PROXIMAL AND REMOTE DETECTION OF WHEAT INFESTED BY WHEAT STEM

SAWFLY (*Cephus cinctus* Norton) VIA MULTITEMPORAL REFLECTANCE

MEASUREMENTS

by

Lochlin Scott Ermatinger

A thesis submitted in partial fulfillment
of the requirements for the degree

of

Master of Science

in

Land Resources and Environmental Sciences

MONTANA STATE UNIVERSITY
Bozeman, Montana

May 2025

DEDICATION

To my family and those closest to me, for your irreplaceable support in completing this journey.

ACKNOWLEDGEMENTS

TABLE OF CONTENTS

TABLE OF CONTENTS CONTINUED

LIST OF TABLES

LIST OF FIGURES

viii

LIST OF FIGURES CONTINUED

LIST OF FIGURES CONTINUED

ABSTRACT

For more than a century, the wheat stem sawfly (WSS, *Cephus cinctus* Norton) has been one of the most important insect pests of wheat (*Triticum aestivum* L.) production in North America. Effective use of management tactics is impaired by the difficulty in monitoring impacts on WSS. Extensive monitoring of WSS populations is cost prohibitive because comprehensive stem dissection surveys are required. The efficacy of surveys may be enhanced with remotely sensed (RS) data, yet little work has been conducted on this approach. We assessed the potential for using RS to estimate WSS infestation at the end of the growing season at the canopy and sub-field spatial scales. We investigated RS of WSS at the canopy level by experimentally infesting wheat plants with WSS. We collected weekly hyperspectral measurements to identify the spectral and temporal scales relevant to RS of WSS. We used sparse multiway partial least squares regression to model variation in multitemporal hyperspectral reflectance of wheat canopies as a function of WSS infestation. This approach accurately estimated the proportion of WSS infested stems ($R^2 = 0.68$, RMSE = 13.5%) and identified spectral readings from the near-infrared shortwave infrared spectral regions collected from the entire experimental period as important. Building off these findings, we evaluated RS of WSS at the sub-field scale using multitemporal images from Sentinel 2 to estimate WSS infestation across 9 production wheat fields. From these fields, we dissected 43,155 wheat stems collected from 1,158 unique locations. For each field, we produced a model to estimate the proportions of total WSS infestation, adequate WSS infestation, and WSS-cut stems. We then compared the performance of these models and found that on average, models describing total WSS ($R^2 = 0.57$) or adequate WSS infestation ($R^2 = 0.57$) were more accurate than models of WSS cut ($R^2 = 0.34$). Our findings suggest that multitemporal passive RS of WSS infestation at the sub-field scale can be useful for mapping patterns of total WSS infestation, but more work is required to effectively map WSS stem cutting. RS shows promise for supplementing research of infield management tactics to better manage WSS.

CHAPTER ONE

LITERATURE REVIEW

The Wheat Stem Sawfly: A Significant Pest of North American
<u>Small Cereal Grains</u>

Cephus cinctus Norton was commonly referred to as the 'western grass-stem sawfly' prior to the early 20th century (Ainslie 1920) as it was most commonly found to inhabit uncultivated grasses. The species was described by Norton in 1872 using a specimen obtained from grass native to Colorado, USA (Norton 1872). The first observations of WSS infesting wheat were reported in Manitoba, Canada in 1895 (Fletcher 1896; Wallace and McNeal 1966). By the 1920's *C. cinctus* garnered the attention of North American economic entomologists as infestations became prevalent in cultivated grasses and small cereal grains across the Canadian provinces and United States (Criddle 1922; Ainslie 1929). Persistent infestations in wheat (*Triticum aestivum* L.) lead entomologists to rename the western grass-stem sawfly the 'wheat stem sawfly' (WSS) (Criddle 1923). The ability of WSS to reproduce in uncultivated grasses and cultivated small cereal grains has led to the propagation of damaging populations along the interface of prairies and dryland agriculture across north-central North America (Lesieur et al. 2016). The areas currently impacted by WSS include the Canadian provinces of Alberta, Saskatchewan, Manitoba, and the U.S. states of Washington, Idaho, Montana, North Dakota, South Dakota, Minnesota, Wyoming, Colorado, Nebraska, and Kansas (Shanower and Waters 2006; Beres et al. 2007; Lesieur et al. 2016; Bekkerman and Weaver 2018; Olfert et al. 2019; McCullough et al. 2020; Cockrell et al. 2021). Across these region, economic losses attributed to WSS have been estimated up to $350 million annually (Beres et al. 2011b). Despite

agroeconomic and scientific interest in the pest, WSS has remained one of most damaging pests to the production of wheat across North America for over a century (Criddle 1922; Beres et al. 2011b; Weaver 2023).

<p style="text-align:center">Wheat Stem Sawfly Biology</p>

Dispersal and Oviposition

WSS adults emerge from stubble depending on temperature and relative humidity and live for about 5 – 8 days (Wallace and McNeal 1966; Perez-Mendoza and Weaver 2006). The onset and duration of the emergence period is influenced by the accumulation of growing degree days but most often occurs during May and June (Fulbright et al. 2017; McCullough et al. 2020). This period of adult emergence can last for several weeks up to well over a month (Perez-Mendoza et al. 2006). The males have smaller bodies and emerge before the females facilitating the fertilization of early emerging females (Fulbright et al. 2017). Copulation is not a prerequisite to oviposition as unfertilized eggs are males (haploid) and fertilized eggs are females (diploid) (Mackay 1955).

Adult WSS do not have a complete digestive tract so their lifespan is constrained by the depletion of internal energy stores (Wallace and McNeal 1966). They may consume water or nectar that slightly increases longevity, but this does not change fecundity (Rand et al. 2019). Because they have no need to search for nutrition, their adult lifespan is dedicated to host seeking (Ainslie 1920). Despite their reliance on endogenous fuel, they have been documented to travel up to a half mile for viable hosts. The host seeking system of WSS females is not fully understood but it is known that they rely on their olfactory senses to detect volatile organic compounds such as (Z)-3-hexenyl acetate, β-ocimene, Z-3hexen-1-ol, and 6-methyl-5-hepten-2-

one that serve as attractants for suitable hosts (Piesik et al. 2008; Weaver et al. 2009; Bhandari 2020; Strand et al. 2025). Females display a preference of hardier, larger, and more succulent stems and will not oviposit until the stem has at least reached the jointing phase of development (Ainslie 1929; Wallace and McNeal 1966; Morrill et al. 2000; Weaver et al. 2009; Buteler and Weaver 2012). Female adult WSS do not appear to have a mechanism to discern whether an egg has been laid in a stem or not thus it is common for multiple WSS eggs to be laid in the same stem (Wallace and McNeal 1966; Buteler et al. 2009). In these cases, the first larva to hatch will likely cannibalize the smaller conspecifics and only one larva will ultimately survive (Criddle 1923; Buteler et al. 2015; Achhami et al. 2020b).

Due to relatively limited dispersal and the lack of adult foraging for nutrition, infestation is often most extensive near areas having large numbers of emerging adults. Cultural practices such as no till and crop/fallow rotation further influence the field distribution of WSS which can localize significant infestations to field edges (Munro 1945; Nansen et al. 2005a). The combination of these factors often produces a gradient of infestation that dissipates as sampling progresses further into a given field (Nansen et al. 2005b; McCullough et al. 2020).

WSS are known to lay eggs in a wide variety of cultivated crops including spring and winter wheat (*Triticum aestivum*), durum wheat (*Triticum turgidum* subsp. *durum*), rye (*Secale cereale* L.), and barley (*Hordeum vulgare* L.) (Ainslie 1920; Cockrell et al. 2017; Achhami et al. 2020a; Rand et al. 2024). Alongside cropped fields, WSS are found to successfully reproduce uncultivated grasses like smooth brome (*Bromus inermis* Leyss.), western wheatgrass (*Pascopyrum smithii* (Rydb.)), bluebunch wheatgrass (*Pseudoroegneria spicata* (Pursh) A. Löve), and slender wheatgrass (*Elymus trachycaulus* (Link) Gould ex Shinners) (Criddle 1922;

Perez-Mendoza et al. 2006; Rand et al. 2024). The wide suite of hosts has enabled the geographic expansion of WSS along the crop prairie interface of North America. Moreover, abundant host access ensures perpetuity of WSS populations. Consequentially, WSS demands long term monitoring for effect management (Weaver 2023).

Wheat Stem Sawfly Larval Cycle and Damage to Host

Once an egg is inside the stem it will hatch in approximately 7 days (Ainslie 1920). Upon hatching the larvae traverse the stem length feeding on the pith and vascular tissue (Ainslie 1929). WSS larvae are not exclusively herbivorous, in the event multiple larvae are present in a stem, the first to mature will cannibalize its peers (Ainslie 1920; Buteler et al. 2015). The larvae continue to feed and burrow through stem internodes as the growing season progresses which has been documented to impair the stem's ability to transport water and nutrients (Morrill et al. 1994). Morrill et al. (1992) observed the presence of subnodal dark spots due to this mechanism of WSS injury. The disruption of the stem function can negatively impact the overall photosynthetic processes (Peterson and Higley 1993) as sucrose produced in the leaves fails to reach its destination (Macedo et al. 2006). This mode of injury alone is seen to reduce yield in infested stems by 20 - 30% (Seamans 1928; Delaney et al. 2010).

During the end of the growing season when the host begins to senesce, desiccation and increased light penetration into the stem cavity signals the larva to travel down the lowest portion of the stem (Ainslie 1929). The larva chews a V shaped notch above itself and uses its excrement or frass to create a plug under this notch. The larva then creates a hibernaculum to protect itself from environmental conditions and predator attacks during diapause (Salt 1947; Holmes et al. 1963; Portman et al. 2018). The purpose of chewing the V shaped notch is to weaken the stem so

that it will eventually fall in the presence of natural environmental effects like gravity, wind, and precipitation. This will provide the overwintering individual an exit once it emerges as an adult the following spring (Munro 1945). This event is referred to as stem lodging which is the most noticeable form of WSS crop damage (Morrill et al., 1992). Severe lodging alone can account for yield losses of up to 80% in a given field (Knodel et al. 2016).

After the larva has created its hibernaculum, its activity slows as it transitions into diapause (Salt 1947). Once winter arrives, the larva will stay dormant until the warmer temperatures of spring arrive, at this point the insect may resume further morphological development or re-enter diapause if environmental conditions prove unfavorable (Salt 1947; Perez-Mendoza and Weaver 2006). In Montana, a temperature range of 20-25 °C and 60-75% relative humidity represents optimal conditions for post-diapause development (Perez-Mendoza and Weaver 2006).

<u>Management Options</u>

<u>Chemical Control</u>

While pesticide use is one of the most prominent agricultural pest control tactics, wheat producers only account for ~5% of total pesticide usage in the United States, despite wheat accounting for the 3rd largest acreage of any U.S. crop (Fernandez-Cornejo et al. 2014). Fernandez-Cornejo et al. (2014) also found that insecticide use only accounted for 3% (by application area) of pesticide application while herbicides accounted for 91% of total use in wheat nationwide. The overall low usage of insecticides extends to management of WSS in wheat. The lack of a chemical control strategy of WSS is due to its life history and side effects imposed by studied control agents (Knodel et al. 2010; Montana Department of Agriculture,

2015). In 1949, Munro et al. found that applying the insecticides BHC, DDD, DDT, toxaphene, and parathion proved fruitless in suppressing WSS infestation in spring wheat. The ability of WSS to evade insecticide contact is attributed to the physical protection offered by the stem wall (Holmes and Peterson 1960; Holmes et al. 1963). It has been proposed to focus chemical control efforts during WSS emergence to force contact between insecticides and adult WSS, but this approach is constrained by the difficulty of predicting emergence and the cost of multiple applications to counter a long period of adult emergence (Knodel et al. 2010). In 2015, the Montana Department of Agriculture licensed phorate, as Thimet®20-G, a temporary emergency registration for control of feeding WSS larvae (Montana Department of Agriculture, 2015). While the insecticide has demonstrated an ability to manage WSS infestation with a 64-100% reduction in cutting (Wanner and Tharp, 2015), elevated toxicity to wildlife and the requirement of post-crop emergence subsurface application no later than 85 days before harvest made it an unpopular choice among producers and the registration was not renewed after December 31, 2019. As of 2025, there are no insecticides permitted for suppressing WSS.

<u>Cultural Controls</u>

     <u>Biological Control</u> WSS has two endemic specialist parasitoids: *Bracon cephi* (Gahan) and *B. lissogaster* Muesebeck (Hymenoptera: Braconidae). These parasitoids attack WSS by identifying and locating larvae feeding in the stem, inserting their ovipositor, and paralyzing the WSS larvae before depositing their eggs (Holmes et al. 1963). Parasitism from *B. cephi* and *B. lissogaster* has been documented to kill up to 34% of WSS (Buteler et al. 2015) with earlier reports indicating greater population suppression is possible (Morrill et al. 1994; Runyon et al. 2002). These two biocontrol agents are responsible for irreplaceable mortality levels when the

numbers are sufficient on the landscape (Buteler et al. 2015). The life history traits of these parasitoids such as egg load, egg volume, and longevity are increased when their diets are supplemented with sucrose (Rand et al. 2019; Reis et al. 2019). Expanding on this, Cavallini et al. (2022) found that parasitoids can achieve these benefits when reared on several carbohydrates combined with amino acids, as well as on extrafloral nectar from cowpea, *Vigna unguiculata* (L.) Walp., and buckwheat, *Fagopyrum esculentum* Moench, floral nectar (Cavallini et al. 2023).

Harvest Practices Despite the practice of no-till agriculture repressing soil erosion (Phillips et al. 1980), it also shows merit as part of a long-term strategy in reducing WSS infestation (Knodel et al. 2016). Sustained no-till practice lends itself to WSS management by preserving populations of parasitoids (Runyon 2001). Even higher retention rates of parasitoids can be attained using a stripper head or cutting wheat at least 25 cm above the soil, with a recent survey indicating that 75% of no-till fields had higher parasitism rates than neighboring tilled fields (Knodel et al. 2016).

Plant Resistance Exploiting the phenotypic properties of wheat varieties as a method for WSS control was first studied by Christian Farstad in 1937 (Farstad 1940). Farstad found that an increased volume of pith in the stem lumen can constrain the movements of the larvae resulting in mortality. Currently, both mortality and pronounced sublethal effects on population dynamics can be attributed to solid-stem wheat (Carcamo et al. 2005; Buteler et al. 2015; Peirce et al. 2022; Bathini et al. 2023). The first commercial wheat variety produced to utilize this effect was a hard red spring wheat named Rescue in 1947 (Platt et al. 1948). This variety gained traction among growers across the North American Great Plains which sparked further development of solid-stemmed varieties. Some of the modern spring wheat varieties with notable stem solidness

and overall WSS resistance include Vida, Choteau, Conan, Corbin, Fortuna, and WB Gunnison (Lanning et al., 2006; Jones et al., 2021). Development and adoption of solid-stemmed winter wheat varieties began in earnest in the 1990s, when damage due to WSS began to worsen in winter wheat fields in Montana (Morrill et al. 1992). Today, popular solid-stemmed winter wheat varieties include Warhorse, Bobcat, Keldin, Yellowstone, and Brawl (NASS-MFO, 2023). While solid-stemmed resistant varieties offer an increased rate of larval mortality, they are unpopular cultivar choices due to a lower yield potential when compared to hollow-stemmed varieties in the absence of WSS pressure (Weiss and Morrill 1992). Furthermore, degree of pith expression is influenced by environmental factors such as seasonal weather patterns which marks another concern for producers (Farstad 1940; Platt 1941; Beres et al. 2017; Subedi et al. 2021).

Trap Crops Seeding the field edges of a high yielding hollow-stemmed wheat with a resistant crop or wheat variety has been suggested as a trap crop strategy (Seamans 1928; Morrill et al. 2001) and has been evaluated using solid stem winter wheat around spring wheat (Morrill et al., 2001). However, this tactic has not been widely adopted by growers due to additional costs. Moreover, successful WSS infestation rates of only 10-15% have been reported to precede infestation of up to 80% the following year (Holmes 1982). Planting immune crops like oat or flax after years of exceptional WSS cutting has shown promise as a means to diminish future populations (Farstad 1940; Farstad 1944). Producer preference and/or market conditions have often made this practice unfavorable (Weiss and Morrill 1992).

Detection of WSS Infestation in Wheat

Sweep Nets

During the period of adult emergence, sweep net surveys can be conducted to capture live adults and understand patterns of WSS dispersal and sex ratios (Goosey 1999; Sing 2002; McCullough et al. 2020; Cockrell et al. 2021). Because of the prolonged period of adult activity on the landscape and staggered emergence between the sexes, it is important that these surveys are conducted more than once in a field to get a clear picture of adult activity (McCullough et al. 2020). The results of these surveys can be influenced by weather as adult WSS rest on stems during inclement weather and are most active when conditions are calm and the temperature is between 17 – 32 °C (Seamans 1945; Goosey 1999). Sweep net surveys are a useful tool for early season scouting but do not provide sufficient information to understand WSS effects on yield or forecasting the WSS population the following year (McCullough et al. 2020).

Stem Dissections

Following emergence, stems must be dissected to detect the presence of eggs, larvae, or excrement (Ainslie 1920). At the end of the growing season, once the crop has been harvested and WSS have cut the stems, crop residue can be collected and dissected to provide information of overall infestation, causes of mortality, and estimate the number of WSS that were successful in cutting (Buteler et al. 2015). Postharvest stem dissection campaigns offer the most robust information for understanding the effect of cultivar, parasitism, and other agronomic practices on WSS infestation and mortality. While this method of monitoring offers some of the most useful data, it is labor and resource intensive.

Stem Lodging Surveys

Field surveys of stem lodging in ripened crops is one of the earliest methods used to estimate WSS infestation as it is assumed to correlate with WSS infestation intensity (Seamans 1928). However, lodging occurrence is not always a reliable proxy for overall infestation for the following reasons: 1) lodging in wheat can occur without WSS infestation (Dahiya et al. 2018), 2) larvae may die or become parasitized before they cut the stem (Buteler et al. 2015) 3) lodged areas of fields may contain a mix of stems with WSS infestation or cutting and stems without WSS infestation (Munro 1945) 4) Lodging rates can be affected by planting densities (Beres et al. 2011a) 5) the results of in-situ lodging surveys are subject to observer variability and bias (Rabieyan et al. 2023). Thus, lodging surveys alone can be susceptible to type I (false positive) and type II (false negative) error. The only accurate method of quantifying infestation is dissecting sufficiently tall stems collected from the end of the growing season (Ainslie, 1920). Moreover, it is imperative that surveys conducted for management capture difference between overall infestation and cutting as host plant resistance and parasitism are the major causes of WSS mortality (Buteler et al. 2015). Conducting any of these field sampling methods with a high degree of accuracy at the field scale requires many observations as statistical power is influenced by both spatial scale and the frequency of WSS infestations (Cárcamo et al. 2007; Davis 2013).

Host Physiological Responses to Wheat Stem Sawfly Infestation

Because monitoring of insect pest infestations in production agricultural fields is often cost prohibitive, there has been much interest in developing scalable detection methods based on ex-situ measurements and a relatively smaller set of infield pest observations (Myers and Allen 1968). These methods rely on the manifestation of discernable changes in crop physiology parameters like respiration (Neves et al. 2006), emission of volatile organic compounds (VOCs) (Fuentes et al. 2021), and reflectance (Baumgardner et al. 1970) change as a result of attack from the insect of interest. Reconciling variation in the physiological parameter(s) and *in-situ* pest observations through statistical models allows for estimating pest occurrence in unsampled areas with a known degree of precision (Hatfield and Pinter 1993; Stein et al. 1998). However, the relationships between insect herbivory and responses in host physiology are often nuanced and can be obfuscated by extrinsic factors, impeding the utility of these models (Peterson and Higley 1993). Exploiting host physiological changes for the purposes of identifying a specific insect attack require an understanding of how the host is expected to respond to the feeding guild (Atstatt and O'Dowd 1976). Identifying host responses to WSS infestation has been well documented but there are currently no reliable methods for bolstering the efficacy of in-field WSS infestation observations with supplementary *ex-situ* measurements.

Changes in Photosynthesis

Measuring gas exchange rates of photosynthesis and photochemical efficiency has also shown merit in discerning between uninfested and WSS infested wheat stems (Macedo et al. 2005; Macedo et al. 2006; Macedo et al. 2007; Delaney et al. 2010). Macedo et al. (2005) found that the impacts of WSS infestation on the photosynthetic rates of leaves were affected by environment. No differences in photosynthetic capacity related to WSS infestation were

observed for plants in the field or the greenhouse, while plants in the growth chamber that received less light and CO_2 were negatively impacted by WSS infestation (Macedo et al. 2005). Macedo et al. (2007) and Delaney et al. (2010) reported that reductions in the photosynthetic capacity of WSS infested plants were similar to those of uninfested wheat plants that suffered from water stress. Interestingly, Macedo et al. (2007) found the relationship between WSS infestation and water stress on photosynthesis was additive while Delaney et al. (2010) found it was interactive. Specifically, Delaney et al. (2010) found the magnitude of these effects on photosynthesis varied across cultivars of wheat and photosynthesis was suppressed further when plants were also deprived of phosphorus. The observed variation in physiological responses points to an ability of hosts to tolerate or even compensate for WSS infestation (Macedo et al. 2006; Achhami et al. 2020c). For instance, increased efficiency in photosystem II has been observed in the head glumes of WSS infested wheat but not in the leaves (Macedo et al. 2007) and the barley varieties 'Craft', 'Haxby', and 'Hockett' have inconsistently produced greater yields in response to WSS infestation (Achhami et al. 2020c).

Changes in Appearance

In 1992, Morrill et al. first used the presence of subnodal dark bands in stems at the grain filling stage to detect WSS infestation in winter wheat. The formation of these bands is believed to be the accumulation of assimilate caused by WSS feeding on the phloem and xylem (Morrill et al. 1994). They were able to predict the occurrence of larva in a stem with up to 95% accuracy using this approach (Morrill et al. 1992). However, they did note that similar banding patterns can materialize naturally in some cultivars or manifest due to pathogen attack. This occurrence of banding in relation to WSS feeding also appears to be influenced by cultivar and external factors

such as water and nutrient availability (Unpublished Data). Despite this, Morrill et al. (1992)

demonstrated that WSS infestation can cause detectable changes to the physical appearance of

wheat stems beyond lodging.

Remote Sensing

Remote sensing (RS) colloquially refers to the practice of collecting information about a

target of interest using an instrument that does not need to directly come into contact with it

(Fisher et al. 1963). This information often comes in the form of spectral measurements that can

be linked to variation in the condition of the ground target. Within the realm of monitoring

vegetation, insights to plant physiology can be gained through standardized measurements of

vegetation's reflectance and supplementary experimentation to explain causes of variation in

reflectance (Knipling 1970). Remote sensors are generally classified as passive or active sensors

(Yates 1970). Passive sensors gather ambient radiation, most often from the visible through

shortwave infrared region of the electromagnetic spectrum (350 – 2500 nm, VSWIR). Internal

pigments and plant tissues dictate how plants absorb and reflect radiation across the VSWIR,

making this region useful for RS of vegetation (Gates et al. 1965). Active sensors emit energy

and record information about its return such as travel time and polarity state which can be used

to understand the physical structure of vegetation (Moore and Simonett 1967). Active and

passive sensors be used in close proximity to a target or can be mounted on unnamed aerial

vehicles (UAVs), planes, and satellites to facilitate the collection of the remotely sensed data

across larger areas (Macdonald et al. 1975; Everaerts 2008). This suite of platforms enables

researchers to use remotely sensed data from various spatial and temporal scales compatible with

the system of interest.

Passive Sensing of Vegetation

The reflectance of plants is controlled by their internal pigments, mesophyll structure,

water content, and angle of incident light (Tucker et al. 1980; Neuwirthová et al. 2017). The

visible (VIS) portion of the electromagnetic spectrum is chiefly influenced by concentrations of

the pigments chlorophyll, xanthophyll, and carotene (Gates et al. 1965). The dominant pigment

in most leaves, chlorophyll, preferentially absorbs light in the blue and red portions of the

spectrum which is then converted into heat or inflorescence and used to create chemical energy

through photosynthesis (Emerson and Rabinowitch 1960). Green light is not heavily absorbed by

the abundant plant pigments thus it is reflected, giving plants their green appearance (Gates et al.

1965). Healthy plants generally reflect highly in the near infrared (NIR) portion of the spectrum

due to a high surface area of mesophilic tissue (Slaton et al. 2001). The NIR reflectance begins to

increase as senescence begins and cells begin to shrink but significantly decreases as senescence

progresses (Gausman 1985). The water content of leaves largely dictates their shortwave infrared

(SWIR) reflectance (Hunt and Rock 1989). In general, water absorbs light in this spectrum, thus

higher reflectance in this region indicates a decrease in leaf water content (Seelig et al. 2008).

The designs of commercially employed passive sensors leverage this knowledge of plant

interactions with VSWIR to optimize the spectral regions that are measured (Jensen 1983).

Multispectral sensors contain three to a dozen or so individual sensors that aggregate light across

a region of adjacent wavelengths, referred to as a band, to produce a principal measurement of

reflectance (Wiersma and Landgrebe 1980). Hyperspectral sensors incorporate 100's to 1000's of

these bands that sense light across small spectral regions to create a near continuous

representation of reflectance across the VSWIR (Bioucas-Dias et al. 2013). The fine spectral

resolution of hyperspectral data has enabled researchers to elucidate nuanced effects of pest and

pathogen infestation with greater precision than multispectral data (Nansen and Elliott 2016; Thomas et al. 2018). Passive sensors for RS of vegetation often contain bands in red, blue, green, NIR, and SWIR (Holmes and MacDonald 1969). Satellite platforms such as those operated by the Landsat and Sentinel missions offer standardized multispectral data products available at moderate spatial resolutions (Landsat 9: 15 – 100 m, Sentinel 2: 10 – 60 m) and consistent revisit intervals (Landsat 9: 16 days, Sentinel 2: 5 days) (Claverie et al. 2018). Landsat, managed by the National Aeronautics and Space Administration (NASA), and Sentinel by European Space Agency (ESA), offer data from these missions freely available which has propagated a rich history of RS agricultural research (Song et al. 2021).

Satellite remote sensing data has been effectively used with in-situ measurements to estimate and map abiotic and biotic stressors of wheat such as nitrogen deficiency (Nino et al. 2024), water stress (Solgi et al. 2023), saline soils (Wen et al. 2023), wheat streak mosaic (WSM) virus (Mirik et al. 2011), hessian fly infestation (*Mayetiola destructor* (Say)) (Bhattarai et al. 2019). While these studies investigated different forcings on wheat reflectance, they all employ similar workflows to model the phenomena of concern. In each study, researchers used statistical models to reconcile variation of the in-situ observations of the stressor they were interested in with corresponding variation in reflectance. Mirik et al. (2011) and Bhattari et al. (2019) found that single image analysis could be useful for estimating the prevalence of WSM and hessian flies, respectively. However, it is often the case that multiple images collected over weeks or months are required to elucidate the impact of stressors when their impact is subtle (Solgi et al. 2023; Nino et al. 2024). When compared to single image crop analysis, integrating multi-

temporal images allows for more robust estimates of attributes that are influenced by the life history of the crop, like yield (Fieuzal et al. 2020; Qiao et al. 2021).

<u>Remote Sensing Specific to WSS</u>

Nansen et al. (2009) found that reflectance of leaves can be altered by the presence of WSS infestation. Reflectance measurements were recorded weekly from multiple leaves of WSS infested and uninfested wheat plants for four weeks using a hyperspectral camera with 213 bands between 402 – 838 nm. To evaluate the use of proximally collected images for detection of WSS infestation, they analyzed differences in the mean reflectance of selected wavelengths (452 nm, 553 nm, 657 nm, 725 nm, 760 nm), variogram parameters nugget and sill (Woodcock et al. 1988), and normalized difference vegetation index (NDVI, Tucker 1979) between the WSS infested and uninfested plants. They reported detectable differences in NDVI and the variogram parameter sill between infested and uninfested leaves were apparent starting three weeks after infestation (Nansen et al., 2009). Similar to the findings of Macedo et al. (2006), it was also observed that the effect of WSS infestation on the reflectance derived parameters was dependent on the leaf it was collected from.

RS in the context of WSS has been only documented at two diametric spatial scales: leaf and landscape (Nansen et al. 2009; Lestina et al. 2016). Lestina et al. (2016) used remotely sensed measurements of the enhanced vegetation index (EVI) in conjunction with ancillary data like terrain roughness, monthly temperature and precipitation, and soil survey data to produce statewide suitability maps of WSS for Colorado. Presence / absence data were collected from 2012 - 2015 with sweep net surveys conducted across the northeastern quadrant of the state during WSS emergence. Interestingly, when considering the entire suite of environmental

variables, Lestina et al. (2016) found that the EVI from the month of April was the single strongest predictor variable of WSS occurrence for a given year. This potentially suggests that monitoring of early season green up can be used as proxy for the effects of temperature and humidity on WSS development and resultant emergence (Morrill et al. 1993; Perez-Mendoza and Weaver 2006). Nansen et al. (2009) demonstrated that physiological changes induced by larval WSS feeding can alter the reflectance of individual wheat leaves. Collecting proximal reflectance measurements of individual leaves is not feasible at the field scale and comparing the reflectance of single leaves to a canopy is not linear due to variations in incidence of light, leaf orientation, light transmission through leaves, reflectivity of backgrounds, and heterogeneity of spectral responses from plant appendages (Knipling 1970). These studies demonstrate the utility of RS data for modeling the occurrence of WSS adults at the landscape scale and internal larval feeding in individual stems.

Both of the aforementioned studies apply a qualitative perspective to WSS that is not advantageous to modeling WSS population dynamics at intermediate spatial scales. Moreover, there are currently no studies that explore the use of RS for describing the distribution of WSS infestation at the field or sub-field scale. Because effective decision-making for WSS management relies on understanding the impact of infestation patterns and mortality factors of WSS, it is imperative to develop quantitative estimates of WSS infestation at the field or subfield scale.

Research Objectives

The motivating goal of this work is to support the development of scalable WSS monitoring tools for researchers and wheat farmers. The absence of literature investigating RS for WSS at the canopy and sub-field scale indicate natural gaps to fill for enhancing our ability to monitor WSS population dynamics. This project seeks to provide a better understanding of how RS of WSS may be effective at the canopy scale to subsequently inform sub-field scale efforts in RS of WSS. Chapter 2 builds off the findings of Nansen et al. (2009) by using a hyperspectral sensor to monitor the reflectance of wheat canopies and describe reflectance changes resulting from variable degrees of WSS infestation. The experiment in chapter 2 was designed to simulate data collected from a hyperspectral drone flown weekly throughout a growing season. Chapter 3 evaluated quantitative RS of WSS infestation at the sub-field scale in production winter and spring wheat fields using georegistered post-harvest residue of WSS infestation and multitemporal Sentinel 2 images. For each field, we produce models to estimate metrics of WSS infestation describing the overall percentage of WSS infested stems, percentage of stems with WSS infestation exceeding two internodes, and the percentage of WSS cut stems. Evaluating the performance of these models sheds light on how passive multitemporal RS can be used for quantifying WSS infestation at the sub-field scale. The conclusion of this study in Chapter 4 summarizes pertinent findings of these studies and suggests future directions of RS research for WSS.

References

Achhami B, Peterson R, Sherman J, Reddy G, Weaver D. 2020. Multiple decrement life tables of *Cephus cinctus* Norton (Hymenoptera: Cephidae) across a set of barley cultivars: The importance of plant defense versus cannibalism. PLOS ONE. 15. doi: 10.1371/journal.pone.0238527.

Achhami B, Reddy G, Sherman J, Peterson R, Weaver D. 2020. Effect of precipitation and temperature on larval survival of *Cephus cinctus* (Hymenoptera: Cephidae) in barley cultivars. Journal of Economic Entomology. 113:1982–1989. doi:10.1093/jee/toaa097.

Achhami B, Reddy G, Sherman J, Weaver D, Peterson R. 2020. Antixenosis, antibiosis, and potential yield compensatory response in barley cultivars exposed to wheat stem sawfly (Hymenoptera: Cephidae) under field conditions. Journal of Insect Science. 20:1–14. doi: 10.1093/jisesa/ieaa091.

Ainslie CN. 1929. The western grass-stem sawfly (*Cephus cinctus* Norton): A pest of small grains. U.S Department of Agriculture Technical Bulletin Report No.: 157.

Ainslie CN. 1920. The western grass-stem sawfly. Washington, D.C. : U.S. Dept. of Agriculture.

Atstatt PR, O'Dowd DJ. 1976. Plant defense guilds: Many plants are functionally interdependent with respect to their herbivores. Science. 193(4247):24–29. doi: 10.1126/science.193.4247.24.

Bathini A, Mendu L, Singh N, Cook J, Weaver D, Sherman J, Hager M, Mondal S, Mendu V. 2023. A "solid" solution for wheat stem sawfly (Hymenoptera: Cephidae) resistance: Genetics, breeding and development of solid stem wheat. Crop Science. 63. doi: 10.1002/csc2.20998.

Baumgardner MF, Leamer RW, Shay JR. 1970. Remote sensing techniques used in agriculture today. In: Aerospace Science and Agricultural Development. 189(1): 9-26

Bekkerman A, Weaver DK. 2018. Modeling joint dependence of managed ecosystems pests: the case of the wheat stem sawfly. Journal of Agricultural and Resource Economics. 43(2):172–194. doi: 10.22004/ag.econ.273445

Beres B, Hill B, Carcamo H, Knodel J, Weaver D, Cuthbert R. 2017. An artificial neural network model to predict wheat stem sawfly cutting in solid-stemmed wheat cultivars. Canadian Journal of Plant Science. 97. doi: 10.1139/CJPS-2016-0364.

Beres BL, Cárcamo HA, Byers JR. 2007. Effect of wheat stem sawfly damage on yield and quality of selected Canadian spring wheat. Journal of Economic Entomology. 100(1):79–87. doi: 10.1093/jee/100.1.79.

Beres BL, Cárcamo HA, Yang R-C, Spaner DM. 2011. Integrating spring wheat sowing density with variety selection to manage wheat stem sawfly. Agronomy Journal. 103(6):1755–1764. doi: 10.2134/agronj2011.0187.

Beres BL, Dosdall LM, Weaver DK, Cárcamo HA, Spaner DM. 2011. Biology and integrated management of wheat stem sawfly and the need for continuing research. Canadian Entomologist. 143(2):105–125. doi: 10.4039/n10-056.

Bhandari R. 2020. Assessment of host selection behaviors and oviposition preferences of *Cephus cinctus* Norton (Hymenoptera: Cephidae) using wheat and smooth brome [Master's thesis]. Bozeman, MT (USA). Montana State University.

Bhattarai GP, Schmid RB, McCornack BP. 2019. Remote sensing data to detect hessian fly infestation in commercial wheat fields. Scientific Reports. 9(1). doi: 10.1038/s41598-019-42620-0.

Bioucas-Dias JM, Plaza A, Camps-Valls G, Scheunders P, Nasrabadi N, Chanussot J. 2013. Hyperspectral remote sensing data analysis and future challenges. IEEE Geoscience and Remote Sensing Magazine. 1(2):6–36. doi: 10.1109/MGRS.2013.2244672.

Buteler M, Peterson RKD, Hofland ML, Weaver DK. 2015. Multiple decrement life table reveals that host plant resistance and parasitism are major causes of mortality for the wheat stem sawfly. Environmental Entomology. 44(6):1571–1580. doi: 10.1093/ee/nvv128.

Buteler M, Peterson RKD, Weaver DK. 2009. Oviposition behavior of the wheat stem sawfly when encountering plants infested with cryptic conspecifics. Environmental Entomology. 38(6):1707–1715. doi: 10.1603/022.038.0624.

Buteler M, Weaver DK. 2012. Host selection by the wheat stem sawfly in winter wheat and the role of semiochemicals mediating oviposition preference. Entomologia Experimentalis et Applicata. 143(2):138–147. doi: 10.1111/j.1570-7458.2012.01237.x.

Carcamo H, Beres B, Clarke F, Byers R, Mündel H, May K, DePauw R. 2005. Influence of plant host quality on fitness and sex ratio of the wheat stem sawfly (Hymenoptera: Cephidae). Environmental Entomology. 34:1579–1592. doi: 10.1603/0046-225X-34.6.1579.

Cárcamo H, Entz T, Beres B. 2007. Estimating *Cephus cinctus* wheat stem cutting damage – can we cut stem counts? Journal of Agri cultural and Urban Entomology. 24(3):117–124. doi: 10.3954/1523-5475-24.3.117.

Cavallini L, Peterson R, Weaver D. 2023. Dietary sugars and amino acids increase longevity and enhance reproductive parameters of *Bracon cephi* and *B. lissogaster*, two parasitoids that specialise on wheat stem sawfly. Physiological Entomology. 48(1):24-34. doi: 10.1111/phen.12399.

Cavallini L, Peterson R, Weaver D. 2023. Cowpea extrafloral nectar has potential to provide ecosystem services lost in agricultural intensification and support native parasitoids that suppress the wheat stem sawfly. Journal of Economic Entomology. 116(3):752-760. doi: 10.1093/jee/toad083.

Claverie M, Ju J, Masek JG, Dungan JL, Vermote EF, Roger J-C, Skakun SV, Justice C. 2018. The harmonized Landsat and Sentinel-2 surface reflectance data set. Remote Sensing of Environment. 219:145–161. doi: 10.1016/j.rse.2018.09.002.

Cockrell DM, Griffin-Nolan RJ, Rand TA, Altilmisani N, Ode PJ, Peairs F. 2017. Host plants of the wheat stem sawfly (Hymenoptera: Cephidae). Environmental Entomology. 46(4):847–854. doi: 10.1093/ee/nvx104.

Cockrell DM, Randolph T, Peirce E, Peairs FB. 2021. Survey of wheat stem sawfly (Hymenoptera: Cephidae) infesting wheat in Eastern Colorado. Journal of Economic Entomology. 114(2):998–1004. doi: 10.1093/jee/toab015.

Criddle N. 1922. The western-stem sawfly and its control. Dominion of Canada Department of Agriculture.(6):1–8.

Criddle N. 1923. Popular and practical entomology: The life habits of *Cephus cinctus* Norton in Manitoba. The Canadian Entomologist. 55(1):1–4. doi: 10.4039/Ent551-1.

Dahiya S, Sihag S, Chaudhary C. 2018. Lodging: Significance and preventive measures for increasing crop production. International Journal of Chemical Studies. 6:700–705. E-ISSN: 2321-4902

Davis RA. 2013. Mechanisms for reproductive isolation in two congeneric parasitoids of the wheat stem sawfly. Montana State University - Bozeman, College of Agriculture. [MS Thesis]. Bozeman, MT (USA). Montana State University.

Delaney KJ, Weaver DK, Peterson RKD. 2010. Photosynthesis and yield reductions from wheat stem sawfly (Hymenoptera: Cephidae): Interactions with wheat solidness, Water stress, and phosphorus deficiency. Journal of Economic Entomology. 103(2):516–524. doi: 10.1603/EC09229.

Emerson R, Rabinowitch E. 1960. Red drop and role of auxiliary pigments in photosynthesis. Plant Physiol. 35(4):477–485.

Everaerts J. 2008. The use of unmanned aerial vehicles (UAVs) for remote sensing and mapping. In: The International Archives of the Photogrammetry, Remote Sensing and Spatial Information Sciences. Vol. 37.

Farstad C. 1940. The development of Western wheat stem sawfly (*Cephus cinctus* Norton) in various host plants as an index of resistance. Iowa State College Journal of Science.(15):67–69. doi: 10.31274/RTD-180813-14901.

Farstad CW. 1944. Wheat stem sawfly in flax. Scientific Agriculture. 24(8):383–386. doi: 10.4141/sa-1944-0025.

Fernandez-Cornejo J, Nehring RF, Osteen C, Wechsler S, Martin A, Vialou A. 2014. Pesticide use in U.S. agriculture: 21 selected crops, 1960-2008. USDA-ERS Economic Information Bulletin Number 124. doi: 10.2139/ssrn.2502986.

Fieuzal R, Bustillo V, Collado D, Dedieu G. 2020. Combined use of multi-temporal Landsat-8 and Sentinel-2 images for wheat yield estimates at the intra-plot Spatial Scale. Agronomy. 10(3):327. doi: 10.3390/agronomy10030327.

Fisher DS, Miller CD, Morgan JO, Parker DC. 1963. Remote sensing of environment. Infrared Laboratory, Institute of Science and Technology, University of Michigan Report No.: 4864-6- F.

Fletcher J. 1896. The western wheat stem sawfly (*Cephus pygmaeus* L.). Dominion of Canada, Department of Agriculture, Report of the Dominion Entomologist. 1(1896):147–149.

Fuentes S, Tongson E, Unnithan RR, Gonzalez Viejo C. 2021. Early detection of aphid infestation and insect-plant interaction assessment in wheat using a low-cost electronic nose (E-Nose), near-infrared spectroscopy and machine learning modeling. Sensors. 21(17):5948. doi: 10.3390/s21175948.

Fulbright J, Wanner K, Bekkerman A, Weaver D. 2017. Wheat stem sawfly biology. Montana State University Extension, MontGuide, MT201107AG.

Gates DM, Keegan HJ, Schleter JC, Weidner VR. 1965. Spectral properties of plants. 4(1):11-20. doi: 10.1364/AO.4.000011

Gausman HW. 1985. Plant leaf optical properties in visible and near-infrared light. [PhD thesis]. Lubbock, TX (USA): Texas Technical University.

Goosey HB. 1999. In field distributions of the wheat stem sawfly, (Hymenoptera: Cephidae), and evaluation of selected tactics for an integrated management program. [MS Thesis] Bozeman, MT (USA). Montana State University.

Hatfield PL, Pinter PJ. 1993. Remote sensing for crop protection. Crop Protection. 12(6):403–413. doi: 10.1016/0261-2194(93)90001-Y.

Holmes ND. 1982. Population dynamics of the wheat stem sawfly, *Cephus cinctus* (Hymenoptera: Cephidae), in wheat. The Canadian Entomologist. 114(9):775–788. doi: 10.4039/Ent114775-9.

Holmes ND, Nelson WA, Peterson LK, Farstad CW. 1963. Causes of variations in effectiveness of *Bracon cephi* (Gahan) (Hymenoptera: Braconidae) as a parasite of the wheat stem sawfly. The Canadian Entomologist. 95(2):133–126. doi: 10.4039/Ent95113-2.

Holmes ND, Peterson LK. 1960. The influence of the host on oviposition by the wheat stem sawfly, *Cephus cinctus* Norton. (Hymenoptera: Cephidae). Can J Plant Sci. 40(1):29–46. doi: 10.4141/cjps60-004.

Holmes RA, MacDonald RB. 1969. The physical basis of system design for remote sensing in agriculture. Proceedings of the IEEE. 57(4):629–639. doi: 10.1109/PROC.1969.7018.

Hunt ER, Rock BN. 1989. Detection of changes in leaf water content using near- and middle-infrared reflectances. Remote Sensing of Environment. 30(1):43–54. doi: 10.1016/0034-4257(89)90046-1.

Jensen JR. 1983. Biophysical remote sensing. Annals of the Association of American Geographers. 73(1):111–132. doi: 10.1111/j.1467-8306.1983.tb01399.x.

Jones BH, Blake NK, Heo H-Y, Martin JM, Torrion JA, Talbert LE. 2021. Allelic response of yield component traits to resource availability in spring wheat. Theoretical Applied Genetics. 134(2):603–620. doi: 10.1007/s00122-020-03717-7.

Knipling EB. 1970. Physical and physiological basis for the reflectance of visible and near-infrared radiation from vegetation. Remote sensing of environment. doi:10.1016/S0034-4257(70)80021-9.

Knodel J, Shanower T, Beauzay P. 2016. Distribution and history. Fargo, ND.: North Dakota State University, Extension Service.

Knodel J, Shanower T, Beauzay PB. 2010. Integrated pest management of wheat stem sawfly in North Dakota. North Dakota State University Cooperative Extension Bulletin. E-1479.

Lanning SP, Fox P, Elser J, Martin JM, Blake NK, Talbert LE. 2006. Microsatellite markers associated with a secondary stem solidness locus in wheat. Crop Science. 46(4):1701–1703. doi: 10.2135/cropsci2005.10-0379.

Lesieur V, Martin J-F, Weaver DK, Hoelmer KA, Smith DR, Morrill WL, Kadiri N, Peairs FB, Cockrell DM, Randolph TL, et al. 2016. Phylogeography of the wheat stem sawfly, *Cephus cinctus* Norton (Hymenoptera: Cephidae): implications for pest management. PLOS ONE. 11(12):e0168370. doi: 10.1371/journal.pone.0168370.

Lestina J, Cook M, Kumar S, Morisette J, Ode PJ, Peairs F. 2016. MODIS imagery improves pest risk assessment: A case study of wheat stem sawfly (*Cephus cinctus*, Hymenoptera: Cephidae) in Colorado, USA. Environmental Entomology. 45(6):1343–1351. doi: 10.1093/ee/nvw095.

Macdonald RB, Hall FG, Erb RB. 1975. The use of LANDSAT data in a large area crop inventory experiment (LACIE). In *LARS Symposia*, p. 46. 1975.

Macedo TB, Peterson RKD, Weaver DK, Morrill WL. 2005. Wheat stem sawfly, *Cephus cinctus* Norton, impact on wheat primary metabolism: An ecophysiological approach. Environmental Entomology. 34(3): 719-726. doi: 10.1603/0046-225X-34.3.719

Macedo TB, Weaver DK, Peterson RKD. 2006. Characterization of the impact of wheat stem sawfly, *Cephus cinctus* Norton, on pigment composition and photosystem II photochemistry of wheat heads. Environmental Entomology. 35(4): 1115-1120. doi: 10.1603/0046-225X-35.4.1115

Macedo TB, Weaver DK, Peterson RKD. 2007. Photosynthesis in wheat at the grain filling stage is altered by larval wheat stem sawfly (Hymenoptera: Cephidae) injury and reduced water availability. Journal of Entomological Science. 42(2): 228 – 238. doi: 10.18474/0749-8004-42.2.228

Mackay MR. 1955. Cytology and parthenogenesis of the wheat stem sawfly, *Cephus cinctus* Norton. (Hymenoptera: Cephidae). Canadian Journal of Zoology. 33(3):161–174. doi: 10.1139/z55-011.

McCullough CT, Hein GL, Bradshaw JD. 2020. Phenology and dispersal of the wheat stem sawfly (Hymenoptera: Cephidae) into winter wheat fields in Nebraska. Journal of Economic Entomology. 113(4):1831–1838. doi: 10.1093/jee/toaa093.

Mirik M, Jones DC, Price JA, Workneh F, Ansley RJ, Rush CM. 2011. Satellite remote sensing of wheat infected by wheat streak mosaic virus. Plant Disease. 95(1):4–12. doi: 10.1094/PDIS-04-10-0256.

Montana Department of Agriculture (MDA). (2015). Thimet® 20-G. EPA SLN No.MT-150001.

Moore RK, Simonett DS. 1967. Radar remote sensing in biology. BioScience. 17(6):384–390. doi: 10.2307/1293798.

Morrill WL, Gabor JW, Kushnak GD. 1992. Wheat stem sawfly (Hymenoptera: Cephidae): damage and detection. Journal of Economic Entomology. 85(6): 2413-2417. doi: 10.1093/jee/85.6.2413

Morrill WL, Gabor JW, Weaver DK, Kushnak GD, Irish NJ. 2000. Effect of host plant quality on the sex ratio and fitness of female wheat stem sawflies (Hymenoptera: Cephidae). Environmental Entomology. 29(2):195–199. doi: 10.1093/ee/29.2.195.

Morrill WL, Gabor JW, Wichman D. 1993. Mortality of the wheat stem sawfly (Hymenoptera: Cephidae) at low temperatures. Environmental Entomology. 22(6):1358–1361. doi: 10.1093/ee/22.6.1358.

Morrill WL, Kushnak GD. 1999. Planting Date Influence on the Wheat Stem Sawfly (Hymenoptera: Cephidae) in Spring Wheat. Journal of Agricultural and Urban Entomology. 16(2): 123-128.

Morrill WL, Kushnak GD, Bruckner PL, Gabor JW. 1994. Wheat stem sawfly (Hymenoptera: Cephidae) damage, rates of parasitism, and overwinter survival in resistant wheat lines. Journal of Economic Entomology. 87(5):1373–1376. doi: 10.1093/jee/87.5.1373.

Morrill WL, Weaver DK, Johnson GD. 2001. Trap strip and field border modification for management of the wheat stem sawfly (Hymenoptera: Cephidae). Journal of Entomological Science. 36(1):34–45. doi: 10.18474/0749-8004-36.1.34.

Munro JA. 1945. Wheat stem sawfly and harvest loss. North Dakota Agricultural Experimental Station Bimonthly Bulletin. 7(4): 12-16.

Myers VI, Allen WA. 1968. Electrooptical remote sensing methods as nondestructive testing and measuring techniques in agriculture. Applied Optics. 7(9):1819–1838. doi: 10.1364/AO.7.001819.

Nansen C, Elliott N. 2016. Remote sensing and reflectance profiling in entomology. Annual Review of Entomology. 61(1):139–158. doi: 10.1146/annurev-ento-010715-023834.

Nansen C, Macedo T, Swanson R, Weaver DK. 2009. Use of spatial structure analysis of hyperspectral data cubes for detection of insect-induced stress in wheat plants. International Journal of Remote Sensing. 30(10):2447–2464. doi: 10.1080/01431160802552710.

Nansen C, Macedo TB, Weaver DK, Peterson RKD. 2005. Spatiotemporal distributions of wheat stem sawfly eggs and larvae in dryland wheat fields. Canadian Entomologist. 137(4):428–440. doi: 10.4039/n04-094.

Nansen C, Weaver DK, Sing SE, Runyon JB, Morrill WL, Grieshop MJ, Shannon CL, Johnson ML. 2005. Within-field spatial distribution of *Cephus cinctus* (Hymenoptera: Cephidae) larvae in Montana wheat fields. Canadian Entomologist. 137: 202 – 214.

National Agricultural Statistics Service, Mountain Regional Field Office. 2023. Montana 2023 wheat varieties. United States Department of Agriculture. Available at: https://www.nass.usda.gov/Statistics_by_State/Montana/Publications/Special_Interest_Reports/MT-Wheat-Varieties-2023.pdf.

Neuwirthová E, Lhotáková Z, Albrechtová J. 2017. The effect of leaf stacking on leaf reflectance and vegetation indices measured by contact probe during the season. Sensors. 17(6):1202. doi: 10.3390/s17061202.

Neves AD, Oliveira RF, Parra JRP. 2006. A new concept for insect damage evaluation based on plant physiological variables. An Acad Bras Ciênc. 78:821–835. doi: 10.1590/S0001-37652006000400015.

Nino P, D'Urso G, Vanino S, Di Bene C, Farina R, Falanga Bolognesi S, De Michele C, Napoli R. 2024. Nitrogen status of durum wheat derived from Sentinel-2 satellite data in central Italy. Remote Sensing Applications: Society and Environment. 36:101323. doi: 10.1016/j.rsase.2024.101323.

Norton E. 1872. Notes on North American Tenthredinidae, with descriptions of new species. Transactions of the American Entomological Society (1867-1877). 4:77–86. doi: 10.2307/25076265.

Olfert O, Weiss RM, Catton H, Cárcamo H, Meers S. 2019. Bioclimatic assessment of abiotic factors affecting relative abundance and distribution of wheat stem sawfly (Hymenoptera: Cephidae) in western Canada. The Canadian Entomologist. 151(1):16–33. doi: 10.4039/tce.2018.46.

Peirce E, Cockrell D, Mason RE, Haley S, Peairs F, Nachappa P. 2022. Solid stems and beyond: challenges and future directions of resistance to wheat stem sawfly (Hymenoptera: Cephidae). Journal of Integrated Pest Management. 13(1): 29. doi: 10.1093/jipm/pmac023.

Perez-Mendoza J, Weaver DK. 2006. Temperature and relative humidity effects on postdiapause larval development and adult emergence in three populations of wheat stem sawfly (Hymenoptera: Cephidae). Environmental Entomology. 35(5):1222–1231. doi: 10.1093/ee/35.5.1222.

Perez-Mendoza J, Weaver DK, Morrill WL. 2006. Infestation of wheat and downy brome grass by wheat stem sawfly and subsequent larval performance. Environmental Entomology. 35(5):1279–1285. doi: 10.1093/ee/35.5.1279.

Peterson RKD, Higley LG. 1993. Arthropod injury and plant gas exchange: current understandings and approaches for synthesis. Trends in Agricultural Science. 1:93–100.

Phillips RE, Thomas GW, Blevins RL, Frye WW, Phillips SH. 1980. No-Tillage agriculture. Science. 208(4448): 1108-1113. doi: 10.1126/science.208.4448.1108.

Piesik D, Weaver DK, Runyon JB, Buteler M, Peck GE, Morrill WL. 2008. Behavioural responses of wheat stem sawflies to wheat volatiles. Agricultural and Forest Entomology. 10(3):245–253. doi: 10.1111/j.1461-9563.2008.00380.x.

Platt AW. 1941. The influence of some environmental factors on the expression of the solid stem character in certain wheat varieties. Scientific Agriculture. 22(3): 139-151.

Platt AW, Farstad CW, Callenbach JA. 1948. The Reaction of Rescue Wheat to Sawfly Damage. Scientific Agriculture. 28(4):154–161. doi: 10.4141/sa-1948-0026.

Portman S, Jaronski S, Weaver D, Reddy G. 2018. Advancing biological control of the wheat stem sawfly: new strategies in a 100-yr struggle to manage a costly pest in the Northern Great Plains. Annals of the Entomological Society of America. 111:85–91. doi: 10.1093/aesa/say002.

Qiao M, He X, Cheng X, Li P, Luo H, Zhang L, Tian Z. 2021. Crop yield prediction from multi-spectral, multi-temporal remotely sensed imagery using recurrent 3D convolutional neural networks. International Journal of Applied Earth Observation and Geoinformation. 102:102436. doi: 10.1016/j.jag.2021.102436.

Rand TA, Kula RR, Gaskin JF. 2024. Evaluating the use of common grasses by the wheat stem sawfly (Hymenoptera: Cephidae) and its native parasitoids in rangeland and Conservation Reserve Program grasslands. Journal of Economic Entomology. 117(3):858–864. doi: 10.1093/jee/toae046.

Rand TA, Titus EF, Waters DK. 2019. Do floral resources benefit the herbivorous sawfly, *Cephus cinctus* (Hymenoptera: Cephidae), a major pest of wheat in North America? Journal of Economic Entomology. 112(2):565–570. doi: 10.1093/jee/toy408.

Rabieyan E, Darvishzadeh R, Alipour H. 2023. Identification and estimation of lodging in bread wheat genotypes using machine learning predictive algorithms. Plant Methods. 19(1):109. doi:10.1186/s13007-023-01088-w.

Reis DA, Hofland ML, Peterson RKD, Weaver DK. 2019. Effects of sucrose supplementation and generation on life-history traits of *Bracon cephi* and *Bracon lissogaster*, parasitoids of the wheat stem sawfly. Physiological Entomology. 44(3–4):266–274. doi: 10.1111/phen.12303.

Runyon JB. 2001. Wheat stem sawfly parasitism in varying field sizes and tillage systems in dryland wheat in Montana. [Master's thesis]. Bozeman, MT (USA) :Montana State University.

Runyon JB, Morrill WL, Weaver DK, Miller PR. 2002. Parasitism of the wheat stem sawfly (Hymenoptera: Cephidae) by Bracon cephi and B. lissogaster (Hymenoptera: Braconidae) in wheat fields bordering tilled and untilled fallow in Montana. Journal of Economic Entomology. 95(6):1130–1134. doi: 10.1603/0022-0493-95.6.1130.

Salt RW. 1947. Some effects of temperature on the production and elimination of diapause in the wheat stem sawfly, *Cephus cinctus* Norton. Canadian Journal of Research. 25d(2): 66–86. doi: 10.1139/cjr47d-004.

Seamans HL. 1945. A preliminary report on the climatology of the wheat stem sawfly (*Cephus cinctus* Norton) on the Canadian Prairies. Scientific Agriculture. 25(7):432–457. doi: 10.4141/sa-1945-0012.

Seelig HD, Hoehn A, Stodieck LS, Klaus DM, Adams WW, Emery WJ. 2008. The assessment of leaf water content using leaf reflectance ratios in the visible, near-, and short-wave-infrared. International Journal of Remote Sensing. 29(13):3701–3713. doi: 10.1080/01431160701772500.

Shanower T, Waters D. 2006. A survey of five stem-feeding insect pests of wheat in the Northern Great Plains. Journal of Entomological Science. 41. doi: 10.18474/0749-8004-41.1.40.

Sing SE. 2002. Spatial and biotic interactions of the wheat stem sawfly with wild oat and Montana dryland spring wheat. [PhD Thesis]. Bozeman, MT (USA): Montana State University.

Slaton MR, Raymond Hunt Jr. E, Smith WK. 2001. Estimating near-infrared leaf reflectance from leaf structural characteristics. American Journal of Botany. 88(2):278–284. doi: 10.2307/2657019.

Solgi S, Ahmadi SH, Seidel SJ. 2023. Remote sensing of canopy water status of the irrigated winter wheat fields and the paired anomaly analyses on the spectral vegetation indices and grain yields. Agricultural Water Management. 280:108226. doi: 10.1016/j.agwat.2023.108226.

Song X-P, Huang W, Hansen MC, Potapov P. 2021. An evaluation of Landsat, Sentinel-2, Sentinel-1 and MODIS data for crop type mapping. Science of Remote Sensing. 3:100018. doi: 10.1016/j.srs.2021.100018.

Stein A, Bastiaanssen ,W. G. M., De Bruin, S., Cracknell ,A. P., Curran, P. J., Fabbri, A. G., Gorte, B. G. H., Van Groenigen, J. W., Van Der Meer, F. D., and Saldana, A. 1998. Integrating spatial statistics and remote sensing. International Journal of Remote Sensing. 19(9):1793–1814. doi: 10.1080/014311698215252.

Strand J, Moya O, Peterson R, Sterling T, Weaver D. 2025. Sensory and behavioral responses of braconid parasitoids to changes in volatile emissions induced by wheat stem sawfly (Hymenoptera: Cephidae) larval feeding in winter wheat and smooth brome. Journal of Insect Science. 25. doi: 10.1093/jisesa/ieaf016.

Subedi M, Cárcamo HA, Knodel JJ, Weaver DK, Cuthbert RD, Pozniak CJ, Nilsen KT, Beres BL. 2021. Stability analysis of stem solidness, grain yield, and grain protein concentration in spring wheat. Canadian Journal of Plant Science. 101(4):456–475. doi: 10.1139/cjps-2020-0089.

Thomas S, Kuska MT, Bohnenkamp D, Brugger A, Alisaac E, Wahabzada M, Behmann J, Mahlein AK. 2018. Benefits of hyperspectral imaging for plant disease detection and plant protection: a technical perspective. Journal of Plant Diseases and Protection. 125(1):5–20. doi: 10.1007/s41348-017-0124-6.

Tucker CJ. 1979. Red and photographic infrared linear combinations for monitoring vegetation. Remote Sensing of Environment. 8(2): 127-150. doi.org/10.1016/0034-4257(79)90013-0

Tucker CJ, Elgin JH, McMurtrey JE. 1980. Relationship of crop radiance to alfalfa agronomic values. International Journal of Remote Sensing. 1(1). doi: 10.1080/01431168008948211.

Wanner K, Tharp C. 2015. Thimet 20-G® for wheat stem sawfly management. Montana State University, Extension, Pesticide News. Available at: https://pesticides.montana.edu/news/msupestnews/20150506_PN_Thimet.html.

Wallace, L. E. and McNeal, F. H. (1966). Stem sawflies of economic importance in grain crops in the United States. Washington, DC: Agricultural Research Service, United States Department of Agriculture.

Weaver DK. 2023. Wheat stem sawfly (Cephus cinctus Norton). Chapter 5, in Eigenbrode, SD, Rashed A, (eds.) Advances in Understanding Insect Pests Affecting Wheat and Other Cereals, pp. 93–134. doi: 10.19103/as.2022.0114.13.

Weaver DK, Buteler M, Hofland ML, Runyon JB, Nansen C, Talbert LE, Lamb P, Carlson GR. 2009. Cultivar preferences of ovipositing wheat stem sawflies as influenced by the amount of volatile attractant. Journal of Economic Entomology. 102(3): 1009-1017. doi:10.1603/029.102.0320.

Weiss MJ, Morrill WL. 1992. Wheat stem sawfly (Hymenoptera: Cephidae) revisited. American Entomologist. 38(4):241–245. doi: 10.1093/ae/38.4.241.

Wen W, Timmermans J, Chen Q, van Bodegom PM. 2023. Evaluating crop-specific responses to salinity and drought stress from remote sensing. International Journal of Applied Earth Observation and Geoinformation. 122:103438. doi: 10.1016/j.jag.2023.103438.

Wiersma DJ, Landgrebe DA. 1980. Analytical design of multispectral Sensors. IEEE Transactions on Geoscience and Remote Sensing. GE-18(2):180–189. doi: 10.1109/TGRS.1980.350271.

Woodcock CE, Strahler AH, Jupp DLB. 1988. The use of variograms in remote sensing: real digital images. Remote Sensing of Environment. 25(3):349–379. doi: 10.1016/0034-4257(88)90109-5.

Yates HW. 1970. A general discussion of remote sensing of the atmosphere. Applied Optics, AO. 9(9):1971–1975. doi: 10.1364/AO.9.001971.

CHAPTER TWO

MULTITEMPORAL HYPERSPECTRAL

CHARACTERIZATION OF WHEAT INFESTED BY WHEAT

STEM SAWFLY, *Cephus cinctus* NORTON

Contribution of Authors and Co-Authors

Manuscript in Chapter 2

Author: Lochlin S. Ermatinger
Contributions: Conducted experiments; analyzed data; drafted initial manuscript; revised, read, and approved the final manuscript.

Co-Author: Scott L. Powell
Contributions: Participated in the review of the ongoing project; revised, read, and approved the final manuscript.

Co-Author: Robert K.D. Peterson
Contributions: Participated in the review of the ongoing project; revised, read, and approved the final manuscript.

Co-Author: David K. Weaver
Contributions: Conceived the project; Participated in the review of the ongoing project; revised, read, and approved the final manuscript.

Manuscript Information

Lochlin S. Ermatinger, Scott L. Powell, Robert K.D. Peterson, David K. Weaver

Status of Manuscript:
☐ Prepared for submission to a peer-reviewed journal
☐ Officially submitted to a peer-reviewed journal
☐ Accepted by a peer-reviewed journal
☒ Published in a peer-reviewed journal

Abstract

Wheat (*Triticum aestivum* L.) production in the Northern Great Plains of North America has been challenged by wheat stem sawfly (WSS), *Cephus cinctus* Norton, for a century. Damaging WSS populations have increased, highlighting the need for reliable surveys. Remote sensing (RS) can be used to correlate reflectance measurements with nuanced phenomena like cryptic insect infestations within plants, yet little has been done with WSS. To evaluate interactions between WSS-infested wheat and spectral reflectance, we grew wheat plants in a controlled environment, experimentally infested them with WSS and recorded weekly hyperspectral measurements (350–2500 nm) of the canopies from prior to the introduction of WSS to full senescence. To assess the relationships between WSS infestation and wheat reflectance, we employed sparse multiway partial least squares regression (N-PLS), which models multidimensional covariance structures inherent in multitemporal hyperspectral datasets. Multitemporal hyperspectral measurements of wheat canopies modeled with sparse N-PLS accurately estimated the proportion of WSS-infested stems ($R^2 = 0.683$, RMSE = 13.5%). The shortwave-infrared (1289–1380 nm) and near-infrared (942–979 nm) spectral regions were the most important in estimating infestation, likely due to internal feeding that decreases plant-water content. Measurements from all time points were important, suggesting aerial RS of WSS in the field should incorporate the visible through shortwave spectra collected from the beginning of WSS emergence at least weekly until the crop reaches senescence.

Introduction

The wheat stem sawfly (WSS) (*Cephus cinctus* Norton) is one of the most important insect pests of wheat (*Triticum aestivum* L.) production in the Northern Great Plains of North America (Criddle 1922; Beres et al. 2011). For over a century, crop losses have occurred due to a lack of effective control strategies and the difficulty in monitoring infestation levels of this cryptic insect pest (Knodel et al. 2010). More than 95% of the WSS's life cycle takes place within a host stem. Evidence of WSS infestation is often not apparent until the end of the growing season when stem lodging occurs; these losses can be very problematic in areas with large WSS infestations. Because of this cryptic feeding habit, the means of detection have largely been limited to careful observation during the period of adult emergence or manual dissection of stems to determine infestation status after the period of adult flight, at any point during the growing season. The effort required to comprehensively inventory WSS occurrence in fields is compounded by large expanses of dryland wheat across the Northern Great Plains of North America. The longstanding prominence of this pest and recent increases in damaging populations of WSS in Colorado, Nebraska, and Kansas (McCullough et al. 2020; Cockrell et al. 2021) underscore the need for a rapid and efficient means of identifying and monitoring infestation levels. Linking the spectral reflectance of standing wheat crops to the degree of WSS infestation may present an objective tool for estimating the severity of WSS on the landscape and prescribing subsequent management or intervention.

WSS is an obligate internally feeding stem miner that requires its host to reach maturity to cause visually apparent damage; thus, its effects on host physiology while feeding are relatively subtle compared to many other forms of insect injury. WSS mainly feeds on the

parenchymous tissue in the innermost stem's lining (Holmes 1954), which is initially a relatively benign form of damage when the larvae are neonates. When larvae exhaust the resources in a given internode, they burrow through stem nodes, which can result in damage to the vascular tissue of the host (Morrill et al. 1992; Macedo et al. 2006; Delaney et al. 2010). This damage to the xylem and phloem disrupts the transport of carbohydrates leading to visible dark bands beneath burrowed nodes (Morrill et al. 1992) and eventually leads to 20 to 30% yield reductions (Seamans et al. 1944; Delaney et al. 2010). Stem mining by WSS also reduces the photosynthetic capacity of the flag leaves of the host (Macedo et al. 2007; Delaney et al. 2010). However, the presence of sub-nodal dark spots or decreased gas ex-change parameters is often not detectable until at least the grain-filling stage (Morrill et al. 1992; Macedo et al. 2007; Delaney et al. 2010). Injury caused by WSS also increases photochemical efficiency in the head glumes of wheat (Macedo et al. 2006). These findings suggest that the physiological changes in wheat caused by the internal feeding of WSS may be expressed asymmetrically across plant tissues and are more likely to be detected at later growth stages.

Many studies have demonstrated the utility of remotely sensed data in quantifying the physiological status of wheat, such as nitrogen deficiency (Rodriguez et al. 2006; Tilling et al. 2007), Hessian fly infestation (Bhattarai et al. 2019), wheat streak mosaic virus (Mirik et al. 2011), Fusarium head blight (Bauriegel et al. 2011; Ma et al. 2021), and senescence (Collins 1978), among other applications. However, comparatively little work has been conducted to determine the efficacy of remote sensing (RS) for the detection of wheat stem mining pests such as WSS, although RS has been used to assess WSS habitat suitability (Lestina et al. 2016). Nansen et al. (2009) conducted the only study to date on remote detection of WSS. They

experimentally infested wheat with WSS and used a hyperspectral camera with a spectral range of 402–838 nm to take images of the wheat leaves three weeks after infestation. They found that differences in the reflectance of infested and uninfested leaves were detectable in the red-edge and near-infrared (NIR) portions of the electromagnetic spectrum. However, the reflectance of individual leaves is not directly comparable to the reflectance of the entire plant or the crop canopy, as radiation measured by the sensor is influenced by the incidence angle of light, head and leaf orientation, and light transmission through the canopy, which has been found to vary up to 15% when comparing leaves to canopies (Knipling 1970). Furthermore, the camera used by Nansen et al. (2009) was not able to measure light in the shortwave-infrared (SWIR) portion of the electromagnetic spectrum, which is between 1300 and 2500 nm and has been found to be sensitive to changes in leaf-water content (Gates et al. 1965; Tucker 1980; Seelig et al. 2008). Therefore, we de-vised an experiment to collect multitemporal hyperspectral measurements of the visible—shortwave infrared (VSWIR, 350–2500 nm) from wheat canopies subjected to WSS infestation to more closely simulate the nature of data captured by aerial or satellite RS platforms.

Hyperspectral data offer identification of subtle reflectance differences due to their broad spectral range and fine spectral resolution, resulting in hundreds to thousands of contiguous bands (Thomas et al. 2018). The large number of very narrow bands leads to redundancy in the data, which is further compounded when hyperspectral measurements are repeated over multiple points in time. This redundancy and the high degree of complexity can lead to a decay in modeling performance, referred to as the Hughes phenomenon (Hughes 1986), which is often dealt with by employing dimensionality reductions, such as feature selection (Georganos et al.

2018), feature extraction (Romero et al. 2016), and multivariate modeling like partial least squares (PLS) (Schweiger et al. 2018). However, the aforementioned methods are not designed to account for repeated measures data. Hyperspectral reflectance profiles collected from the same sample over multiple points in time are repeated measures, which are more appropriately modeled with high-order arrays (Yu et al. 2021), otherwise known as tensors. Recent studies using repeated measures of multispectral and hyperspectral data have found satisfactory modeling performance using multiway partial least squares (N-PLS) (Yu et al. 2021; Lopez-Fornieles et al. 2022). N-PLS accounts for the repeated measures of these data by employing a trilinear method of decomposition (Wold et al. 1987; Bro 1996) along the multidimensional tensor structure to account for the correlation among samples, wavelengths, and points in time. This method allows for a simplified model of the data using latent variables and beta coefficients that preserve the interpretation of the spectral and temporal dimensions.

The objective of our study is to evaluate the efficacy of repeated measures hyper-spectral reflectance data for estimating the level of WSS infestation in a group of wheat plants exposed to female adults. We designed the experiment to emulate the manner in which RS of WSS across a wheat field would be carried out by assessing WSS infestation on a continuous scale within a group of adjacent wheat plants and by collecting reflectance measurements from above the canopy with a nadir orientation. We measured the canopy reflectance weekly starting just prior to introducing the WSS treatment and continuing until the wheat reached full senesce. This design captures the entirety of the growing season relevant to WSS interactions with wheat at an interval and duration that are similar to the temporal resolution of RS platforms like drones and satellites. The goal of this study is to identify spectral regions and time points that are important for RS of

WSS. This knowledge may prove useful for estimating WSS infestations across larger areas based on RS platforms that measure reflectance in spectral regions found to be important in this study.

Materials and Methods

Plant Cultivation

The spring wheat cultivar Reeder was grown in 25.4 cm diameter pots with 10 seeds planted in the center. Reeder was chosen because it is a hollow-stem cultivar that is susceptible to WSS injury (Varella et al. 2019) and remains the second most planted cultivar among Montana spring wheat producers (NASS MRFO 2023) The plants were seeded in a 50:50 mix of Soil Mix (loam, washed concrete sand, and Canadian Sphagnum peat moss) and Sunshine Mix #1 (Canadian Sphagnum peat moss, perlite, vermiculite, starter nutrient charge, wetting agent, and dolomitic lime), which has a pH of 7.3. Plants were watered daily and fertilized twice weekly (Tuesdays and Thursdays) once they reached the three-leaf stage (Zadoks 13). For fertilizer, we used Jack's Professional Nutrients (J.R. Peters, Allentown, PA, USA) of 20N:20P:20K applied at a rate of 100 ppm (200 ppm per week). The greenhouse maintained a temperature of 21 ± 3 °C and provided the plants with ambient sunlight in addition to a 15L:9D supplemental lighting period (GE Multivapor lamps model MVR1000/C/U, GE Lighting, General Electric Co., Cleveland, OH, USA). Fertilizer and watering were tapered off after reaching Zadoks 70 and ended at around Zadoks 80. In each pot, the seeds were placed together in the center to minimize the variation in canopy shape among samples.

This experiment consisted of five planting groups of 30 pots staggered in one-week intervals. Once a majority of the tillers in a planting group reached Zadoks 32, the 20 most

uniform pots were selected and enclosed by mesh nets to begin the experimental treatment. For

each planting group, 20 newly emerged female and five male adult WSS were introduced to each

of the randomly assigned treatment pots (n = 15). The control pots (n = 5) were also fitted with

mesh nets, but no WSS were introduced. After three days, the nets and WSS adults were

removed. This unbalanced sample design favoring the treatment group was selected after

attempting this same experiment during 2021 and 2022, which resulted in limited and variable

infestation levels. These earlier trials also informed the arrangement of the seeds, where linear-

or row-style orientations were observed to increase the between-sample spectral variability when

compared to placing all seeds around the center. At the conclusion of the experiment, the stems

were dissected individually to quantify the WSS-infested stems as a proportion of the total

number of stems within each pot (Figure A1). Stems were categorized in one of the following

four categories: uninfested, dead neonate, WSS bur-rowed through two or more nodes (feeding

injury in three or more internodes), or WSS cut (Figure A2). WSS cut is the most damaging

category as larva will burrow through all, or almost all nodes, encountering the xylem and

phloem each time, before descending to the base of the stem where they ultimately severe the

stem in the process of creating a hibernaculum in the lowest chamber. Because WSS mainly

confers damage to the host by burrowing through internodes with stem cutting afterwards, we

only considered stems in the categories of WSS cut or WSS burrowed through two or more

nodes for our response variable, the proportion of adequately infested stems, p, defined in the

following equation (Equation 1).

Spectral Reflectance Sampling

Nadir reflectance measurements of the canopy of each pot in a replicate were collected weekly starting the day the WSS were introduced and continuing until the plants reached full senescence, evidenced by the dried wheat heads angling downwards. In total, each pot was sampled nine times, with the last sample taking place 56 days after the introduction of WSS (DAI). The last planting group matured at a much faster rate than the other groups resulting in only seven weeks of spectral sampling. This entire group was removed from the analysis because of its advanced rate of senescence. Two other sample pots died before the completion of the experiment and were also removed, leaving a final sample size of n = 78 pots (control = 19, treatment = 59). Reflectance samples were recorded with an ASD FieldSpec Pro spectrometer (Malvern Panalytical, Boulder, CO, USA) fitted to a sampling environment supplied with artificial lights (work lights with tungsten halogen bulbs 110–130 V, 300 W, color temperature = 2800 K, Qingdao, China,) and opaque walls with minimal reflectance to eliminate outside light (Figure 1). Halogen lights were chosen as they emit light across the majority of the spectrum sampled by the ASD FieldSpec Pro (350–2500 nm) and have been found to be a suitable supplementary light source in laboratory settings (Lee et al. 2023). The ASD FieldSpec Pro collects a reflectance reading centered at each wavelength between 350 and 2500 nm, yielding 2151 measurements across the spectrum. The trials in 2021 and 2022 demonstrated optimal spectral sampling was achieved by fixing the sensor sufficiently far above the top of a canopy to achieve a sampling area of 30 cm.

This specific distance was solved for using the equation defined by Danner et al. (2015), which relates the ASD's field of view, α, and the distance between sensor and target, d, to the observed sampling area, A (Equation 2). At the beginning of each sampling event the mean

height of the planting group's canopy was measured, and the telescoping top of the sampling environment was adjusted accordingly. Next, we turned on the halogen lights and waited 10 min for them to warm up to allow for a stabilized emission spectrum as determined by preliminary empirical tests. A 30.5 × 30.5 cm Spectralon® white reference standard (Labsphere Inc., North Sutton, NH, USA) was placed in the sampling environment to calibrate the sensor before collecting the spectral samples. To collect the hyperspectral reflectance profiles, each pot was placed in the sampling environment, and the floor was secured around the base of the stems to remove the effect of soil on the spectral measurement. The mean reflectance of each wavelength was then recorded over a 10 s period.

Data Preprocessing

Spectral data were input into R (R Core Team, 2023) and converted from digital numbers to reflectances using the white reference and dark current measurements from each sampling event with the package asdreader (version 0.1.3) (Roudier et al. 2017). To account for measurement drift caused by internal heating over the course of sampling, the prospectr package (version 0.2.7) was used to apply a splice correction to each reflectance spectrum (Stevens, 2024). This process normalizes the reflectance measurements from the VNIR and SWIRII diodes of the ASD FieldSpec Pro to its central SWIRI diode (Hatchell 1999; Danner et al. 2015). The reflectance data were then grouped by their values of DAI, centered and scaled, and stored in a three-way array, as outlined by Bro (1996) and Wold et al. (1987).

Studies of hyperspectral data often discard regions of the spectrum because of noise or lack of emitted radiation, yet few describe an objective method to identify noisy spectra. We employed the inter-band redundancy analysis (IBRA) to identify and remove noisy regions of the

spectrum (Morales et al. 2021). The IBRA is a dimensionality reduction technique that calculates the variable inflation factor (VIF) between all pairs of bands to define the degree of collinearity between a band and its spectral neighbors (Morales et al. 2021). A Python package of the algorithm and accompanying details a can be found at https://github.com/NISL-MSU/HSI-BandSelection (accessed on 3 March 2024). The result of this algorithm is the identification of salient bands based on how many bands left or right are needed to arrive at a band that holds sufficiently different information. This method works well in highlighting noisy spectral regions that are due to a lack of emitted radiation from a supplemental light source. Inconsistent and low emission in a given region creates unstable reflectance readings across adjacent narrow bands that are not filtered out by the algorithm but rather represented as salient information de-noted by a lesser VIF value (Figure 2). To identify noisy spectra, we applied this algorithm to samples from the control group collected 14 days after the start of the experiment to ensure that canopies were filled in. Because the tungsten–halogen bulbs we used do not emit much radiation in the ultraviolet spectrum or in the longer shortwave infrared (Thoms and Girwidz 2015), we do not expect these regions to provide stable reflectance. Based on this analysis, we only considered bands greater than 520 nm but less than 1870 nm as suitable (Figure 2).

Sparse Multiway Partial Least Squares Regression
<u>Modeling</u>

To account for the binomial nature of our response variable, y, and the proportion of adequately infested stems, p, we transformed the data with a logit link function. Because these data contained control samples with no infestation, a small displacement factor was added to every value to ensure the transformation of zeros would not result in a value of negative infinity (Equation 3).

The data were then sorted in descending order based on these logit values, and every seventh value was placed into the validation group, while the remaining 85% were used to calibrate the model. The data were parsed out in this stratified manner because most samples had low infestation resulting in a non-normal distribution (Figure A3).

The package sNPLS (version 1.0.27) (Hervas 2022) was used in R (version 3.0.0) to fit the sparse N-PLS models. In this context, sparsity implies that insignificant spectral–temporal features are given a beta coefficient of 0, effectively dropping them from the model. Features retained by the model are fitted with a non-zero beta coefficient, where the magnitude is equivalent to the feature's importance in explaining the variance in the proportion of adequately WSS-infested stems. A positive beta coefficient suggests increasing reflectance of the spectral–temporal feature is associated with an increase in the proportion of adequately WSS-infested stems. A negative beta coefficient indicates that decreased reflectance of the spectral–temporal feature is correlated with an increase in the proportion of infestation. Hervas et al. (2018) implemented sparsity in the N-PLS algorithm using the least absolute shrinkage and selection operator (LASSO) (Tibshirani 1996). Evaluation of root mean square error (RMSE) in the calibration set and the cross- validation set was used to select the optimal number of latent variables in the N-PLS model (Goodarzi and Freitas 2009; Lopez-Fornieles et al. 2022). After selecting the final model, the logit values were back transformed to proportion of adequately infested stems per pot for interpretability. The methods used for data collection, preprocessing, and model selection are organized in Figure 3.

<u>Results</u>

The spectral reflectance of the wheat canopies over time is characterized by a waveform of absorption and reflectance features throughout the VSWIR that simplifies toward the end of the experiment (Figure 4). The pigments of young and vigorous plants utilize blue, green, but mostly red radiation for photosynthesis leading to low reflectance in the visible (VIS, 580–680 nm) (Knipling 1970). In the early stages of the experiment the wheat canopies display elevated reflectance in the NIR (750–1250 nm), indicative of adequate nitrogen concentration (Rodriguez et al. 2006) and healthy mesophyll tissue (Knipling 1970). Low reflectance in the SWIR (>1300 nm) is owed to the water content of the wheat (Tilling et al. 2007). As the wheat and WSS larvae mature, the absorption features of VIS and SWIR dramatically increase in reflectance due to the plants undergoing senescence. During this process, the wheat plants redistribute nutrients to further develop the seed head (Bidinger et al. 1977), leading to a degradation of the photosystems (Knipling 1970) and a decrease in plant water content (Hunt and Rock 1989). Concurrent with plant senescence, the undulation across the NIR region ap-pears to diminish.

The sparse N-PLS model that yielded the smallest RMSE for the validation dataset contained 13 latent variables (Figure 5). This model explained 58.3% of the variation in the calibration dataset and 68.3% of the variation in the validation dataset, as indicated by the coefficient of determination (R^2) (Figure 6). The RMSE of the validation set implies the modeled estimate for a given pot, is on average 13.5 percentage points away from the actual value of proportion of adequately WSS-infested stems. Agreement between the relatively small values of the standard error (SE) and bias suggests no issues with under or overfitting.

After eliminating noisy spectra using the IBRA, 1351 wavelengths were found suitable for modeling, and with nine repeated measures of each spectrum, this represents 12,159 covariates. The final sparse N-PLS model selected 400 spectral–temporal features, amounting to only 3.3% of the input data (Figure 7). Of these features, there were 87 unique wavelengths with every time point retained. The wavelengths selected were not distributed randomly across the spectrum but rather grouped in spectrally adjacent clusters. The clusters in the VIS and near-infrared (NIR) regions at around 580 nm and 940 nm, respectively, were selected most consistently over time. Wavelengths selected from the SWIR region also exhibited spectral clustering but were more diffuse from the clustering pattern of the VIS and NIR regions and were selected less consistently over time. The values of the beta coefficients alternated from positive or negative over time but remained consistent within spectral clusters. The SWIR clusters centered on 1320 nm and 1400 nm are where the signs of the neighboring beta coefficients appear uncorrelated within a given time point.

The radiation in the NIR and SWIR regions of the spectrum was most heavily weighted in the model (Figure 8 & Table 1), as indicated by the magnitudes of the beta coefficients. Notably, 18 of the 20 most important spectral–temporal features were wavelengths greater than 1250 nm from the SWIR region. Importance of features is relative to the magnitude of their beta coefficient as LASSO removed insignificant features (Tibshirani 1996) and the reflectance values are standardized across the spectral and temporal dimensions (Lopez-Fornieles et al. 2022). The feature with the greatest weight was 1339 nm from 56 DAI with a beta coefficient of 1.72, almost four times larger than second largest beta coefficient (−0.46 1308 nm given 21

DAI). Most of these heavily weighted features were spectral measurements collected in the first four weeks of the experiment.

Discussion

Our results indicate that multitemporal hyperspectral data fitted to a sparse N-PLS model can be used to estimate the level of adequate WSS infestation within wheat canopies, as suggested by the R2 of 0.68 with an RMSE of 13.5%. Imposing sparsity in the N-PLS algorithm reduced the number of spectral–temporal features by 96.7%, highlighting the redundancy inherent in multitemporal hyperspectral data (Zhang et al. 2019). The model that explained the greatest amount of variation in the validation dataset required 13 latent variables. Wavelengths retained by the final model belonged to discrete clusters throughout the VSWIR, yet the greatest weight was applied to wavelengths in the NIR and SWIR. All time points studied were found to be important in the model, illustrating the need for multitemporal measurements to detect the subtle spectral changes attributed to WSS infestation.

The spectral clusters that were found to be important were the VIS around green light (575 nm), NIR around 940 nm, and SWIR around 1300 nm. Spectral reflectance characteristics of vegetation in these regions is dictated by pigmentation and absorption for photosynthesis (Woolley 1971), integrity of mesophyll and cellular structure (Gates et al. 1965), and absorption related to water content (Hunt and Rock 1989), respectively.

The spectral–temporal feature with the beta coefficient of the greatest magnitude was 1309 nm at 56 DAI. The large positive slope of this coefficient indicates increasing reflectance of that spectral temporal feature is correlated with an increasing proportion of adequate WSS infestation. Previous studies have indicated that water-stressed plants illicit greater spectral

reflectance at approximately 1300 nm compared to un-stressed plants (Hunt and Rock 1989; Seelig et al. 2008). Macedo et al. (2007) found the photosynthetic capacity of wheat infested by WSS was impacted to a similar degree as it was by water deficit. This suggests that wheat with a greater degree of adequate WSS infestation likely has less water content at 56 DAI, leading to greater reflectance at 1309 nm compared to wheat with a lesser or no degree of adequate WSS infestation. Morrill et al. (1992) posited internodal travel by WSS may lead to damage of the xylem and phloem, in turn disrupting the transport of water and nutrients, which is corroborated by the increased reflectance at 1309 nm at 56 DAI. Overall, this spectral region contained the features given the greatest weight in the model highlighting the utility of the SWIR region in identifying WSS infestation in wheat.

The model beta coefficients within a spectral region exhibited an alternating pattern of positive and negative correlations between reflectance and proportion of adequately WSS-infested stems over time. This may suggest that the relationship between proportion of adequately WSS-infested stems and reflectance over time does not man-fest in a linear relationship. This pattern is similar to the inconsistent effects of WSS infestation on vegetation indices over time that Nansen et al. (2009) observed. In this same vein, Macedo et al. (2005 & 2007) studied the effects of WSS infestation on the photochemical efficiency of wheat and found its impact on photosynthesis was dependent on environment (growth chamber, greenhouse, and field) and growth stage. In this study, wavelengths in the green region of light (500–600 nm) were important, which have a known link to photosynthesis (Liu and van Iersel 2021). The alternating correlations between reflectance of a given spectra over time and proportion of adequate WSS infestation is likely a function of the complex relationship drawn among the 13

latent variables required for this model. To understand the exact nature of WSS infestation and wheat reflectance as a consequence of the variation in physiology, studies with destructive vegetative tissue sampling are required. Nevertheless, the complexity pre-sent in the model adds to the growing body of evidence that WSS infestation impacts wheat physiology in a relatively subtle manner.

Radiation in the NIR (about 940 nm), especially during the beginning of the experiment, was important in estimating proportion of adequate WSS infestation. This region of light has a known utility for assessing plant condition, as seen in vegetation indices such as the normalized difference vegetation index (Tucker 1979), normalized difference nitrogen index (Serrano et al. 2001), and the normalized difference water index (Gao 1996). It has also been observed that plant conditions, such as height and stem diameter, play important roles in female WSS host selection (Buteler and Weaver 2012). While we only selected the pots with the most uniform growing wheat and randomly assigned the treatment, it is possible that subtle differences in plant allometry or vigor impacted the success of WSS oviposition. This is consistent with the model weight applied to the early reflectance of the NIR and SWIR. This is likely true of other important spectral regions in the beginning of the experiment, whereas the reflectance at the end of the host life cycle is likely affected by WSS feeding impacts on host plant physiology. The prevalence of spectral features from early time points in this non-choice experiment indicate that RS of WSS infestation in wheat benefits from accounting for early plant condition. Furthermore, field conditions contrast this experiment in that WSS populations are not controlled and, there-fore, may be drawn to locations of the field based on these same principles.

Nansen et al. (2009) found evidence to suggest the spectral reflectance within the range of 402–838 nm of wheat leaves can be altered by WSS infestation up to 21 DAI, especially in the red-edge and NIR regions. Our results differ slightly in that the spectral region given the most importance was the SWIR, and all time points up to 56 DAI were important in estimating proportion of adequate WSS infestation. However, it is important to note that there are significant differences among these study designs: (1) we sampled canopy reflectance with a greater spectral range 520–1870 nm from before WSS introduction to full senescence of the host plant; (2) we employed a statis-tical method to incorporate the repeated measures of the data rather than treat measurements as independent; (3) we used LASSO to select important spectral temporal features as opposed to visual determination of wavelengths of interest; and (4) we considered the proportion of adequately WSS-infested stems in place of a binary out-come of infested or not. Both studies illustrate the need for multitemporal measurements and demonstrate the NIR region is important in discerning WSS infestation status in leaf and canopy reflectance of wheat. Our findings are consistent with previous studies of physiology of wheat infested by WSS in that impacts are often relatively nuanced (Macedo et al. 2005; Macedo et al. 2007; Nansen et al. 2009).

Our results indicate that radiation across the VSWIR, but especially in the SWIR region, is important for assessing the degree of adequate WSS infestation from multitemporal hyperspectral measurements of wheat canopies. It also seems that accurate and precise estimates of this infestation are best achieved when spectral measurements are repeated across the life cycles of both WSS and its host. This suggests that RS of WSS infestation at the field scale is best suited to platforms that collect multiple bands throughout the VSWIR. The well-known

satellite missions of Landsat and Sentinel-2 provide optical imagery throughout the VSWIR about every 10–16 days (depending on mission and latitude) at a spatial resolution of 10–60 m depending on the band. Many studies have demonstrated the utility of these satellites for estimating wheat yield (Xiao et al. 2024), disease infection (Ma et al. 2018), and nutrient deficiency (Crema et al. 2020), among many other applications of wheat production. Given the large acreages dryland wheat is often planted to within the Northern Great Plains of North America, these two satellite missions may provide adequate spatial, spectral, and temporal requirements for estimating WSS infestation within wheat fields. However, more research should be conducted to understand the spatial distribution and variability of reflectance of WSS-infested host plants over a larger studied area.

Conclusions

To our knowledge, this is the first account of multitemporal hyperspectral non-imaging spectrometry of wheat canopies subjected to WSS infestation. This study is also novel in its use of the IBRA for eliminating noisy spectra and application of sparse N-PLS to multitemporal hyperspectral data. Estimating the proportion of adequately WSS-infested stems relies on measurements across the VSWIR with the greatest emphasis placed on the SWIR. It is also necessary that these measurements are recorded throughout the duration of larval feeding by WSS and concurrent developmental change in the plant host. These findings imply that field RS of WSS infestation will benefit from sensors that capture the aforementioned spectral range with a high temporal density over the course of the growing season.

Acknowledgements

Figures

Fig 2.1. (top left): Interior view of lights; (bottom left) view of the plant from where the sensor is situated; (right) outside view of the entire sampling environment. Sampling environment telescopes vertically to adjust sampling area of the ASD FieldSpec Pro to the canopy of each pot.

Fig 2.2. Mean reflectance at 14 days after infestation: (a) red vertical lines indicate cut-off points of noisy spectra; (b) black lines are the VIF values calculated from the IBRA to the reflectance spectrum of all control samples from 14 days after infestation.

Data Collection

0 DAI

```
┌─────────────────────────┐
│ planting group reaches  │
│       Zadok's 32        │
└─────────────────────────┘
            ↓
┌─────────────────────────┐
│ select 20 most uniform  │
│          pots           │
└─────────────────────────┘
            ↓
┌─────────────────────────┐
│  record first spectral  │
│        reading          │
└─────────────────────────┘
            ↓
┌─────────────────────────┐
│    randomly assign      │
│ experimental treatment  │
│  and introduce WSS adults │
└─────────────────────────┘
```

3 DAI

```
┌─────────────────────────┐
│    remove WSS from      │
│     treatment pots      │
└─────────────────────────┘
```

7 – 56 DAI

```
┌─────────────────────────┐
│ record spectral readings │
│ once weekly until planting │
│  group reaches full     │
│       senescence        │
└─────────────────────────┘
            ↓
┌─────────────────────────┐
│      dissect stems      │
└─────────────────────────┘
```

Data Preprocessing and Model Selection

Reflectance Data

```
┌─────────────────────────┐
│   convert radiance to   │
│      reflectance        │
└─────────────────────────┘
            ↓
┌─────────────────────────┐
│  apply prospectr splice │
│       correction        │
└─────────────────────────┘
            ↓
┌─────────────────────────┐
│   apply IBRA to mean    │
│ reflectance at 14 DAI to │
│ identify noisy regions of │
│      the spectrum       │
└─────────────────────────┘
            ↓
┌─────────────────────────┐
│  remove noisy spectra from │
│  all reflectance profiles │
└─────────────────────────┘
            ↓
┌─────────────────────────┐
│ group reflectance profiles │
│ by DAI, apply centering │
│      and scaling        │
└─────────────────────────┘
```

Stem Splitting Data

```
┌─────────────────────────┐
│ sort data in descending │
│    order by logit of    │
│ proportion of adequately │
│   WSS infested stems    │
└─────────────────────────┘
            ↓
┌─────────────────────────┐
│ withhold every seventh pot │
│ for the validation dataset │
└─────────────────────────┘
```

```
┌─────────────────────────────────────────────┐
│ fit N-PLS model with LASSO operator to allow │
│          for feature selection              │
└─────────────────────────────────────────────┘
            ↓
┌─────────────────────────────────────────────┐
│ select final N-PLS model based on joint     │
│ evaluation of RMSE in calibration and       │
│          validation datasets                │
└─────────────────────────────────────────────┘
```

Fig 2.3. Flowchart illustrating the experimental, data preprocessing, and analysis steps followed to link multitemporal hyperspectral reflectance to the proportion of adequately infested wheat stem sawfly (WSS) stems within a pot.

Fig 2.4. Opposing viewpoints of the multitemporal reflectance of all sampled wheat canopies averaged at each point in time. Early time points are characterized by strong absorption features while these regions increase in reflectance as plant phenology and wheat stem sawfly infestation progresses.

Fig 2.5. RMSE of calibration and validation dataset based on number of latent variables. The vertical black dashed line indicates the sparse N-PLS model with 13 latent variables produced the optimal fit based on RMSE with the calibration and validation datasets.

Fig 2.6. Predicted vs. fitted values amongst the calibration and validation datasets. Spread of points along the 1:1 line suggests no issues with heteroscedasticity. The green dashed line represents the line of best fit, where the gray area is the 95% confidence interval.

Fig 2.7. Distribution of spectral–temporal features retained by the final sparse N-PLS model. Imposing sparsity via LASSO significantly reduced the number of spectral–temporal features from 12,159 to 400. The signs of the beta coefficients indicate the features' relationship with estimating the proportion of adequate WSS infestation.

Fig 2.8. Mean spectral reflectance and beta coefficients given days after infestation. The average spectral reflectance increased over time, especially in the VIS and SWIR absorption features, as phenology advanced and plants senesced. The signs and magnitudes of the beta coefficients represent their correlations and weights in estimating the proportion of adequately WSS-infested stems within a pot.

Fig A2.1. Picture of wheat stem sawfly (WSS) larva feeding inside a wheat stem. The frass is excrement produced during and after feeding by WSS larvae. Photo by Jackson R. Strand.

Fig A2.2. Examples of possible wheat stem sawfly (WSS) infestation categories recorded at the conclusion of the experiment. A first instar larva that lived and died within a single internode is represented on the far left (a), denoted as *dead neonate*. A larva that burrowed through *two or more nodes* but ultimately died before cutting the stem is depicted in (b). The most significant possible form of WSS damage, *WSS cut* (c), occurs when a WSS larva burrows through all, or almost all nodes, and eventually severs the stem near the soil surface, where it creates a hibernaculum to prepare for diapause. An *uninfested* stem that did not experience WSS infestation will be devoid of frass and all nodes remain intact (d).

Fig A2.3. Proportion of adequately wheat stem sawfly infested stems within a pot by planting replicate. Replicates were planted weekly with A being the first and D being the last. Infestation varied by planting replicate and did not display a normal distribution even when considering all replicates together.

Tables

Table 1. 20 most important spectral–temporal features in sparse N-PLS model for estimating the proportion of adequately WSS-infested stems per pot as ranked by magnitude of beta coefficient.

Wavelength	Days after Infestation	Beta Coefficient
1339	56	1.72
1308	21	−0.46
1339	35	0.39
1300	0	−0.37
1380	14	0.28
1308	14	−0.27
1289	56	0.27
1300	21	0.26
1381	14	0.25
1301	0	−0.24
979	0	−0.22
1380	0	0.22
1308	7	−0.21
1308	56	−0.19
1381	0	0.19
978	0	−0.17
1380	56	−0.16
1301	21	0.16
942	0	0.16
1308	42	−0.16

Equations

$$p_i = \frac{WSS\ burrowed\ through\ two\ or\ more\ nodes_i + WSS\ cut_i}{total\ stems_i} \tag{2.1}$$

$$A = \pi \left(tan\ \frac{\alpha}{2} \times d\right)^2 \tag{2.2}$$

$$y_i = logit(p_i) = ln\left(\frac{p_i + 0.01}{1-(p_i + 0.01)}\right) \tag{2.3}$$

References

Bauriegel E, Giebel A, Geyer M, Schmidt U, Herppich WB. 2011. Early detection of fusarium infection in wheat using hyper-spectral imaging. Computers and Electronics in Agriculture. 75(2):304–312. doi: 10.1016/j.compag.2010.12.006.

Beres BL, Dosdall LM, Weaver DK, Cárcamo HA, Spaner DM. 2011. Biology and integrated management of wheat stem sawfly and the need for continuing research. Canadian Entomologist. 143(2):105–125. doi: 10.4039/n10-056.

Bhattarai GP, Schmid RB, McCornack BP. 2019. Remote sensing data to detect hessian fly infestation in commercial wheat fields. Scientific Reports. 9(1). doi: 10.1038/s41598-019-42620-0.

Bidinger F, Musgrave RB, Fischer RA. 1977. Contribution of stored pre-anthesis assimilate to grain yield in wheat and barley. Nature. 270(5636):431–433. doi: 10.1038/270431a0.

Bro R. 1996. Multiway calibration. multilinear PLS. Journal of Chemometrics. 10(1):47–61. doi: 10.1002/(SICI)1099-128X(199601)10:1<47::AID-CEM400>3.0.CO;2-C.

Buteler M, Weaver DK. 2012. Host selection by the wheat stem sawfly in winter wheat and the role of semiochemicals mediating oviposition preference. Entomologia Experimentalis et Applicata. 143(2):138–147. doi: 10.1111/j.1570-7458.2012.01237.x.

Cockrell DM, Randolph T, Peirce E, Peairs FB. 2021. Survey of wheat stem sawfly (Hymenoptera: Cephidae) infesting wheat in Eastern Colorado. Journal of Economic Entomology. 114(2):998–1004. doi: 10.1093/jee/toab015.

Collins W. 1978. Remote sensing of crop type and maturity. Photogrammetric Engineering and Remote Sensing. 44(1):43-55

Crema A, Boschetti M, Nutini F, Cillis D, Casa R. 2020. Influence of soil properties on maize and wheat nitrogen status assessment from Sentinel-2 data. Remote Sensing. 12(14). doi: https://doi.org/10.3390/rs12142175.

Criddle N. 1922. The western-stem sawfly and its control. Dominion of Canada Department of Agriculture.(6):1–8.

Danner M, Locherer M, Hank T, Richter K. 2015. Spectral sampling with the ASD Fieldspec 4 EnMAP Field Guides Technical Report. doi: 10.2312/enmap.2015.008.

Delaney KJ, Weaver DK, Peterson RKD. 2010. Photosynthesis and yield reductions from wheat stem sawfly (Hymenoptera: Cephidae): Interactions with wheat solidness, Water stress, and phosphorus deficiency. Journal of Economic Entomology. 103(2):516–524. doi: 10.1603/EC09229.

Gao B-C. 1996. NDWI a normalized difference water index for remote sensing of vegetation liquid water from Space. Remote Sensing of Environment. 58:257-266. doi: 10.1016/S0034-4257(96)00067-3

Gates DM, Keegan HJ, Schleter JC, Weidner VR. 1965. Spectral properties of plants. 4(1):11-20. doi: 10.1364/AO.4.000011

Georganos S, Grippa T, Vanhuysse S, Lennert M, Shimoni M, Kalogirou S, Wolff E. 2018. Less is more: optimizing classification performance through feature selection in a very-high-resolution remote sensing object-based urban application. GIScience and Remote Sensing. 55(2):221–242. doi: 10.1080/15481603.2017.1408892.

Goodarzi M, Freitas MP. 2009. On the use of PLS and N-PLS in MIA-QSAR: Azole antifungals. Chemometrics and Intelligent Laboratory Systems. 96(1):59–62. doi: 10.1016/j.chemolab.2008.11.007.

Hatchell DC. 1999. ASD technical guide 3rd ed. section 0-1 technical guide. Boulder, CO.: Analytical Spectral Devices.

Holmes ND. 1954. Food relations of the wheat stem Sawfly,. The Canadian Entomologist. 86(4):159–167. doi: 10.4039/Ent86159-4.

Hughes FG. 1986. On the mean accuracy of statistical pattern recognizers. IEEE. IT-14(1):55–63. doi: 10.1109/TIT.1968.1054102

Hunt ER, Rock BN. 1989. Detection of changes in leaf water content using near- and middle-Infrared reflectances. Remote Sensing of Environment. 30(1):43–54. doi: 10.1016/0034-4257(89)90046-1.

Hervas D. sNPLS. 2022. Available online: https://cran.r-project.org/web/packages/sNPLS/index.html

Hervás D, Prats-Montalbán JM, Lahoz A, Ferrer A. Sparse N-way partial least squares with R package sNPLS. Chemometrics and Intelligent Laboratory Systems. 2018, 179, 54–63.

Knipling EB. 1970. Physical and physiological basis for the reflectance of visible and near-infrared radiation from vegetation. Remote sensing of environment. doi:10.1016/S0034-4257(70)80021-9.

Knodel J, Shanower T, Beauzay PB. 2010. Integrated pest management of wheat stem sawfly in North Dakota. North Dakota State University Cooperative Extension Bulletin. E-1479.

Lee H, Cho S, Lim J, Lee A, Kim G, Song D-J, Chun S-W, Kim M-J, Mo C. 2023. Performance comparison of tungsten-halogen light and phosphor-converted nir led in soluble solid content estimation of apple. Sensors. 23(4):1961. doi: 10.3390/s23041961.

Lestina J, Cook M, Kumar S, Morisette J, Ode PJ, Peairs F. 2016. MODIS imagery improves pest risk assessment: A case study of wheat stem sawfly (*Cephus cinctus*, Hymenoptera: Cephidae) in Colorado, USA. Environmental Entomology. 45(6):1343–1351. doi: 10.1093/ee/nvw095.

Liu J, van Iersel MW. 2021. Photosynthetic physiology of blue, green, and red light: light intensity effects and underlying mechanisms. Frontiers in Plant Science. 12. doi: 10.3389/fpls.2021.619987.

Lopez-Fornieles E, Brunel G, Rancon F, Gaci B, Metz M, Devaux N, Taylor J, Tisseyre B, Roger JM. 2022. Potential of multiway pls (N-PLS) regression method to analyse time-series of multispectral images: a case study in agriculture. Remote Sensing. 14(1). doi: 10.3390/rs14010216.

Ma H, Huang W, Dong Y, Liu L, Guo A. 2021. Using uav-based hyperspectral imagery to detect winter wheat fusarium head blight. Remote Sensing. 13(15). doi: 10.3390/rs13153024.

Ma H, Jing Y, Huang W, Shi Y, Dong Y, Zhang J, Liu L. 2018. Integrating early growth information to monitor winter wheat powdery mildew using multi-temporal landsat-8 imagery. Sensors. 18(10) 3290. doi: 10.3390/s18103290.

Macedo TB, Peterson RKD, Weaver DK, Morrill WL. 2005. Wheat stem sawfly, *Cephus cinctus* Norton, impact on wheat primary metabolism: An ecophysiological approach. Environmental Entomology. 34(3): 719-726. doi: 10.1603/0046-225X-34.3.719

Macedo TB, Weaver DK, Peterson RKD. 2006. Characterization of the impact of wheat stem sawfly, *Cephus cinctus* Norton, on pigment composition and photosystem II photochemistry of wheat heads. Environmental Entomology. 35(4): 1115-1120. doi: 10.1603/0046-225X-35.4.1115

Macedo TB, Weaver DK, Peterson RKD. 2007. Photosynthesis in Wheat at the Grain Filling Stage Is Altered by Larval Wheat Stem Sawfly (Hymenoptera: Cephidae) Injury and Reduced Water Availability 1. Journal of Entomological Science. 42(2): 228 – 238. doi: 10.18474/0749-8004-42.2.228

McCullough CT, Hein GL, Bradshaw JD. 2020. Phenology and dispersal of the wheat stem sawfly (Hymenoptera: Cephidae) into winter wheat fields in Nebraska. Journal of Economic Entomology. 113(4):1831–1838. doi: 10.1093/jee/toaa093.

Mirik M, Jones DC, Price JA, Workneh F, Ansley RJ, Rush CM. 2011. Satellite remote sensing of wheat infected by wheat streak mosaic virus. Plant Disease. 95(1):4–12. doi: 10.1094/PDIS-04-10-0256.

Morales G, Sheppard JW, Logan RD, Shaw JA. 2021. Hyperspectral dimensionality reduction based on inter-band redundancy analysis and greedy spectral selection. Remote Sensing. 13(18). doi: 10.3390/rs13183649.

Morrill WL, Gabor JW, Kushnak GD. 1992. Wheat stem sawfly (Hymenoptera: Cephidae): Damage and detection. Journal of Economic Entomology. 85(6): 2413-2417. doi: 10.1093/jee/85.6.2413

Nansen C, Macedo T, Swanson R, Weaver DK. 2009. Use of spatial structure analysis of hyperspectral data cubes for detection of insect-induced stress in wheat plants. International Journal of Remote Sensing. 30(10):2447–2464. doi: 10.1080/01431160802552710.

National Agricultural Statistics Service, Mountain Regional Field Office. 2023. Montana 2023 wheat varieties. United States Department of Agriculture. Available at: https://www.nass.usda.gov/Statistics_by_State/Montana/Publications/Special_Interest_Reports/MT-Wheat-Varieties-2023.pdf.

R Core Team. R Language Definition; R Foundation for Statistical Computing: Vienna, Austria, 2023

Rodriguez D, Fitzgerald G, Belford R, Christensen L. 2006. Detection of nitrogen deficiency in wheat from spectral reflectance indices and basic crop eco-physiological concepts. Australian Journal of Agricultural Research. 57:781–789. doi: 10.1071/AR05361.

Romero A, Gatta C, Camps-Valls G. 2016. Unsupervised deep feature extraction for remote sensing image classification. IEEE Transactions on Geoscience and Remote Sensing. 54(3):1349–1362. doi: 10.1109/TGRS.2015.2478379.

Roudier P, Lalibert' E. Asdreader. 2017. Available online: https://cran.r-project.org/web/packages/asdreader/index.html

Schweiger AK, Cavender-Bares J, Townsend PA, Hobbie SE, Madritch MD, Wang R, Tilman D, Gamon JA. 2018. Plant spectral diversity integrates functional and phylogenetic components of biodiversity and predicts ecosystem function. Nature Ecology and Evolution. 2(6):976–982. doi: 10.1038/s41559-018-0551-1.

Seamans HL, Manson GF, Farstad CW. 1944. The effect of wheat stem sawfly (*Cephus cinctus*) on the heads and grain of infested stems. Annual Report of the Entomological Society of Ontario 75: 10–15.

Seelig HD, Hoehn A, Stodieck LS, Klaus DM, Adams WW, Emery WJ. 2008. The assessment of leaf water content using leaf reflectance ratios in the visible, near-, and short-wave-infrared. International Journal of Remote Sensing. 29(13):3701–3713. doi: 10.1080/01431160701772500.

Serrano L, Peñuelas J, Ustin SL. 2001. Remote sensing of nitrogen and lignin in Mediterranean vegetation from AVIRIS data: Decomposing biochemical from structural signals. Remote Sensing of Environment. 81(2-3): 355-364. 10.1016/S0034-4257(02)00011-1.

Stevens A, Ramirez-Lopez L. Prospectr. 2024. Available online: https://cran.r-project.org/web/packages/prospectr/index.html

Thomas S, Kuska MT, Bohnenkamp D, Brugger A, Alisaac E, Wahabzada M, Behmann J, Mahlein AK. 2018. Benefits of hyperspectral imaging for plant disease detection and plant protection: a technical perspective. Journal of Plant Diseases and Protection. 125(1):5–20. doi: 10.1007/s41348-017-0124-6.

Thoms L-J, Girwidz R. 2015. Training and assessment of experimental competencies from a distance: Optical spectrometry via the Internet. Il Nuovo Cimento C. 38:113. doi: 10.1393/ncc/i2015-15113-3.

Tibshirani R. 1996. Regression shrinkage and selection via the lasso. Journal of the Royal Statistical Society: Series B (Methodological). 58(1): 267-288. doi: 10.1111/j.2517-6161.1996.tb02080.x

Tilling AK, O'Leary GJ, Ferwerda JG, Jones SD, Fitzgerald GJ, Rodriguez D, Belford R. 2007. Remote sensing of nitrogen and water stress in wheat. Field Crops Research. 104(1–3):77–85. doi: 10.1016/j.fcr.2007.03.023.

Tucker CJ. 1979. Red and photographic infrared l,inear combinations for monitoring vegetation. Remote Sensing of Environment. 8(2): 127-150. doi.org/10.1016/0034-4257(79)90013-0

Tucker CJ. 1980. Remote Sensing of Leaf Water Content in the Near Infrared. Remote Sensing Of Environment. 10(1): 23-32. 10.1016/0034-4257(80)90096-6

Varella AC, Weaver DK, Blake NK, Hofland ML, Heo H-Y, Cook JP, Lamb PF, Jordan KW, Akhunov E, Chao S, et al. 2019. Analysis of recombinant inbred line populations derived from wheat landraces to identify new genes for wheat stem sawfly resistance. Theoretical Applied Genetics. 132(8):2195–2207. doi: 10.1007/s00122-019-03347-8.

Wold S, Geladi P, Esbensen K, Ohman J. 1987. Multi-way principal components-and pls-analysis. Journal of Chemometrics. 1(1):41-56. doi: 10.1002/cem.1180010107

Woolley JT. 1971. Reflectance and transmittance of light by leaves. Plant Physiology. 47(5):656-662. doi: 10.1104/pp.47.5.656

Xiao G, Zhang X, Niu Q, Li Xingang, Li Xuecao, Zhong L, Huang J. 2024. Winter wheat yield estimation at the field scale using sentinel-2 data and deep learning. Computers and Electronics in Agriculture. 216. doi: 10.1016/j.compag.2023.108555.

Yu H, Guo L, Kharbach M, Han W. 2021. Multi-way analysis coupled with near-infrared spectroscopy in food industry: Models and applications. Foods. 10(4). doi: 10.3390/foods10040802.

Zhang W, Li X, Zhao L. 2019. Discovering the representative subset with low redundancy for hyperspectral feature selection. Remote Sensing. 11(11). doi: 10.3390/rs11111341.

CHAPTER THREE

MAPPING WHEAT STEM SAWFLY (*Cephus cinctus* NORTON)

INFESTATIONS IN SPRING AND WINTER WHEAT FIELDS

VIA MULTIWAY MODELLING OF MULTITEMPORAL

SENTINEL 2 IMAGES

<u>Contribution of Authors and Co-Authors</u>

Manuscript in Chapter 3

Author: Lochlin S. Ermatinger
Contributions: Conducted experiments; analyzed data; drafted initial manuscript; revised, read, and approved the final manuscript.

Co-Author: Scott L. Powell
Contributions: Participated in the review of the ongoing project; revised, read, and approved the final manuscript.

Co-Author: Robert K.D. Peterson
Contributions: Participated in the review of the ongoing project; revised, read, and approved the final manuscript.

Co-Author: David K. Weaver
Contributions: Conceived the project; Participated in the review of the ongoing project; revised, read, and approved the final manuscript.

Manuscript Information

Lochlin S. Ermatinger, Scott L. Powell, Robert K.D. Peterson, David K. Weaver

Remote Sensing

Status of Manuscript:
☐ Prepared for submission to a peer-reviewed journal
☒ Officially submitted to a peer-reviewed journal
☐ Accepted by a peer-reviewed journal
☐ Published in a peer-reviewed journal

Abstract

The wheat stem sawfly (WSS, *Cephus cinctus* Norton) is a major insect pest of wheat (*Triticum aestivum* L.) in North America. Few management tactics exist, and quantifying their efficacy is confounded by the difficulty in monitoring infestation at the field scale. Accurate estimates of WSS infestation are cost prohibitive as they rely on comprehensive stem dissection surveys due to the concealed life cycle of the pest. Consolidating the available management tactics into an effective strategy requires inexpensive spatially explicit estimates of WSS infestation that are compatible with the large field size dryland wheat is often sown to. Therefore, we investigated using multitemporal satellite passive remote sensing (RS) to estimate various metrics of WSS infestation collected from field surveys at the subfield scale. To do this we dissected 43,155 individual stems collected from 1,158 unique locations across 9 production wheat fields in Montana, USA. Cloud-free Sentinel 2 images were collected from Google Earth Engine for each field from across the growing season and sparse multiway partial least squares regression was used to produce a model for total WSS infestations, adequate WSS infestations, and WSS cut stems, for each sampled field. Upon comparing the performance of these models, we found that on average, the metrics total ($R^2 = 0.57$) and adequate WSS infestations ($R^2 = 0.57$) were more accurately estimated than WSS cut ($R^2 = 0.34$). The results of this study indicate that multitemporal RS can help estimate total and adequate WSS infestations, but more holistic methods of field level sensing should be explored, especially for estimating WSS cutting.

Introduction

The production of wheat (*Triticum aestivum* L.) in North America has been challenged by the wheat stem sawfly (WSS, *Cephus cinctus* Norton) for more than a century (Criddle 1922; Beres et al. 2011; Weaver 2023). The long-standing distinction of WSS as a major pest of wheat is attributed to the difficulty in estimating WSS infestations, a wide variety of hosts, ineffective insecticides, and subsequently a lack of control strategies (Weaver et al. 2024). Quantifying WSS infestation throughout fields is difficult because visual cues of WSS infestation can be subtle and confounded by other factors, thus reliable estimates of infestation depend on extensive stem dissection (Morrill et al. 1992). Therefore, combining stem dissection survey data with remotely sensed imagery may present an efficient method of estimating WSS infestation to better inform management of WSS.

The first reports of WSS in the late 19th century were confined to native grasses (Norton 1872), but in the decades to follow damaging populations were often described in wheat fields (Fletcher 1896; Criddle 1923). By the early 20th century, WSS was considered one of the most important insect pests to the production of small grains in North America (Ainslie 1929). Since then, the geographic range of damaging WSS populations has expanded and currently encompasses the Canadian provinces of Alberta, Saskatchewan, Manitoba, and the U.S. states of Washington, Idaho, Montana, North Dakota, South Dakota, Minnesota, Wyoming, Colorado, Nebraska, and Kansas (Shanower and Waters 2006; Beres et al. 2007; Lesieur et al. 2016; Bekkerman and Weaver 2018; Olfert et al. 2019; McCullough et al. 2020; Cockrell et al. 2021; Weaver 2023). Although WSS infestations are commonly observed in wheat and recently barley (*Hordeum vulgare* L.) (Varella et al. 2018; Achhami et al. 2020a), WSS populations maintain the

ability to reproduce in a wide range of wild grass species found outside of cropped fields (Ainslie 1920; Wallace and McNeal 1966; Peirce et al. 2021; Rand et al. 2024; Strand et al. 2024). The geographic expansion of damaging WSS populations, recent adaptation to barley, and access to hosts outside of managed lands highlight the perpetual threat that WSS poses to the production of small grains in North America.

The lack of control strategies for WSS outbreaks is largely explained by the concealed nature of their lifecycle. The WSS life cycle begins in the spring (mid-May through July) when adults emerge from stubble (Morrill and Kushnak 1999). This period of emergence lasts for about 6-8 weeks, but an individual adult only lives for about five to eight days (Weaver et al. 2024). During this time the adult females use their ovipositors to insert eggs into stem tillers (Criddle 1923). Once a larva hatches inside a stem, it tunnels throughout, feeding mainly on parenchymal tissues until it needs to burrow through a node to access larger reserves (Roemhild 1954). Traveling between internodes forces the larvae to chew through vascular tissue which impairs the transport of nutrients leading to dark spots under nodes (Morrill et al. 1994). The larva continues this feeding behavior within the stem until the end of the growing season when its host begins to senesce and increased light penetration (Villacorta et al. 1971; Holmes 1982) signals the larva to descend towards the soil surface where it cuts the stem and creates a hibernaculum to prepare for diapause (Holmes 1975). In areas where many stems are cut, they can lodge in the presence of strong wind and fall on top of each other to create a domino effect where most of the grain heads fall to the ground (Ainslie 1920). This is the most noticeable symptom of WSS infestation and economic loss as the fallen grain heads are difficult to recover.

There are currently no viable forms of WSS control but there is a diverse suite of management tactics. The long period of adult emergence makes the use of contact insecticides ineffective and there are currently no options for systemic pesticides to act on the larval stage (Weaver 2023; Weaver et al. 2024). Wheat producers experiencing heavy WSS pressure benefit from planting solid-stem cultivars because strong pith expression results in a higher rate of larval mortality compared to hollow-stem varieties. However, in the absence of WSS, hollow-stem varieties often produce higher yields than solid-stem varieties. The use of trap crops like oat (*Avena sativa* L.) which attract WSS to lay eggs but are 100% lethal to the larvae is also a good, but population-dependent option (Criddle 1923; Seamans 1928; Weaver et al. 2004; Beres et al. 2009; Weaver et al. 2024). For long term management, producers are encouraged to cut stubble high and practice conservation tillage to maintain a healthy population of the wasp species, *Bracon cephi* (Gahan) and B. *lissogaster Muesebeck*, which are the most important natural enemies of WSS (Beres et al. 2024). Additionally, the benefits of these parasitoids may be enhanced by catering to their diet and providing plants that produce extrafloral nectar (Reis et al. 2019; Cavallini et al. 2023) and maintaining field margins that contain grass species that are WSS sinks and parasitoid sources (Strand et al. 2024). Using these management tactics for economic benefit requires measuring their effect on the local WSS population and subsequent yield that would have been lost in the absence of their use. This depends on the ability to accurately and precisely monitor WSS over time.

Although a majority of the WSS lifecycle takes place concealed within a stem, there are several ways to sample for WSS depending on the phase of the growing season. During the period of WSS emergence, surveys can be conducted using sweep nets to capture live adults

(Morrill et al. 2001; McCullough et al. 2020). However, these surveys are time intensive and adult WSS do not directly damage the crop. Crop damage due to WSS occurs from larval feeding resulting in reduced head wheat (Delaney et al. 2010) and when grain heads are lodged and not recovered (Ainslie 1929; Sjolie et al. 2024). Following the period of emergence, stems can be dissected to determine the presence of WSS larvae, either by direct observation of eggs, larvae, or their excrement, frass. Right before harvest, estimates of cutting can be made with in-situ observations but are subject to observer variability and stem lodging can also be caused by factors like heavy rains or hail (Dahiya et al. 2018). Stem lodging due to WSS infestation can potentially be underestimated in years that do not have high wind or rain to topple the stems, or if harvest occurs before the full extent of stem cutting unfolds. Currently, the most accurate method for estimating WSS infestation and crop damage at the field scale requires dissecting many stem samples collected throughout the field and from the end of the growing season to observe the full extent of feeding injury, instances of parasitism, and cutting (Cárcamo et al. 2007).

Combining spatially explicit stem dissection surveys with remotely sensed data presents the opportunity to estimate WSS infestation across larger areas. Lestina et al. (2016) found data from Moderate Resolution Imaging Spectroradiometer (MODIS) imagery could be used with ancillary environmental data to predict the presence of WSS at the landscape scale. Proximally sensed data of the visible through shortwave infrared (VSWIR, 350 – 2500 nm) have also demonstrated utility in predicting WSS infestation status in wheat at the leaf and canopy scale (Nansen et al. 2009; Ermatinger et al. 2024). Nansen et al., 2009 and Ermatinger et al., 2024 indicated that WSS infestation can be detected by subtle variation in wheat reflectance

throughout the VSWIR from multiple points in time. Although experiments in the greenhouse have demonstrated the efficacy of remote sensing (RS) for estimating WSS infestation, no prior studies have evaluated using RS to map WSS infestation at the field scale.

Satellite RS platforms like Sentinel 2 and the Landsat missions that use passive sensors measuring ambient energy have a proven history for monitoring crop condition down to the sub-field scale (Haack 1982; Segarra et al. 2020). Their coverage of the VSWIR, high repeat frequency, and fine to moderate spatial resolution, makes them optimal tools for monitoring the large field sizes commonly observed in agricultural systems of dryland small grain. The Sentinel 2 constellation provides a finer temporal and spatial resolution than Landsat, thus it is a good starting point for exploring the capability of RS of WSS.

Studies that use passive RS for detecting insect infestation in wheat such as Hessian fly, *Mayetiola destructor* (Say), greenbugs, *Schizaphis graminum* (Rondani), and Russian wheat aphid, *Diuraphis noxia* (Mordvilko), have found success by exploiting changes in vegetation reflectance that are caused by feeding and subsequent injury (Yang et al. 2009; Bhattarai et al. 2019). WSS however requires its host to reach maturity and consequentially induces subtle changes to host physiology that can potentially be obscured given the right environmental conditions (Macedo et al. 2005; Macedo et al. 2007) or masked by compensatory host responses (Achhami et al. 2020b). Thus, solely observing the reflectance of crops following WSS infestation may not provide the sensitivity required to estimate the level of WSS infestation. Cropped areas with heavy stem lodging because of WSS infestation, can likely be detected with RS methods as it has been demonstrated for hail-induced lodging events (Gobbo et al. 2021). Nevertheless, stem lodging alone may not always manifest from WSS infestation. In the

beginning of the growing season, prior to or concurrent with WSS emergence, spectral variability related to crop condition may, in part, coincide with WSS infestation, as WSS is known as an edge effect pest (Sing 2002; Nansen, et al. 2005a; Nansen et al. 2005b) and females exhibit a preference for the most robust stems available (Buteler and Weaver 2012). Moreover, accurate field estimates of WSS infestation based on passive RS likely require spectral observations from across the growing season.

Estimating the overall extent of stem feeding by WSS larvae for a given field enables producers and researchers to understand how environmental variability, parasitism, choice of variety, and agronomic practices interacted with WSS infestation and severity. Stem dissection surveys from the end of the growing season afford the opportunity to quantify the intricacies of WSS larval feeding, yet it is unknown how to best synthesize stem dissection data for the purpose of estimating WSS infestation with RS. To evaluate this, we collected georegistered wheat residue samples and dissected each stem to quantify WSS infestation across many field years over the latitudinal gradient of Montana to capture the variability presented in climate, wheat cultivar, and WSS infestation pressure. The main objective of this study is to understand how RS of WSS infestation is most accurately predicted using multitemporal satellite imagery. To address this, we quantified the WSS infestation of each sample's location into three metrics: total WSS infestation, adequate WSS infestations, and WSS cut. These metrics were chosen to represent various degrees of WSS feeding severity. We then modeled each metric for each field following the methods of Ermatinger et al. (2024) and compared the coefficients of determination (R^2) across the models to understand which metric is most accurately predicted

using this methodology. This study is intended to benefit future endeavors of producing spatially explicit estimates of WSS infestation within wheat fields.

<p style="text-align:center">Materials and Methods</p>

Site Selection & Ground Reference Data Collection

We selected wheat fields near Three Forks, Moccasin, Carter, and Big Sandy to capture environmental variation experienced in major wheat-producing regions (Figure 1). Both spring and winter wheat fields were selected in areas where producers had knowledge of damaging WSS populations. To quantify WSS infestation throughout a given field we collected samples from discrete locations across each field. Sampling blocks were placed on the field edges adjacent to the nearest neighboring WSS source and non-source fields with transects leading inwards (Figure 2). In larger fields, additional sampling blocks were placed throughout the interior to account for variation in crop condition. The distance between sampling locations along a transect was closest near the field edge and further apart as the transect moved inwards. The high density of sampling locations close to field edges was informed by previous studies (Sing 2002; Nansen, et al. 2005a; Nansen et al. 2005b) that found WSS infestation severity and variation was greatest at the field edge and dissipated towards the interior. This general sampling scheme does not apply to Big Sandy 2020 as it was sampled before defining the aforementioned sampling criteria. In Big Sandy 2020, a small subset of infestation samples (n = 45) was collected before harvest from a small area to avoid trampling a large area of the growing crop. After harvest, a larger set was collected from the opposite side of the field (n = 100). Each wheat sample consisted of all the stems within 30 cm of a row and its corresponding location recorded with a RS2 GNSS receiver (Emlid Reach, Richfield, OH). The GPS data for the sample locations

were post processed using temporally matched continuous operating reference station (CORS) data from the nearest CORS to each site in Emlid Studio (version 1.8). On average, the root mean square error (RMSE) of the corrected locations was less than a meter, well within the spatial resolution of the Sentinel 2 data (10 – 60 m).

The stem samples were then manually dissected to quantify the proportion of WSS infestation at each sample location. Stems were categorized in one of the following four categories: uninfested, dead neonate, WSS burrowed through at least one node, or WSS cut. The most intensive feeding injury is represented by WSS cut as stems in this category have multiple nodes burrowed through and a complete severance at the base of the stem. Quantifying infestation at the sample level in this manner allowed us to represent and model WSS infestation in multiple ways. The most rudimentary of which is total WSS infestations, $p_{total\,WSS}$, represented as the proportion of stems within a sample that contained any evidence of WSS infestation (Equation 1).

We removed dead neonates to model WSS infestation as the proportion of instances where a larval WSS burrowed through at least one node or ultimately cut the stem (WSS cut), $p_{adequate\,WSS}$ (Equation 2).

Finally, we modeled WSS infestation as only the proportion of WSS cut stems within a sample, $p_{WSS\,cut}$ (Equation 3).

To estimate how these metrics of WSS infestation vary within each field, we fit a generalized linear mixed model (glmm) using R (version 3.0.0) and the package 'glmmTMB' (Brooks et al. 2024) for each field, followed by a post-hoc comparison of means using the Tukey HSD method from the package 'emmeans' (Lenth et al. 2024). Because each of the WSS

infestation metrics is measured as a proportion of the total number of stems, which is binomial, we transformed the values with a logit link function. We incorporated a small adjustment factor that was added to observations of 0 and subtracted from values of 1 to avoid undefined logit values (Equation 4). We also incorporated sample ID as a random effect to account for the fact that measurements of each WSS infestation metric were recorded at each location.

Sentinel 2 Imagery Acquisition and Time Standardization

Sentinel 2 surface reflectance scenes from across the growing season (April 1 – first available image after field's harvest date) were retrieved for each field using Google Earth Engine (Gorelick et al. 2017). Because we were studying fields from 2020-2023, we used the harmonized Sentinel 2 surface reflectance repository, as this collection shifts the range of a scene's digital numbers post 25th January 2022 to match those before it (Main-Knorn et al. 2017). We then manually removed scenes that contained clouds and or shadows over the field of interest and clipped the remaining scenes to the field boundary to create a stack of images for each field. To standardize the image acquisition dates of each field and account for differences in locations, years, and crop type, we converted the date to growing degree days (GDD) (see Equation 5 & Supplementary Figure 1).

Where i represents days for spring wheat fields and j represents days for winter wheat fields. The model only considers days with an average temperature Tavg, above Tbase = 0°C (Miller et al. 2001) starting seven days after the planting date (P) of spring wheat and starting on April 1 for winter wheat fields, as we did not have complete records of winter wheat seeding dates. Daily temperature data used for this were collected from PRISM https://prism.oregonstate.edu/ (accessed on 30 August 2024). For each field, the images were grouped by their values of GDD,

and the reflectance was centered and scaled to set each bands mean equal to 0 and standard deviation to 1 then stored in a three-way array (Wold et al. 1987; Bro 1996). Centering and scaling were applied in this manner to preserve variation in reflectance across GDD but avoid bands with inherently greater magnitudes receiving more weight than those with lesser magnitudes in the modeling process (Hastie et al. 2009).

Sampled WSS Infestation & Available Sentinel 2 Imagery

Fields sown to winter wheat represented the majority of those sampled in this study (six winter wheat, three spring wheat, Table 1). The fields received between 117.3 and 297.5 mm of rainfall during the growing season, as estimated from PRISM https://prism.oregonstate.edu/ (accessed on 30 August 2024). In total we collected 1,158 ground reference samples, from which we manually dissected 43,155 wheat stems to measure WSS infestation. The number of Sentinel 2 images suitable for analysis varied due to cloud cover during the satellite revisits and location in relation to the constellation's orbit. For instance, the Moccasin area benefited from a greater number of available images, as the area is resampled by a Sentinel 2 satellite every second or third day, whereas the other fields studied are revisited every fifth day. After removing images containing clouds and or shadows, fields had between 8 and 17 images suitable for further analysis. Although we were not able to collect all sowing dates, records of harvest dates were complete.

Sparse Multiway Partial Least Squares Regression Models

To investigate our research objective of which metric of WSS infestation is most accurately estimated with multitemporal satellite imagery, we produced a model for each field for each of our three response variables: total WSS, adequate WSS, and WSS cut. The Big Sandy

2020 field did not have stem dissection data that accounted for adequate WSS, thus we only produced models of total WSS and WSS cut for that field. Centering and scaling were then applied to the logit values for each metric from each field to amend overdispersion and improve overall model performance.

For each field, the data were then partitioned into a model calibration and validation set based on spatial blocking and WSS infestation level. Spatial blocking was used to account for the spatial dependence of observations (Roberts et al. 2017) and stratifying by infestation level to account for the non-normal distributions of each WSS infestation metric. For each spatial block, the data were sorted in descending order based on the metric of WSS infestation for a given model and every fifth observation was placed into a validation set while the remaining 80% of the data were used to calibrate the model.

R (version 3.0.0) was used to fit sparse N-PLS models for each WSS infestation metric from each field using the package 'sNPLS' (Hervás et al. 2019). The sNPLS function preforms a trilinear decomposition on the three-way array of images and the response vector of the WSS infestation metric to explain the maximum amount of covariance between both elements (Wold et al. 1987; Bro 1996; Hervás et al. 2019). Feature selection is used to identify bands from images that are important while insignificant spectral measurements are dropped to reduce the overall size of the dataset (Tibshirani 1996; Hervás et al. 2019).

The relationship between the selected spectral measurements and the WSS infestation metric is modeled by a set of orthogonal factors referred to as latent variables (Wold et al. 1987). Model selection is performed by conducting a grid search across all possible combinations of sentinel 2

bands, available images, and number of latent variables by evaluating the RMSE between the calibration and validation set (Goodarzi and Freitas 2009) (Supplementary Tables 2-4).

To determine which WSS infestation metric is most accurately estimated using multitemporal RS, we compared the coefficient of determination from the validation datasets across all models. We chose R^2 as the metric to judge model performance as it is a dimensionless value that subtracts the ratio of the residual sum of squares and total sum of squares from one, to represent how well a model fits a given dataset (Equation 6). In this context, R^2 is bound between negative infinity and one, where an R^2 value of one indicates the model perfectly fits the data and zero or less indicates a poor fit. A one-way repeated measures ANOVA, followed by a post-hoc Tukey HSD test, was conducted using the 'lme4' (Bates et al. 2015) and 'emmeans' (Lenth et al. 2024) packages to assess whether R^2 varied by WSS infestation metric, while accounting for the study's repeated measures design. The Big Sandy 2020 field was removed from this analysis, as we did not have information for adequate WSS infestations. Model diagnostics revealed no issues with normality, residuals, or homoscedasticity. The methods presented in this section are summarized in Figure 3.

<div align="center">Results</div>

Surveyed WSS Infestation

Sampled WSS infestation varied across fields with a range of 5.9 – 45.67% total WSS infestation. The mean total WSS infestation across all sampled fields was 24.7% with a mean adequate WSS percentage of 22.3% and a mean WSS cut percentage of 10.3% (Figure 4). On average, total WSS infestation was 2.5 times greater than the percentage of WSS cut; similarly, the percentage of adequate WSS infested stems was 2.2 times greater than WSS cut (excluding

Big Sandy 2020 for not having adequately WSS infested stems). WSS infestation varied spatially throughout fields (Supplementary Figures 2-4) and many samples had little to no infestation which led to high variance and overdispersion in the datasets (Table 2 or Supplementary Table 1). In all fields, total WSS was found to be significantly different than WSS cut as indicated by a post-hoc comparison of means using a Tukey HSD (p-value <.05; Table 2). In four of the eight fields that had measurements of both total and adequate WSS infestations, these metrics were found to be statistically different.

Modeled WSS Infestation

Model performance varied across fields and infestation metrics, as indicated by the R^2 value from the validation dataset of the optimal model for each WSS infestation metric for a given field (Figure 5). The average R^2 was greatest for total WSS (mean = 0.57, standard deviation (SD) = 0.26) and adequate WSS (mean = 0.57, SD = 0.29), while WSS cut was on average, markedly lower (mean = 0.25, SD = 0.35). Furthermore, the best fitting model for WSS cut of the fields Big Sandy 2022 and Moccasin 2021 A had negative values of R^2, indicating the models produced a larger residual sum of squares than the total sum of squares, resulting in a very poor fit to the validation data.

We found strong evidence to suggest that R^2 varied across models of WSS infestation metrics while accounting for the random effect of field ($\chi2 = 19.38$, df = 2, p < 0.001; Figure 6). The mean R^2 for total and adequate WSS infestation was almost identical at 0.57 (SD = 0.26) and 0.57 (SD = 0.30), respectively. In contrast, the mean R^2 for WSS cut was 0.34 (SD = 0.36). Following this up with pairwise comparisons using Tukey's method showed that the total WSS infestation group was significantly different from the WSS cut group, with an estimated mean

difference of 0.23 (df = 14, t-ratio = 3.85, p-value = 0.005). Similarly, the adequate WSS group

was significantly different from WSS cut, with an estimated mean difference of 0.23, (df = 14, t-

ratio = 3.77 p-value = 0.005) However, the difference between total WSS and adequate WSS was

not statistically significant (df = 14, t-ratio = 0.07, p-value = 0.997). This indicates that while

WSS cut is distinct from the other groups, total WSS and adequate WSS are not significantly

different from each other.

The mapped predictions of each WSS infestation metric display the expected pattern of

clusters of high infestation near field edges with severity of infestation decreasing towards field

interiors (Figures 7-9). The trend of high WSS infestation along field edges is most clearly

illustrated in the total WSS maps for fields Moccasin 2021B, Big Sandy 2022, Three Forks 2022,

Carter 2023, and Moccasin 2023 (Figure 7). Coincidentally, these were also the fields with the

highest observed WSS infestation (Table 1). The maps generally mirror the trend of the sampled

WSS infestation metric they are derived from, as WSS cut is predicted minimally across the

fields (Figure 9), while the adequate WSS maps estimate infestation events to a greater extent

than WSS cut, but to a lesser degree than total WSS. The WSS cut maps primarily confine

predictions of cutting to the edges of the fields, whereas the maps for adequate and total WSS

indicate non-zero values for their respective metrics in areas beyond the field edges to a greater

extent.

Images from the later stages of the growing season were weighted with the greatest

importance across all modeled WSS infestation metrics (Figure 10). This was determined by

extracting the magnitude of the beta coefficients which directly represent the importance of

explanatory variables in N-PLS (Lopez-Fornieles et al. 2022) and normalizing the absolute

values by dividing them by the sum of the absolute beta coefficients for a given model. To understand how beta coefficients are distributed across crop and WSS phenology, we plotted the normalized beta coefficients against quantiles of GDD. This was done by computing four quantiles for the GDD distribution of each field to remedy the variance in GDD ranges observed across all fields. Across models of all WSS infestation metrics, Sentinel 2 images from the last quantile were ascribed the most weight, indicating images closer to the date of harvest are vital to estimating WSS infestation.

In visualizing the relationship between these normalized beta coefficients and their distribution across the wavelengths measured by Sentinel 2 (Figure 11), it appears all bands are useful in explaining variability in WSS infestations. The shortwave infrared (SWIR) bands centered at 1610 and 2190 nm, appear to have more utility to models predicting total or adequate WSS infestation than models of WSS cut.

Discussion

The methods used in this study most accurately estimated the metrics of total and adequate WSS infestation as compared to the proportion of cut stems (Figure 6). Models of cut stems had the greatest variance, and this was the only metric to produce models with negative values of R2 (Figures 5 & 6). These results provide evidence that multitemporal passive RS for estimating the post-harvest level of WSS infestation benefits from complete dissections of available stems and images with bands distributed across the VSWIR.

The fields studied are representative of the diverse areas of wheat production found across Montana and with it, variation in environment, agronomic practices, and WSS populations. We sought to remedy the discrepancies between fields, years, cultivars, and

availability of cloud-free Sentinel 2 images, by calibrating and validating each model within the context of a given field. To standardize the temporal domain across the crop and WSS phenology of field years, we used a GDD model with starting parameters specific to spring or winter wheat (Miller et al. 2001) (Equation 5, Figure A1). Furthermore, we took into account spatial variability and possible effects of lurking variables (heterogeneity of soil conditions, weeds, other insect damage) that we were not able to measure in this study, with the following precautions: (1) partitioning calibration and validation data sets to have proportional levels of infestation equally distributed across the sampling blocks of the field (2) centering and scaling each field's available Sentinel 2 images by band and GDD (3) using a multiway model (sparse N-PLS) to estimate WSS infestation based on the spectral trajectory of the observations while accounting for the correlative nature of the reflectance measurements across the spectral and temporal domains. Despite variation in locations, years, cultivars, agronomic conditions, or available imagery, the results of this study indicate the methods we used for multitemporal passive RS are better suited for estimating total or adequately WSS infested stems as opposed to cut stems.

We found that average R2 was similar for total and adequately WSS infested models but models of WSS cut had a significantly lower R2 while accounting for the random effect of field (Figure 6). This indicates that regardless of spring or winter wheat, location, or variation between years, these methods were least consistent for estimating the proportion of WSS cut stems. Interestingly, the highest R2 of any model was reported for the proportion of cut stems in the field Three Forks 2023 (R2 = 0.92). Then again, the only models with negative values of R2 were also created for the metric cut stems (Moccasin 2021 A, R2 = -0.07 & Big Sandy 2022, R2 = -0.01; Figure 9). It is worth noting that the fields Moccasin 2021A and Big Sandy 2022

produced the lowest performing models for all metrics across all fields studied. We do know that Big Sandy 2022 received the least amount of summer rainfall (Table 1) of any field studied and the producer noted that there was a damaging hail event (unpublished data). It is possible that the influences of prolonged water stress and a hailstorm could mask or confound variation in spectral reflectance related to the distribution of WSS infestation. Moccasin 2021 A did not seem to be subjected to drought or hail but did record the lowest sampled levels of both total and adequate WSS infestation, both of which were over dispersed (Table 2). To ameliorate the effects of overdispersion on model performance, we used centering, scaling, and partitioning of the data to balance the proportions of infestation in the calibration and validation sets (Payne et al. 2017).

It is possible that the small number of observations with measurable infestation create high enough leverage on the model to produce poor validation results (Supplementary Tables 1-3). Despite this, the field Three Forks 2023 had similar issues with low levels of infestation and overdispersion across all WSS infestation metrics (Table 2) but reported high R2 values for all WSS infestation metrics. As previously noted, one of the limitations of this study is the absence of possible lurking variables, which makes it difficult to interpret why some models explained more variation in WSS infestation than others.

Across the best performing models of each WSS infestation metric, the last quantile of GDD was attributed with the greatest relative contribution of beta coefficients (Figure 10). This suggests that RS images from the end of the growing season are particularly important in explaining variation across all WSS infestation metrics. Since our modelling approach enforced sparsity by only selecting covariates (i.e. reflectance of individual bands given GDD) that significantly explained variation in the dependent variable (based on the WSS infestation metric)

(Hervás et al. 2019), and most models incorporated data from more than two GDD quantiles, it can be implied that partial explanatory power is afforded by images from multiple points in the growing season. Moreover, this dispersed pattern of beta coefficients varying by both field and infestation metric is also present across the distribution of Sentinel 2 bands (Figure 11). While model performance varies across fields and WSS infestation metrics, all models benefited from images collected across the entire growing season with Sentinel 2's coverage of the VSWIR.

The models in this paper behaved similarly to a model presented by Ermatinger et al., 2024 trained for proximal estimation of adequate WSS infestations in wheat via multitemporal hyperspectral measurements. In both studies, spectral data throughout the VSWIR over the entire course of WSS host interaction were important, but the greatest emphasis was placed on spectral measurements near host senescence. It is logical to assume this is because the compounding effects of WSS feeding manifest in spectral changes that are most discernable at the end of the growing season. If this were the case, we may expect that images from the last GDD quantile would have greater importance for models of the most invasive forms of WSS infestation metric: WSS cut or adequate, as opposed to total WSS infestation. However, the reason for shared importance of the last GDD quantile across all metrics may be explained by the hierarchal nature of the measured WSS infestation metrics (i.e. total WSS infestation $\geq$ adequate WSS infestations $\geq$ WSS cut; Table 2 & Figure 4). In other words, the areas with the greatest degree of cutting will invariably have an equal or greater degree of adequate and total infestation (Figures A2-4). Therefore, in the case of this study, covariates found to explain variation in WSS cutting will also lend explanatory power to the metrics total and adequate WSS infestation. This nested relationship of the WSS infestation metrics also provides an explanation as to why early season

reflectance measurements have value for estimating all metrics of WSS infestation. From an ecological perspective, early season variation in crop condition across a field may influence where female WSS congregate and in turn lay their eggs (Buteler et al. 2009; Buteler et al. 2010; Buteler and Weaver 2012; Buteler et al. 2015). Thus, it is empirically true that these areas of greatest total WSS infestation have a greater potential for WSS cutting than areas with lesser degree of total WSS infestation. However, factors like pith expression, fungal infection, and parasitism influence a WSS larvae's ability to survive the growing season and cut the stem (Sjolie et al. 2024), which may partially explain why the model $R2$ of WSS cut had the greatest variance and the lowest mean (Figure 6). The comparison of average model performance for each metric demonstrates that multitemporal passive RS of WSS is least compatible with estimating the degree of WSS cutting.

Maps of total or adequate WSS infestation describe dispersal and oviposition patterns of WSS, but these metrics alone do not capture the impact of management techniques on WSS. Precise estimates of cutting, combined with total WSS infestation at the end of the growing season, would offer the most robust insights into how management techniques impact WSS and could help forecast next year's WSS pressure. End-of-season cutting estimates are likely most useful to wheat producers because a lack of viable in-season management options for WSS means decisions need to be made prior to planting. WSS management decisions often involve modifications to planting date, solid-stem varieties, or crop rotation (Weaver et al. 2024). Although some models of cutting were satisfactory, the inconsistent performance among models of cutting illustrates that multitemporal passive RS is likely not sufficient for estimating WSS cutting. This would suggest that future studies should consider active methods of remote sensing

like synthetic aperture radar (SAR) (Ajadi et al. 2020) or light detection and ranging (LiDAR) (Hu et al. 2021) sensors that are sensitive to structural variation, such as crop lodging from WSS cutting. Caution should be owed to the fact that rates of cutting are not always synonymous with the degree of lodging as falling stems can create a domino effect and lodge uncut stems. Moreover, low levels of cutting may not manifest in detectable lodging or events like hailstorms can induce lodging in the absence of WSS infestations. Combining post-harvest stem dissection surveys with multitemporal passive RS and active RS concurrent with WSS cutting may present the most robust approach for estimating both total WSS infestation and cutting.

Conclusions

Damaging populations of WSS have existed for more than a century in North America and are currently expanding their geographic range. Despite a longstanding economic interest in the pest, producers of wheat have a limited number of management techniques at their disposal. This issue has been further compounded by an insufficient ability to monitor WSS populations at the field and regional scale. Due to the concealed lifecycle of WSS, accurate estimates of larval WSS infestation, mortality, and cutting rely on comprehensive stem dissection campaigns from the end of the growing season. The results of this study indicate that these surveys can be combined with multitemporal Sentinel 2 imagery to estimate the level of total and adequate WSS infestations more accurately than the level of WSS cutting. It is likely that RS based models of cutting would benefit from the inclusion of SAR or LiDAR data. Future studies on RS of WSS are encouraged to co-locate stem dissection surveys with measurements of other environmental parameters that influence the reflectance of wheat, such as soil conditions, weed encroachment, and insect herbivory. Long-term monitoring of WSS pressure in the context of environmental

variation and management tactics can help consolidate management techniques into a cohesive strategy to provide resiliency against WSS. This work demonstrates an important first step in using RS technologies to unveil the subtleties of WSS infestation at the field scale across variable growing regions and agronomic practices.
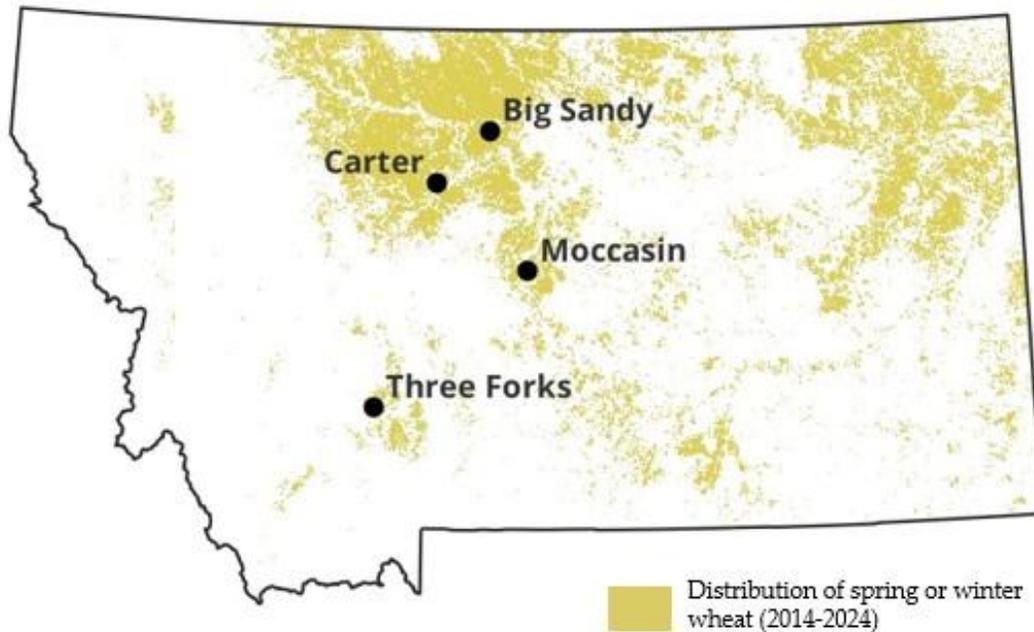
Figures

Fig 3.1. Nearest cities to field locations used in this study. Sites were chosen to provide coverage of the variable wheat growing climates that exist throughout Montana. Gold-colored areas represent locations classified as either spring or winter wheat from 2014-2024 by CropScape. Data were collected from https://nassgeodata.gmu.edu/CropScape/ (accessed on 2 March 2025).

Fig 3.2. Locations of wheat samples collected from each field and the potential of surrounding agricultural lands to provide a wheat stem sawfly (WSS) source. Fields categorized as WSS source were sown to either wheat or barley the year prior. Data for surrounding crop rotations were collected from https://nassgeodata.gmu.edu/CropScape/ (accessed 30th August 2024).

Fig 3.3. Graphical representation of the processing of ground reference and satellite imagery, calibration of models, mapping model results, and testing to see which metric of wheat stem sawfly infestation is most accurately estimated with multitemporal remote sensing.

Fig 3.4. Distribution of the observed wheat stem sawfly (WSS) infestation metric across the studied fields. Boxes represent the interquartile range while the lines indicate the mean value.
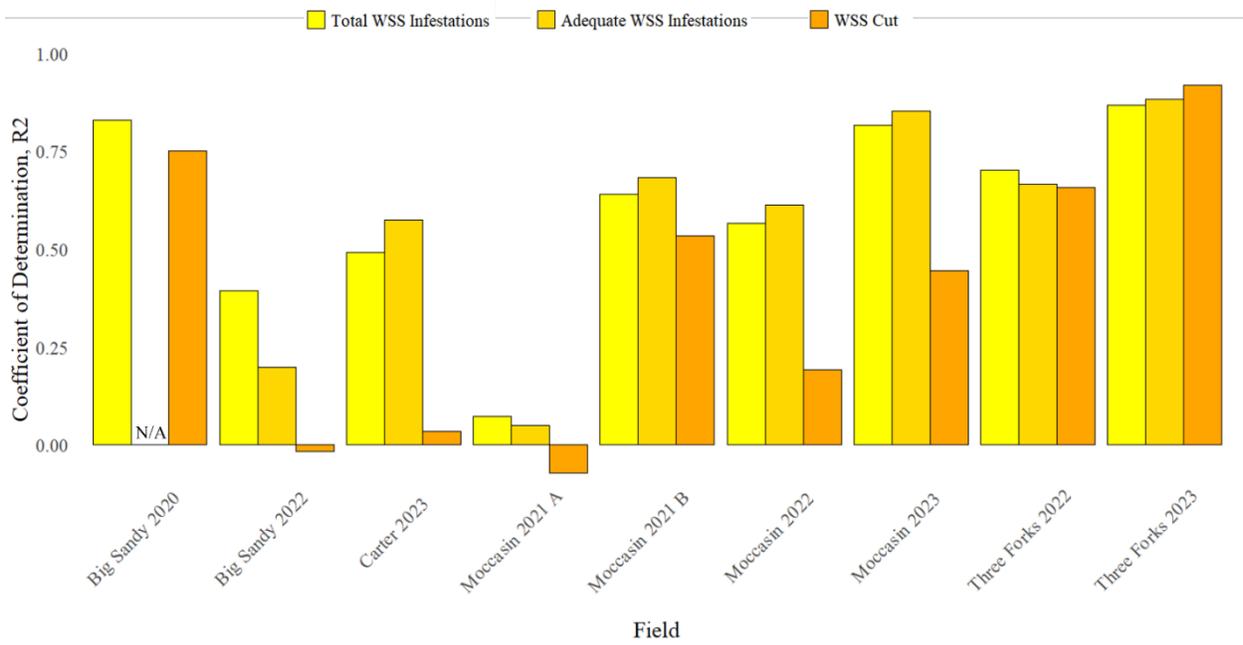
Fig 3.5. Comparison of the validation dataset's coefficient of determination (R²), across fields for the optimal multiway partial least squares regression (N-PLS) model for each wheat stem sawfly (WSS) infestation metric.
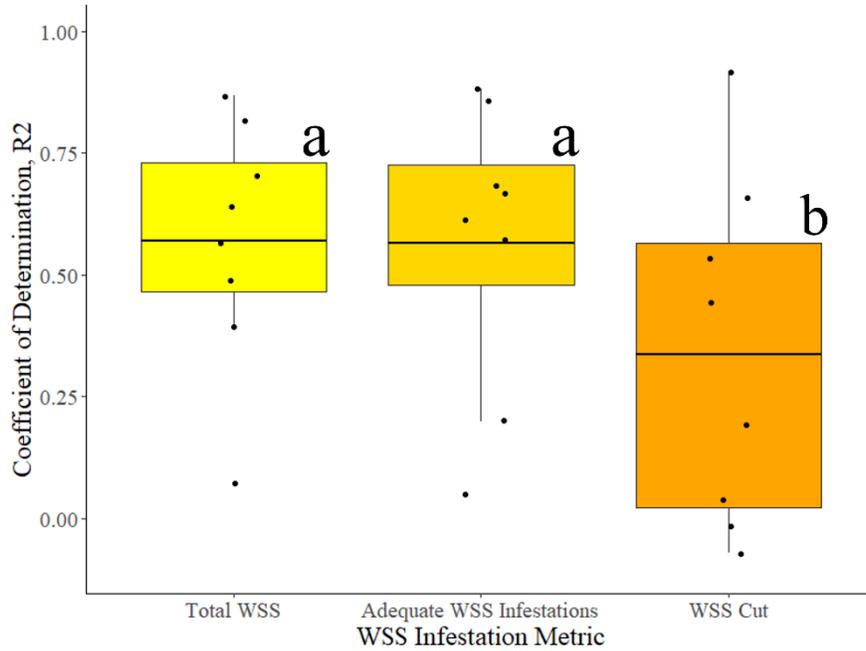
Fig 3.6. Average validation dataset coefficient of determination (R^2) from the optimal model for each wheat stem sawfly (WSS) infestation metric. WSS Infestation metrics with different letters were found to have statistically different mean values of R^2 by a Tukey's post hoc pairwise comparison test with a 5% significance level. The field Big Sandy 2020 was removed because information to quantify adequate WSS infestations was not collected.
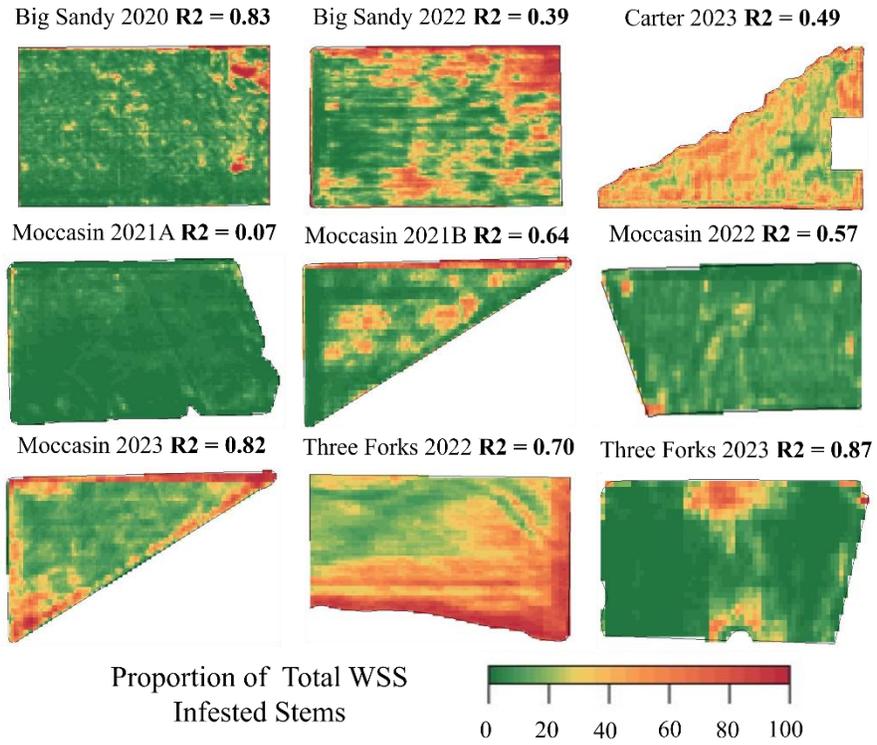
Fig 3.7. Predicted proportion of total WSS infested stems from the optimal model for each field.
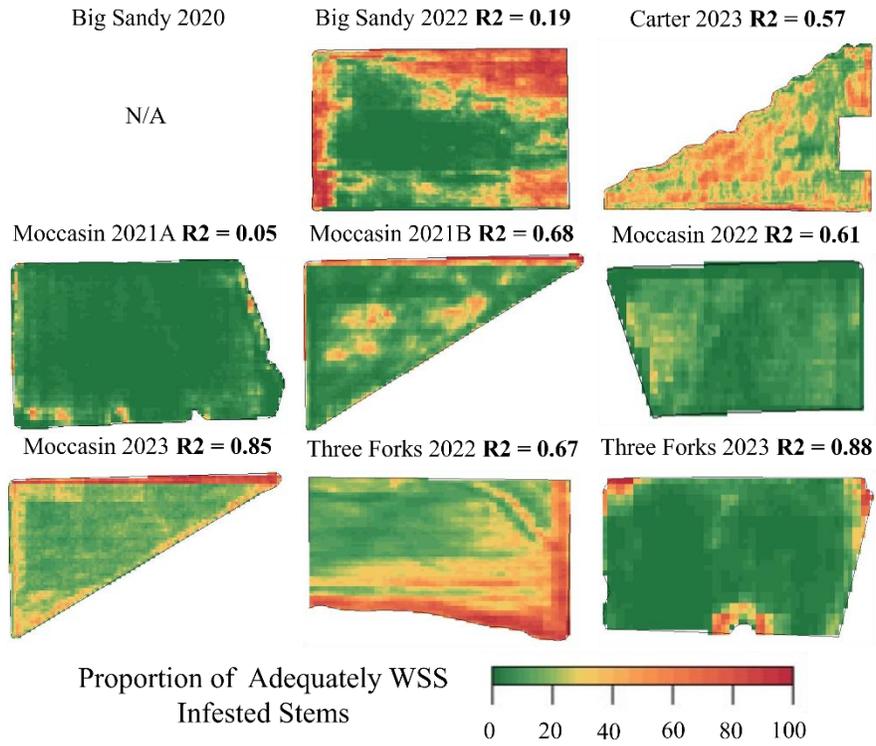
Fig 3.8. Predicted proportion of adequate WSS infested stems from the optimal model for each field.
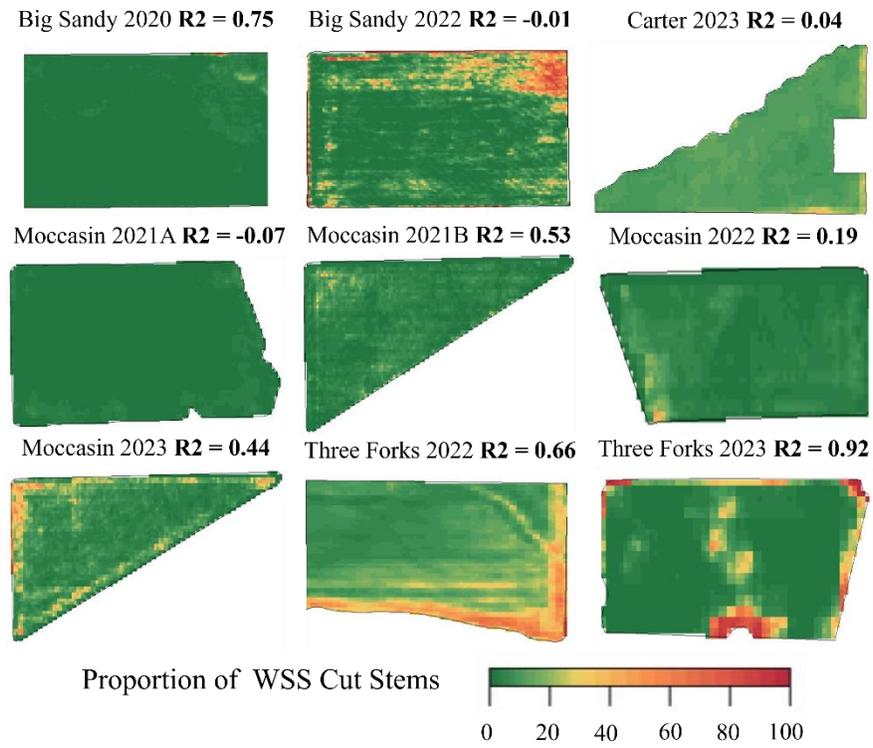
Fig 3.9. Predicted proportion of WSS cut stems from the optimal model for each field.
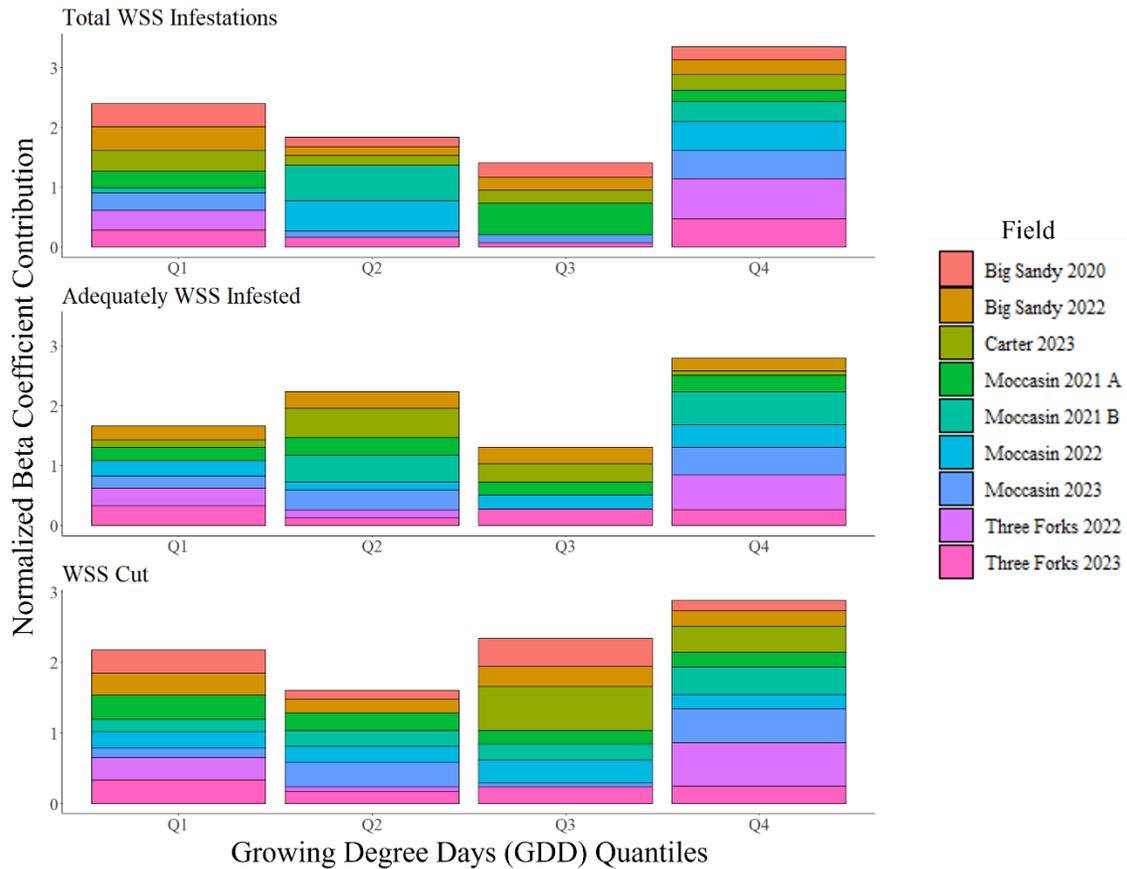
Fig 3.10. Distribution of normalized beta coefficients across GDD quantiles for each modeled WSS infestation metric. The normalized beta coefficients were calculated by taking the absolute value of each spectral temporal feature's beta coefficient and dividing it by the sum of absolute beta coefficients for each model. Growing degree quantiles were calculated for the range of GDD for each model to visualize how each model weighted spectral temporal features based on crop and WSS phenology.
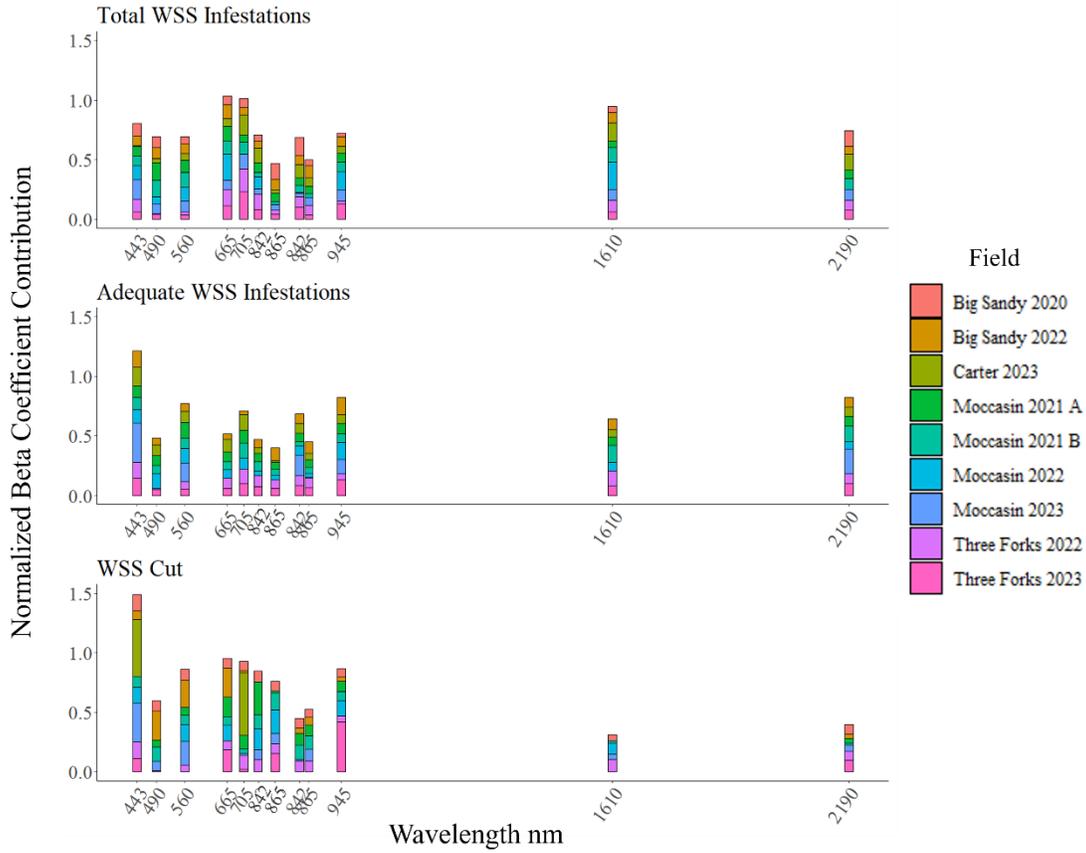
Fig 3.11. Distribution of normalized beta coefficients across the central wavelengths (nm) of the Sentinel 2 bands for each modeled WSS infestation metric. The normalized beta coefficients were calculated by taking the absolute value of each spectral temporal feature's beta coefficient and dividing it by the sum of absolute beta coefficients for each model.

Fig A3.1. Normalized difference vegetation index (NDVI) and GDD for each field, delineated by wheat type. Using GDD helps center the green-up peak of each field despite spring wheat displaying a slightly later NDVI maximum than winter wheat.
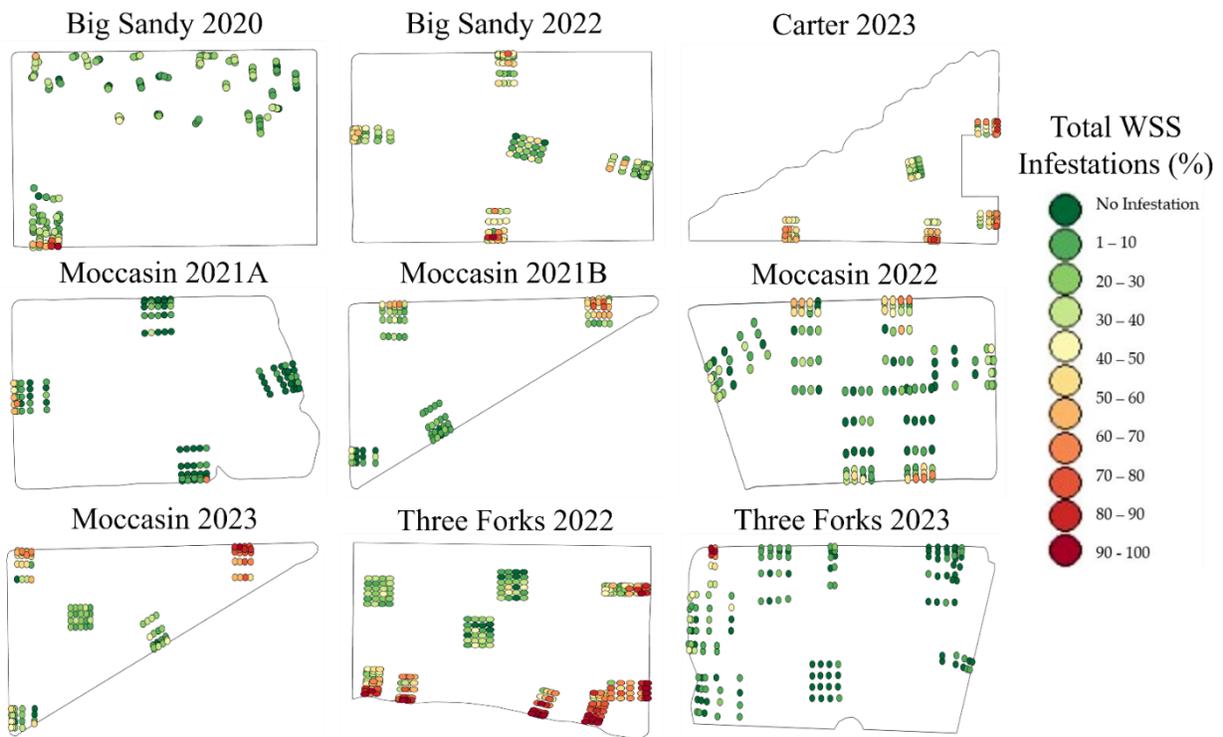
Fig A3.2. Sampled distribution of wheat stem samples from each field symbolized as total WSS infestation.
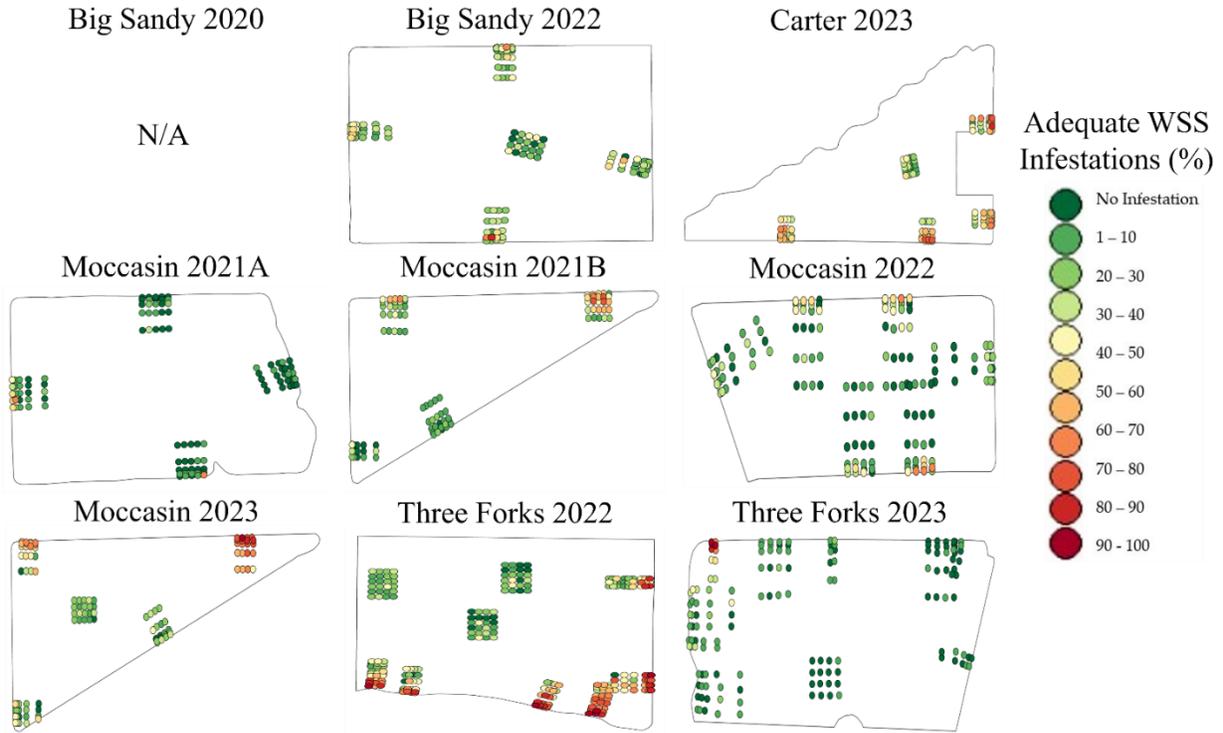
Fig A3.3. Sampled distribution of wheat stem samples from each field symbolized as adequate WSS infestation.
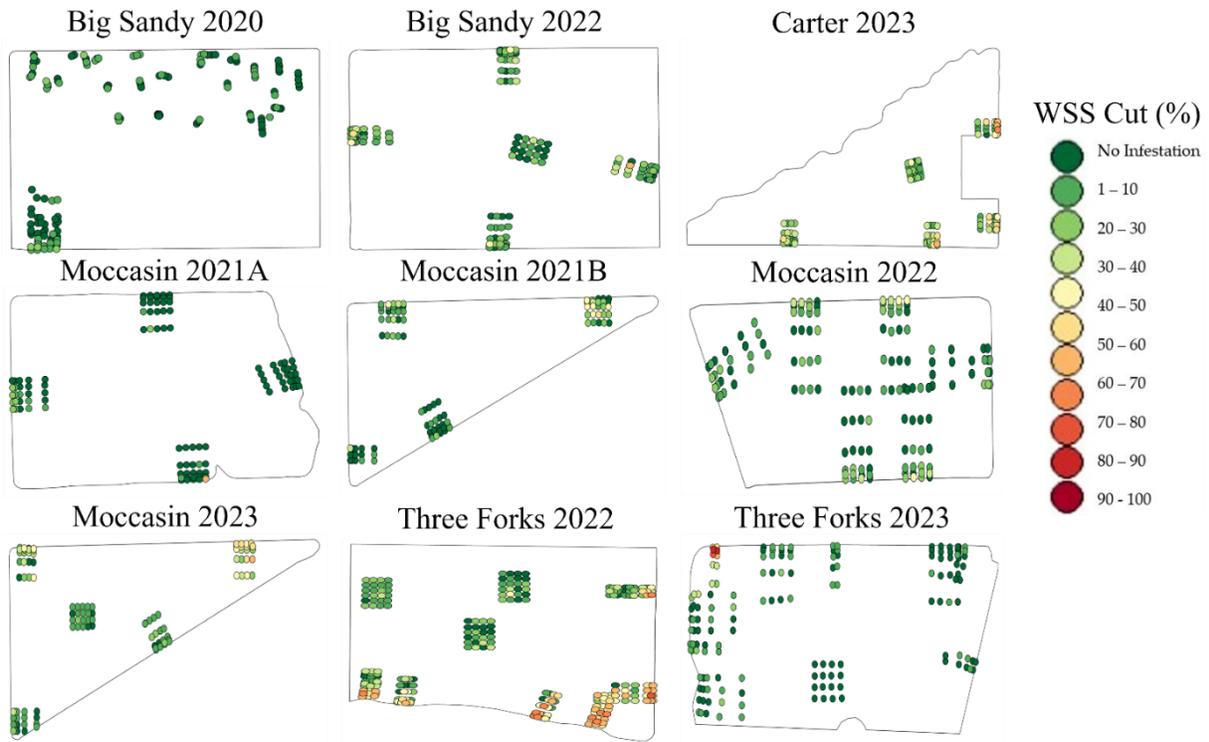
Fig A3.4. Sampled distribution of wheat stem samples from each field symbolized as WSS.

Table 2. Description of field locations, crop type, precipitation during the growing season (15 April – 31 July), number of stem samples collected, cloud free Sentinel 2 images available, planting, and harvest dates.

Field Name	Longitude	Latitude	Crop	Summer Precipitation (mm)	No. of Wheat Samples	No. of Cloud Free Images	Planting Date	Harvest Date
Big Sandy	110° 21' 41.76" W	48° 16' 9.84" N	Spring	165.0	145	10	04/28/2020	08/23/2020
Big Sandy	110° 23' 39.84" W	48° 16' 3.72" N	Spring	117.3	115	10	04/11/2022	08/13/2022
Carter 2023	110° 57' 51.12" W	47° 45' 35.28"	Winter	221.6	98	8	N/A	07/26/2023
Moccasin	109° 52' 39.72" W	47° 5' 47.40" N	Winter	135.2	100	15	N/A	07/30/2021
Moccasin	109° 51' 33.84" W	47° 4' 5.88" N	Winter	135.2	90	17	09/27/2021	07/30/2021
Moccasin	109° 52' 3.36" W	47° 4' 2.64" N	Winter	179.9	139	16	N/A	08/04/2022
Moccasin	109° 51' 33.84" W	47° 4' 5.88" N	Winter	297.5	100	16	N/A	08/08/2023
Three Forks	111° 36' 7.20" W	46° 0' 57.96" N	Spring	177.5	225	12	04/05/2022	08/20/2022
Three Forks	111° 35' 38.04" W	45° 59' 22.20"	Winter	178.3	146	13	09/15/2023	08/21/2023

Table 3. Mean and standard deviation for the proportion of total wheat stem sawfly (WSS) infestations, adequate WSS infestations and WSS cut for each sampled field. Each field was fit to a generalized linear mixed model to account for the proportional nature of the response using a logit link function and a random effect for the repeated measures from sample location. Letters next to the mean indicate significant differences (p-value < .05) among WSS infestation metrics within each field as indicated by a post hoc comparison of means adjusted using the Tukey honest significant difference method.

Field	Total WSS Infestations	Adequate WSS Infestations	WSS Cut
Big Sandy 2020	$15.64^A \pm 15.68$	N/A	$1.51^B \pm 2.97$
Big Sandy 2022	$26.78^A \pm 18.98$	$20.13^B \pm 15.20$	$8.59^C \pm 9.59$
Carter 2023	$40.75^A \pm 20.52$	$36.43^B \pm 19.58$	$18.8^C \pm 15.46$
Moccasin 2021 A	$5.92^A \pm 13.56$	$5.48^A \pm 12.66$	$1.75^B \pm 6.26$
Moccasin 2021 B	$20.35^A \pm 20.40$	$20.24^A \pm 20.39$	$7.76^B \pm 10.88$
Moccasin 2022	$15.18^A \pm 17.29$	$12.31^B \pm 15.60$	$5.57^C \pm 7.89$
Moccasin 2023	$32.42^A \pm 25.36$	$31.26^A \pm 25.0$	$12.79^B \pm 13.13$
Three Forks 2022	$45.67^A \pm 31.01$	$36.90^B \pm 28.80$	$22.92^C \pm 20.30$
Three Forks 2023	$8.18^A \pm 18.12$	$7.89^A \pm 17.65$	$5.72^B \pm 14.57$

Table 4. Model parameters and performance metrics for the optimal sparse multi-way partial least squares regression model produced for adequate WSS infestations for a given field. The normalized root mean square error (RRMSE) calculated by dividing the RMSE of each dataset by its mean to provide comparative power across all models.

Field	No. Latent Variables	No. Time-points	No. Bands	Calibration RRMSE	Validation RRMSE	Calibration r^2	Validation r^2	Calibration R^2	Validation R^2
Big Sandy 2020	10	9	5	0.528	0.438	0.835	0.921	0.698	0.830
Big Sandy 2022	8	9	11	0.557	0.626	0.606	0.663	0.353	0.393
Carter 2023	7	7	3	0.318	0.358	0.788	0.759	0.612	0.491
Moccasin 2021A	9	1	11	0.647	5.039	0.948	0.513	0.894	0.073
Moccasin 2021B	7	1	10	0.528	0.754	0.854	0.859	0.720	0.641
Moccasin 2022	5	1	2	0.884	0.924	0.648	0.791	0.375	0.567
Moccasin 2023	9	1	9	0.396	0.323	0.874	0.911	0.759	0.816
Three Forks 2022	2	1	7	0.338	0.309	0.893	0.874	0.753	0.702
Three Forks 2023	10	1	3	0.757	0.935	0.942	0.942	0.885	0.869

Table 5. Model parameters and performance metrics for the optimal sparse multi-way partial least squares regression model produced for adequate WSS infestations for a given field. The normalized root mean square error (RRMSE) calculated by dividing the RMSE of each dataset by its mean to provide comparative power across all models.

Field	No. Latent Variables	No. Time-points	No. Bands	Calibration RRMSE	Validation RRMSE	Calibration r^2	Validation r^2	Calibration R^2	Validation R^2
Big Sandy 2020					*N/A				
Big Sandy 2022	10	4	12	0.598	0.818	0.587	0.488	0.297	0.199
Carter 2023	10	1	5	0.379	0.352	0.725	0.817	0.513	0.574
Moccasin 2021A	10	11	11	0.626	4.51	0.951	0.404	0.891	0.049
Moccasin 2021B	2	1	11	0.577	0.689	0.819	0.873	0.668	0.682
Moccasin 2022	6	16	11	0.969	1.015	0.666	0.799	0.392	0.612
Moccasin 2023	6	1	1	0.422	0.301	0.866	0.938	0.739	0.854
Three Forks 2022	2	4	8	0.395	0.413	0.877	0.823	0.744	0.665
Three Forks 2023	10	4	11	0.856	0.810	0.922	0.941	0.848	0.882

*Information for adequate WSS infestations was not collected for Big Sandy 2020

Table 6. Model parameters and performance metrics for the optimal sparse multi-way partial least squares regression model produced for WSS cut for a given field. The normalized root mean square error (RRMSE) calculated by dividing the RMSE of each dataset by its mean to provide comparative power across all models.

Field	No. Latent Variables	No. Time-points	No. Bands	Calibration RRMSE	Validation RRMSE	Calibration r^2	Validation r^2	Calibration R^2	Validation R^2
Big Sandy 2020	7	10	11	0.905	0.682	0.709	0.868	0.428	0.752
Big Sandy 2022	10	9	1	0.816	2.275	0.515	0.426	0.219	-0.016
Carter 2023	1	3	2	0.783	1.001	0.358	0.421	0.087	0.035
Moccasin 2021A	9	4	2	0.851	9.25	0.872	0.216	0.705	-0.072
Moccasin 2021B	10	11	1	0.936	0.984	0.728	0.757	0.489	0.534
Moccasin 2022	7	4	1	0.913	1.568	0.715	0.49	0.427	0.191
Moccasin 2023	9	12	7	0.507	0.994	0.874	0.735	0.756	0.444
Three Forks 2022	2	4	8	0.574	0.528	0.762	0.814	0.566	0.657
Three Forks 2023	10	7	1	1.144	0.788	0.877	0.965	0.749	0.918

Equations

$$p_{total\ WSS_i} = \frac{dead\ neonates_i + WSS\ burrowed\ through\ at\ least\ one\ node_i + WSS\ cut_i}{total\ stems_i} \tag{3.4}$$

$$p_{adequate\ WSS_i} = \frac{WSS\ burrowed\ through\ at\ least\ one\ node_i + WSS\ cut_i}{total\ stems_i} \tag{3.5}$$

$$p_{WSS\ cut_i} = \frac{WSS\ cut_i}{total\ stems_i} \tag{3.6}$$

$$y_i = logit(p_i) = ln\left(\frac{p_i \pm 0.01}{1 - (p_i \pm 0.01)}\right) \tag{3.7}$$

$$GDD = \begin{cases} \sum_{i=1}^{n} \max\left(T_{avg,i} - T_{base}\right) & if\ spring\ wheat\ and\ i \geq P + 7 \\ \sum_{j=1}^{m} \max\left(T_{avg,j} - T_{base}\right) & if\ winter\ wheat\ and\ j \geq April\ 1 \end{cases} \tag{3.8}$$

$$R^2 = 1 - \frac{\sum_{i=1}^{n}(y_i - \hat{y}_i)^2}{\sum_{i=1}^{n}(y_i - \bar{y})^2} \tag{3.9}$$

References

Achhami B, Reddy G, Sherman J, Peterson R, Weaver D. 2020. Effect of precipitation and temperature on larval survival of *Cephus cinctus* (Hymenoptera: Cephidae) in barley cultivars. Journal of Economic Entomology. 113:1982–1989. doi:10.1093/jee/toaa097.

Achhami B, Reddy G, Sherman J, Weaver D, Peterson R. 2020. Antixenosis, antibiosis, and potential yield compensatory response in barley cultivars exposed to wheat stem sawfly (Hymenoptera: Cephidae) under field conditions. Journal of Insect Science. 20:1–14. doi: 10.1093/jisesa/ieaa091.

Ainslie CN. 1929. The western grass-stem sawfly (*Cephus cinctus* Norton): A pest of small grains. U.S Department of Agriculture Technical Bulletin Report No.: 157.

Ainslie CN. 1920. The western grass-stem sawfly. Washington, D.C. : U.S. Dept. of Agriculture.

Ajadi OA, Liao H, Jaacks J, Delos Santos A, Kumpatla SP, Patel R, Swatantran A. 2020. Landscape-scale crop lodging assessment across Iowa and Illinois using synthetic aperture radar (SAR) Images. Remote Sensing. 12(23):3885. doi: 10.3390/rs12233885.

Bates D, Mächler M, Bolker B, Walker S. 2015. Fitting linear mixed-effects models using lme4. Journal of Statistical Software. 67:1–48. doi: 10.18637/jss.v067.i01.

Bekkerman A, Weaver DK. 2018. Modeling joint dependence of managed ecosystems pests: the case of the wheat stem sawfly. Journal of Agricultural and Resource Economics. 43(2):172–194. doi: 10.22004/ag.econ.273445

Beres BL, Cárcamo HA, Bremer E. 2009. Evaluation of alternative planting strategies to reduce wheat stem sawfly (Hymenoptera: Cephidae) damage to spring wheat in the Northern Great Plains. Journal of Economic Entomology. 102(6):2137–2145. doi: 10.1603/029.102.0617.

Beres BL, Cárcamo HA, Byers JR. 2007. Effect of wheat stem sawfly damage on yield and quality of selected Canadian spring wheat. Journal of Economic Entomology. 100(1):79–87. doi: 10.1093/jee/100.1.79.

Beres BL, Dosdall LM, Weaver DK, Cárcamo HA, Spaner DM. 2011. Biology and integrated management of wheat stem sawfly and the need for continuing research. Canadian Entomologist. 143(2):105–125. doi: 10.4039/n10-056.

Beres BL, Meers SM, Delaney KJ, Cárcamo HA, Miller PR, Spaner DM, Weaver DK. 2024. Stem height and harvest management influence conservation biological control of wheat stem sawfly by endemic parasitoids. Canadian Journal of Plant Science. doi: 10.1139/cjps-2024-0227

Bhattarai GP, Schmid RB, McCornack BP. 2019. Remote sensing data to detect hessian fly infestation in commercial wheat fields. Scientific Reports. 9(1). doi: 10.1038/s41598-019-42620-0.

Bro R. 1996. Multiway calibration. multilinear PLS. Journal of Chemometrics. 10(1):47–61. doi: 10.1002/(SICI)1099-128X(199601)10:1<47::AID-CEM400>3.0.CO;2-C.

Brooks M, Bolker B, Kristensen K, Maechler M, Magnusson A, McGillycuddy M, Skaug H, Nielsen A, Berg C, Bentham K van, et al. 2024. glmmTMB: Generalized Linear Mixed Models using Template Model Builder. doi: 10.32614/RJ-2017-066

Buteler M, Peterson RKD, Hofland ML, Weaver DK. 2015. Multiple decrement life table reveals that host plant resistance and parasitism are major causes of mortality for the wheat stem sawfly. Environmental Entomology. 44(6):1571–1580. doi: 10.1093/ee/nvv128.

Buteler M, Peterson RKD, Weaver DK. 2009. Oviposition behavior of the wheat stem sawfly when encountering plants infested with cryptic conspecifics. Environmental Entomology. 38(6):1707–1715. doi: 10.1603/022.038.0624.

Buteler M, Weaver DK. 2012. Host selection by the wheat stem sawfly in winter wheat and the role of semiochemicals mediating oviposition preference. Entomologia Experimentalis et Applicata. 143(2):138–147. doi: 10.1111/j.1570-7458.2012.01237.x.

Buteler M, Weaver DK, Bruckner PL, Carlson GR, Berg JE, Lamb PF. 2010. Using agronomic traits and semiochemical production in winter wheat cultivars to identify suitable trap crops for the wheat stem sawfly. The Canadian Entomologist. 142(3):222–233. doi: 10.4039/n09-072.

Cárcamo H, Entz T, Beres B. 2007. Estimating *Cephus cinctus* wheat stem cutting damage – can we cut stem counts? Journal of Agri cultural and Urban Entomology. 24(3):117–124. doi: 10.3954/1523-5475-24.3.117.

Cavallini L, Peterson R, Weaver D. 2023. Cowpea extrafloral nectar has potential to provide ecosystem services lost in agricultural intensification and support native parasitoids that suppress the wheat stem sawfly. Journal of Economic Entomology. 116(3):752-760. doi: 10.1093/jee/toad083.

Cockrell DM, Randolph T, Peirce E, Peairs FB. 2021. Survey of wheat stem sawfly (Hymenoptera: Cephidae) infesting wheat in Eastern Colorado. Journal of Economic Entomology. 114(2):998–1004. doi: 10.1093/jee/toab015.

Criddle N. 1922. The western-stem sawfly and its control. Dominion of Canada Department of Agriculture.(6):1–8.

Criddle N. 1923. Popular and practical entomology: The life habits of *Cephus cinctus* Norton in Manitoba. The Canadian Entomologist. 55(1):1–4. doi: 10.4039/Ent551-1.

Dahiya S, Sihag S, Chaudhary C. 2018. Lodging: Significance and preventive measures for increasing crop production. International Journal of Chemical Studies. 6:700–705. E-ISSN: 2321-4902

Delaney KJ, Weaver DK, Peterson RKD. 2010. Photosynthesis and yield reductions from wheat stem sawfly (Hymenoptera: Cephidae): Interactions with wheat solidness, Water stress, and phosphorus deficiency. Journal of Economic Entomology. 103(2):516–524. doi: 10.1603/EC09229.

Ermatinger LS, Powell SL, Peterson RKD, Weaver DK. 2024. Multitemporal hyperspectral characterization of wheat infested by wheat stem sawfly, *Cephus cinctus* Norton. Remote Sensing. 16(18):3505. doi: 10.3390/rs16183505.

Fletcher J. 1896. The western wheat stem sawfly (*Cephus pygmaeus* L.). Dominion of Canada, Department of Agriculture, Report of the Dominion Entomologist. (1896) 1:147–149.

Gobbo S, Ghiraldini A, Dramis A, Dal Ferro N, Morari F. 2021. Estimation of hail damage using crop models and remote sensing. Remote Sensing. 13(14):2655. doi: 10.3390/rs13142655.

Goodarzi M, Freitas MP. 2009. On the use of PLS and N-PLS in MIA-QSAR: Azole antifungals. Chemometrics and Intelligent Laboratory Systems. 96(1):59–62. doi: 10.1016/j.chemolab.2008.11.007.

Gorelick N, Hancher M, Dixon M, Ilyushchenko S, Thau D, Moore R. 2017. Google Earth Engine: Planetary-scale geospatial analysis for everyone. Remote Sensing of Environment. 202(1):18–27. doi: 10.1016/j.rse.2017.06.031.

Haack BN. 1982. Landsat: A tool for development. World Development. 10(10):899–909. doi: 10.1016/0305-750X(82)90064-X.

Han W, Yang Z, Di L, Mueller R, 2012. CropScape: A Web service based application for exploring and disseminating US conterminous geospatial cropland data products for decision support. Computers and Electronics in Agriculture, 84, 111–123. doi: 10.1016/j.compag.2012.03.005

Hastie T, Tibshirani R, Friedman J, Franklin J. 2009. The elements of statistical learning: data mining, inference, and prediction. The Mathematical Intelligencer. 27(2): 83-85

Hervás D, Prats-Montalbán JM, García-Cañaveras JC, Lahoz A, Ferrer A. 2019. Sparse n-way partial least squares by l1-penalization. Chemometrics and Intelligent Laboratory Systems. 185:85–91. doi: 10.1016/j.chemolab.2019.01.004.

Holmes ND. 1975. Effects of moisture, gravity, and light on the behavior of larvae of the wheat stem sawfly, *Cephus cinctus* (Hymenoptera: Cephidae). The Canadian Entomologist. 107(4):391–401. doi: 10.4039/ent107391-4.

Holmes ND. 1982. Population dynamics of the wheat stem sawfly, *Cephus cinctus* (Hymenoptera: Cephidae), in wheat. The Canadian Entomologist. 114(9):775–788. doi: [10.4039/Ent114775-9](10.4039/Ent114775-9).

Hu X, Sun L, Gu X, Sun Q, Wei Z, Pan Y, Chen L. 2021. Assessing the self-recovery ability of maize after lodging using UAV-LiDAR data. Remote Sensing. 13(12):2270. doi: [10.3390/rs13122270](10.3390/rs13122270).

Lenth RV, Banfai B, Bolker B, Buerkner P, Giné-Vázquez I, Herve M, Jung M, Love J, Miguez F, Piaskowski J, et al. 2024. Emmeans: estimated marginal means, aka least-squares Means. doi: 10.32614/CRAN.package.emmeans

Lesieur V, Martin J-F, Weaver DK, Hoelmer KA, Smith DR, Morrill WL, Kadiri N, Peairs FB, Cockrell DM, Randolph TL, et al. 2016. Phylogeography of the wheat stem sawfly, *Cephus cinctus* Norton (Hymenoptera: Cephidae): implications for pest management. PLOS ONE. 11(12):e0168370. doi: 10.1371/journal.pone.0168370.

Lopez-Fornieles E, Brunel G, Rancon F, Gaci B, Metz M, Devaux N, Taylor J, Tisseyre B, Roger JM. 2022. Potential of multiway pls (N-PLS) regression method to analyze time-series of multispectral images: a case study in agriculture. Remote Sensing. 14(1). doi: [10.3390/rs14010216](10.3390/rs14010216).

Macedo TB, Peterson RKD, Weaver DK, Morrill WL. 2005. Wheat stem sawfly, *Cephus cinctus* Norton, impact on wheat primary metabolism: An ecophysiological approach. Environmental Entomology. 34(3): 719-726. doi: [10.1603/0046-225X-34.3.719](10.1603/0046-225X-34.3.719)

Macedo TB, Weaver DK, Peterson RKD. 2007. Photosynthesis in wheat at the grain filling stage is altered by larval wheat stem sawfly (Hymenoptera: Cephidae) injury and reduced water availability Journal of Entomological Science. 42(2): 228 – 238. doi: [10.18474/0749-8004-42.2.228](10.18474/0749-8004-42.2.228)

Main-Knorn M, Pflug B, Louis J, Debaecker V, Müller-Wilm U, Gascon F. 2017. Sen2Cor for Sentinel-2. In: image and signal processing for remote sensing XXIII. Vol. 10427. SPIE. p. 37–48. doi: [10.1117/12.2278218](10.1117/12.2278218)

McCullough CT, Hein GL, Bradshaw JD. 2020. Phenology and dispersal of the wheat stem sawfly (Hymenoptera: Cephidae) into winter wheat fields in Nebraska. Journal of Economic Entomology. 113(4):1831–1838. doi: 10.1093/jee/toaa093.

Miller P, Lanier W, Brandt S. 2001. Using growing degree days to predict plant stages. Montana State University Extension. MontGuide, MT200103 AG.

Morrill WL, Gabor JW, Kushnak GD. 1992. Wheat stem sawfly (Hymenoptera: Cephidae): Damage and detection. Journal of Economic Entomology. 85(6): 2413-2417. doi: [10.1093/jee/85.6.2413](10.1093/jee/85.6.2413)

Morrill WL, Kushnak GD. 1999. Planting date influence on the wheat stem sawfly (Hymenoptera: Cephidae) in spring wheat. Journal of Agricultural and Urban Entomology. 16(2): 123-128.

Morrill WL, Kushnak GD, Bruckner PL, Gabor JW. 1994. Wheat stem sawfly (Hymenoptera: Cephidae) damage, rates of parasitism, and overwinter survival in resistant wheat lines. Journal of Economic Entomology. 87(5):1373–1376. doi: 10.1093/jee/87.5.1373.

Morrill WL, Weaver DK, Johnson GD. 2001. Trap strip and field border modification for management of the wheat stem sawfly (Hymenoptera: Cephidae). Journal of Entomological Science. 36(1):34–45. doi: 10.18474/0749-8004-36.1.34.

Nansen C, Macedo T, Swanson R, Weaver DK. 2009. Use of spatial structure analysis of hyperspectral data cubes for detection of insect-induced stress in wheat plants. International Journal of Remote Sensing. 30(10):2447–2464. doi: 10.1080/01431160802552710.

Nansen C, Macedo TB, Weaver DK, Peterson RKD. 2005. Spatiotemporal distributions of wheat stem sawfly eggs and larvae in dryland wheat fields. Canadian Entomologist. 137(4):428–440. doi: 10.4039/n04-094.

Nansen C, Weaver DK, Sing SE, Runyon JB, Morrill WL, Grieshop MJ, Shannon CL, Johnson ML. 2005. Within-field spatial distribution of Cephus cinctus (Hymenoptera: Cephidae) larvae in Montana wheat fields. Canadian Entomologist. 137: 202 – 214.

Norton E. 1872. Notes on North American Tenthredinidae, with descriptions of new species. Transactions of the American Entomological Society (1867-1877). 4:77–86. doi: 10.2307/25076265.

Olfert O, Weiss RM, Catton H, Cárcamo H, Meers S. 2019. Bioclimatic assessment of abiotic factors affecting relative abundance and distribution of wheat stem sawfly (Hymenoptera: Cephidae) in western Canada. The Canadian Entomologist. 151(1):16–33. doi: 10.4039/tce.2018.46.

Payne EH, Hardin JW, Egede LE, Ramakrishnan V, Selassie A, Gebregziabher M. 2017. Approaches for dealing with various sources of overdispersion in modeling count data: Scale adjustment versus modeling. Statistical Methods in Medical Research. 26(4):1802–1823. doi: 10.1177/0962280215588569.

Peirce E, Cockrell D, Mason RE, Haley S, Peairs F, Nachappa P. 2022. Solid stems and beyond: challenges and future directions of resistance to wheat stem sawfly (Hymenoptera: Cephidae). Journal of Integrated Pest Management. 13(1): 29. doi: 10.1093/jipm/pmac023.

PRISM Climate Group. 2014. Oregon State University. Available at: https://prism.oregonstate.edu

R Core Team. 2023. R Language Definition; R Foundation for Statistical Computing: Vienna, Austria,

Rand TA, Kula RR, Gaskin JF. 2024. Evaluating the use of common grasses by the wheat stem sawfly (Hymenoptera: Cephidae) and its native parasitoids in rangeland and Conservation Reserve Program grasslands. Journal of Economic Entomology. 117(3):858–864. doi: 10.1093/jee/toae046.

Reis DA, Hofland ML, Peterson RKD, Weaver DK. 2019. Effects of sucrose supplementation and generation on life-history traits of *Bracon cephi* and *Bracon lissogaster*, parasitoids of the wheat stem sawfly. Physiological Entomology. 44(3–4):266–274. doi: 10.1111/phen.12303.

Roberts DR, Bahn V, Ciuti S, Boyce MS, Elith J, Guillera-Arroita G, Hauenstein S, Lahoz-Monfort JJ, Schröder B, Thuiller W, et al. 2017. Cross-validation strategies for data with temporal, spatial, hierarchical, or phylogenetic structure. Ecography. 40(8):913–929. doi: 10.1111/ecog.02881.

Roemhild GR. 1954. Morphological resistance of some of the Gramineae to the wheat stem sawfly (*Cephus cinctus* Norton) [PhD thesis]. Bozeman, MT (USA): Montana State University.

Seamans HL. 1928. The value of trap crops in the control of the wheat stem sawfly in Alberta. Annual Report of the Entomological Society of Ontario 59: 59–64.

Segarra J, Buchaillot ML, Araus JL, Kefauver SC. 2020. Remote sensing for precision agriculture: Sentinel-2 improved features and applications. Agronomy. 10(5):641. doi: 10.3390/agronomy10050641.

Shanower T, Waters D. 2006. A survey of five stem-feeding insect pests of wheat in the Northern Great Plains. Journal of Entomological Science. 41. doi: 10.18474/0749-8004-41.1.40.

Sing SE. 2002. Spatial and biotic interactions of the wheat stem sawfly with wild oat and Montana dryland spring wheat. [PhD Thesis]. Bozeman, MT (USA): Montana State University.

Sjolie DM, Willenborg CJ, Vankosky MA. 2024. The causes of wheat stem sawfly (Hymenoptera: Cephidae) larval mortality in the Canadian prairies. The Canadian Entomologist. 156(e3): 1-15. doi: 10.4039/tce.2023.29.

Strand J, Peterson R, Sterling T, Weaver D. 2024. Agroecological importance of smooth brome in managing wheat stem sawfly (Hymenoptera: Cephidae) via associated braconid parasitoids. Journal of Economic Entomology. doi: 10.1093/jee/toae246.

Tibshirani R. 1996. Regression shrinkage and selection via the lasso. Journal of the Royal Statistical Society: Series B (Methodological). 58(1): 267-288. doi: 10.1111/j.2517-6161.1996.tb02080.x

Varella AC, Talbert LE, Achhami BB, Blake NK, Hofland ML, Sherman JD, Lamb PF, Reddy GVP, Weaver DK. 2018. Characterization of resistance to *Cephus cinctus* (Hymenoptera: Cephidae) in barley germplasm. Journal of Economic Entomology. 111(2):923–930. doi: 10.1093/jee/toy025.

Villacorta A, Bell RA, Callenbach JA. 1971. Influence of high temperature and light on postdiapause development of the wheat stem sawfly. Journal of Economic Entomology. 64(3):749–751. doi: 10.1093/jee/64.3.749.

Wallace, L. E. and McNeal, F. H. (1966). Stem sawflies of economic importance in grain crops in the United States. Washington, DC: Agricultural Research Service, United States Department of Agriculture.

Weaver DK. 2023. Wheat stem sawfly (Cephus cinctus Norton). Chapter 5, in Eigenbrode, SD, Rashed A, (eds.) Advances in Understanding Insect Pests Affecting Wheat and Other Cereals, pp. 93–134. doi: 10.19103/as.2022.0114.13.

Weaver DK, Sing S, Runyon J, Morrill W. 2004. Potential impact of cultural practices on wheat stem sawfly (Hymenoptera: Cephidae) and associated parasitoids. Journal of Agricultural and Urban Entomology. 21:271–287.

Weaver DK, Tallman S, Lane T. 2024. Wheat stem sawfly best management practices. Montana State University Extension. MSU Extension Bulletin EB0244; USDA-NRCS Agronomy Technical Note MT-95. doi: 10.13140/RG.2.2.19133.88805

Wold S, Geladi P, Esbensen K, Ohman J. 1987. Multi-way principal components-and pls-analysis. Journal of Chemometrics. 1(1):41-56. doi: 10.1002/cem.1180010107

Yang Z, Rao MN, Elliott NC, Kindler SD, Popham TW. 2009. Differentiating stress induced by greenbugs and Russian wheat aphids in wheat using remote sensing. Computers and Electronics in Agriculture. 67(1):64–70. doi: 10.1016/j.compag.2009.03.003.

CHAPTER FOUR

CONCLUSIONS

The lack of chemical control options for WSS confines management decisions to a diverse suite of management tactics. Effective use of these tactics relies on our ability to optimize their deployment and equally, to quantify their impact on WSS populations. Due to the concealed life cycle of WSS, estimating WSS infestation relies on stem dissection surveys that are labor and time intensive. We assessed remote sensing (RS) of WSS infestation at the canopy and subfield scale using multitemporal passive RS data to spatially interpolate stem dissection surveys. We found that passive RS data collected over the course of the growing season was useful for estimating the percentage of WSS infested stems from post-harvest stem dissection surveys. Estimates of WSS cutting were on average less precise, highlighting the need for more studies in this area.

The findings of Chapter 2 (Ermatinger et al., 2024) revealed that proximal sensing of wheat canopies for estimating the proportion of adequate WSS infestation in wheat required spectral observations from across the entire life history of WSS and its host. While 96.7% of the spectral-temporal features were discarded by the optimal model, at least one spectral feature from every time point was found to be significant. Moreover, the model presented in Chapter 2 required the construction of complex relationships for temporal patterns across spectra, corroborating the often-subtle responses in host physiology due to WSS herbivory (Macedo et al. 2005; Macedo et al. 2007). Wavelengths within the green, NIR, and SWIR spectral regions were found to be of significance for estimating the proportion of adequately WSS infested stems. The SWIR region contributed the greatest importance to explaining variation in the proportion of

adequately WSS infested stems. Elevated reflectance at 1339 nm during wheat senescence was found to be the single strongest predictor of the proportion of adequate WSS infestation. Increases in SWIR reflectance of vegetation are often used as an indicator of deficient plant water content (Hunt and Rock 1989; Seelig et al. 2008). This finding corroborates the notion that WSS larval feeding can impair the water transport system of the host through feeding on vascular tissue (Morrill et al. 1992; Morrill et al. 1994; Delaney et al. 2010). It is apparent that larval WSS feeding can induce physiological changes to significantly alter the reflectance of individual leaves (Nansen et al. 2009) and the canopy (Chapter 2, Ermatinger et al., 2024).

The methods described in Chapter 2 were applied to the sub-field scale in 9 dryland wheat fields throughout central Montana with Sentinel 2 images and post-harvest residue samples (Chapter 3, Ermatinger et al., Submitted). This field study afforded the opportunity to evaluate the potential of using RS to estimate different metrics of WSS infestation. For each field we produced a model for the proportions of total WSS infestation, adequate WSS infestation, and WSS cut stems and compared accuracy. We found that models of total ($R^2 = 0.57$) or adequate WSS infestations ($R^2 = 0.57$) outperformed models of WSS-cut stems ($R^2 = 0.34$). This may suggest that these methods are better suited to mapping patterns of WSS oviposition as opposed to end of season WSS stem cutting.

The variation in model performance across fields suggests that extrinsic factors should be incorporated in future studies of estimating WSS with remote sensing. Some of the fields with the lower performing models were affected by hail and grasshopper damage which likely obfuscated the impact of WSS infestation and resulting spectral responses. We recommend future studies incorporate co-located measurements of environmental parameters like soil conditions,

insect herbivory, and weed presence with stem dissection surveys. Estimates of WSS may be more accurately achieved by incorporating end of season active RS measurements as this method has shown promise for RS of lodging in wheat (Ajadi et al. 2020). Because the areas of greatest WSS cutting potential are related to the areas of highest total WSS infestation, multitemporal passive RS with end of season active RS might afford accurate estimates for both metrics.

Despite a rich history of ecological and management research, WSS has remained one of the most important pests to the production of wheat in North America for more than a century. Because WSS has access to hosts in agricultural and wildlands, it represents a perpetual threat to the production of wheat and other small cereal grains that requires long term monitoring for effective management. The difficulty in implementing management tactics such as planting solid stem wheat varieties, oats, or crop rotation to legumes or oil seeds is exacerbated by an inability to quantify WSS infestation and cutting across wheat fields. Supplementing estimates of WSS infestation and cutting produced from stem dissection surveys and RS alongside studies of applied management tactics, may help researchers and wheat producers better understand how to manage WSS. This may allow researchers to better study oviposition and mortality patterns in relation to variables of interest. Supplementing this type of monitoring with integrated pest management projects may help elucidate the impacts of individual tactics on WSS populations at the sub-field scale and add to our understanding of these at the landscape level.

CUMULATIVE REFERENCES

Achhami B, Peterson R, Sherman J, Reddy G, Weaver D. 2020. Multiple decrement life tables of *Cephus cinctus* Norton (Hymenoptera: Cephidae) across a set of barley cultivars: The importance of plant defense versus cannibalism. PLOS ONE. 15. doi: 10.1371/journal.pone.0238527.

Achhami B, Reddy G, Sherman J, Peterson R, Weaver D. 2020. Effect of precipitation and temperature on larval survival of *Cephus cinctus* (Hymenoptera: Cephidae) in barley cultivars. Journal of Economic Entomology. 113:1982–1989. doi:10.1093/jee/toaa097.

Achhami B, Reddy G, Sherman J, Weaver D, Peterson R. 2020. Antixenosis, antibiosis, and potential yield compensatory response in barley cultivars exposed to wheat stem sawfly (Hymenoptera: Cephidae) under field conditions. Journal of Insect Science. 20:1–14. doi: 10.1093/jisesa/ieaa091.

Ainslie CN. 1929. The western grass-stem sawfly (*Cephus cinctus* Norton): A pest of small grains. U.S Department of Agriculture Technical Bulletin Report No.: 157.

Ainslie CN. 1920. The western grass-stem sawfly. Washington, D.C. : U.S. Dept. of Agriculture.

Ajadi OA, Liao H, Jaacks J, Delos Santos A, Kumpatla SP, Patel R, Swatantran A. 2020. Landscape-scale crop lodging assessment across Iowa and Illinois using synthetic aperture radar (SAR) Images. Remote Sensing. 12(23):3885. doi: 10.3390/rs12233885.

Atstatt PR, O'Dowd DJ. 1976. Plant Defense Guilds: Many plants are functionally interdependent with respect to their herbivores. Science. 193(4247):24–29. doi: 10.1126/science.193.4247.24.

Bates D, Mächler M, Bolker B, Walker S. 2015. Fitting linear mixed-effects models using lme4. Journal of Statistical Software. 67:1–48. doi: 10.18637/jss.v067.i01.

Bathini A, Mendu L, Singh N, Cook J, Weaver D, Sherman J, Hager M, Mondal S, Mendu V. 2023. A "solid" solution for wheat stem sawfly (Hymenoptera: Cephidae) resistance: Genetics, breeding and development of solid stem wheat. Crop Science. 63. doi: 10.1002/csc2.20998.

Baumgardner MF, Leamer RW, Shay JR. 1970. Remote Sensing Techniques Used in Agriculture Today. In: Aerospace Science and Agricultural Development. 189(1): 9-26

Bauriegel E, Giebel A, Geyer M, Schmidt U, Herppich WB. 2011. Early detection of fusarium infection in wheat using hyper-spectral imaging. Computers and Electronics in Agriculture. 75(2):304–312. doi: 10.1016/j.compag.2010.12.006.

Bekkerman A, Weaver DK. 2018. Modeling joint dependence of managed ecosystems pests: the case of the wheat stem sawfly. Journal of Agricultural and Resource Economics. 43(2):172–194. doi: 10.22004/ag.econ.273445

Beres B, Hill B, Carcamo H, Knodel J, Weaver D, Cuthbert R. 2017. An artificial neural network model to predict wheat stem sawfly cutting in solid-stemmed wheat cultivars. Canadian Journal of Plant Science. 97. doi: 10.1139/CJPS-2016-0364.

Beres BL, Cárcamo HA, Bremer E. 2009. Evaluation of alternative planting strategies to reduce wheat stem sawfly (Hymenoptera: Cephidae) damage to spring wheat in the Northern Great Plains. Journal of Economic Entomology. 102(6):2137–2145. doi: 10.1603/029.102.0617.

Beres BL, Cárcamo HA, Byers JR. 2007. Effect of wheat stem sawfly damage on yield and quality of selected Canadian spring wheat. Journal of Economic Entomology. 100(1):79–87. doi: 10.1093/jee/100.1.79.

Beres BL, Cárcamo HA, Yang R-C, Spaner DM. 2011. Integrating spring wheat sowing density with variety selection to manage wheat stem sawfly. Agronomy Journal. 103(6):1755–1764. doi: 10.2134/agronj2011.0187.

Beres BL, Dosdall LM, Weaver DK, Cárcamo HA, Spaner DM. 2011. Biology and integrated management of wheat stem sawfly and the need for continuing research. Canadian Entomologist. 143(2):105–125. doi: 10.4039/n10-056.

Beres BL, Meers SM, Delaney KJ, Cárcamo HA, Miller PR, Spaner DM, Weaver DK. 2024. Stem height and harvest management influence conservation biological control of wheat stem sawfly by endemic parasitoids. Canadian Journal of Plant Science. doi: 10.1139/cjps-2024-0227

Bhandari R. 2020. Assessment of host selection behaviors and oviposition preferences of *Cephus cinctus* Norton (Hymenoptera: Cephidae) using wheat and smooth brome [Master's thesis]. Bozeman, MT (USA). Montana State University.

Bhattarai GP, Schmid RB, McCornack BP. 2019. Remote sensing data to detect hessian fly infestation in commercial wheat fields. Scientific Reports. 9(1). doi: 10.1038/s41598-019-42620-0.

Bidinger F, Musgrave RB, Fischer RA. 1977. Contribution of stored pre-anthesis assimilate to grain yield in wheat and barley. Nature. 270(5636):431–433. doi: 10.1038/270431a0.

Bioucas-Dias JM, Plaza A, Camps-Valls G, Scheunders P, Nasrabadi N, Chanussot J. 2013. Hyperspectral remote sensing data analysis and future challenges. IEEE Geoscience and Remote Sensing Magazine. 1(2):6–36. doi: 10.1109/MGRS.2013.2244672.

Bro R. 1996. Multiway calibration. multilinear PLS. Journal of Chemometrics. 10(1):47–61. doi: 10.1002/(SICI)1099-128X(199601)10:1<47::AID-CEM400>3.0.CO;2-C.

Brooks M, Bolker B, Kristensen K, Maechler M, Magnusson A, McGillycuddy M, Skaug H, Nielsen A, Berg C, Bentham K van, et al. 2024. glmmTMB: Generalized Linear Mixed Models using Template Model Builder. doi: 10.32614/RJ-2017-066

Buteler M, Peterson RKD, Hofland ML, Weaver DK. 2015. Multiple decrement life table reveals that host plant resistance and parasitism are major causes of mortality for the wheat stem sawfly. Environmental Entomology. 44(6):1571–1580. doi: 10.1093/ee/nvv128.

Buteler M, Peterson RKD, Weaver DK. 2009. Oviposition behavior of the wheat stem sawfly when encountering plants infested with cryptic conspecifics. Environmental Entomology. 38(6):1707–1715. doi: 10.1603/022.038.0624.

Buteler M, Weaver DK. 2012. Host selection by the wheat stem sawfly in winter wheat and the role of semiochemicals mediating oviposition preference. Entomologia Experimentalis et Applicata. 143(2):138–147. doi: 10.1111/j.1570-7458.2012.01237.x.

Buteler M, Weaver DK, Bruckner PL, Carlson GR, Berg JE, Lamb PF. 2010. Using agronomic traits and semiochemical production in winter wheat cultivars to identify suitable trap crops for the wheat stem sawfly. The Canadian Entomologist. 142(3):222–233. doi: 10.4039/n09-072.

Carcamo H, Beres B, Clarke F, Byers R, Mündel H -h, May K, DePauw R. 2005. Influence of plant host quality on fitness and sex ratio of the wheat stem sawfly (Hymenoptera: Cephidae). Environmental Entomology. 34:1579–1592. doi: 10.1603/0046-225X-34.6.1579.

Cárcamo H, Entz T, Beres B. 2007. Estimating *Cephus cinctus* wheat stem cutting damage – can we cut stem counts? Journal of Agri cultural and Urban Entomology. 24(3):117–124. doi: 10.3954/1523-5475-24.3.117.

Cavallini L, Peterson R, Weaver D. 2023. Dietary sugars and amino acids increase longevity and enhance reproductive parameters of *Bracon cephi* and *B. lissogaster*, two parasitoids that specialise on wheat stem sawfly. Physiological Entomology. 48(1):24-34. doi: 10.1111/phen.12399.

Cavallini L, Peterson R, Weaver D. 2023. Cowpea extrafloral nectar has potential to provide ecosystem services lost in agricultural intensification and support native parasitoids that suppress the wheat stem sawfly. Journal of Economic Entomology. 116(3):752-760. doi: 10.1093/jee/toad083.

Claverie M, Ju J, Masek JG, Dungan JL, Vermote EF, Roger J-C, Skakun SV, Justice C. 2018. The harmonized Landsat and Sentinel-2 surface reflectance data set. Remote Sensing of Environment. 219:145–161. doi: 10.1016/j.rse.2018.09.002.

Cockrell DM, Griffin-Nolan RJ, Rand TA, Altilmisani N, Ode PJ, Peairs F. 2017. Host plants of the wheat stem sawfly (Hymenoptera: Cephidae). Environmental Entomology. 46(4):847–854. doi: 10.1093/ee/nvx104.

Cockrell DM, Randolph T, Peirce E, Peairs FB. 2021. Survey of wheat stem sawfly (Hymenoptera: Cephidae) infesting wheat in eastern Colorado. Journal of Economic Entomology. 114(2):998–1004. doi: 10.1093/jee/toab015.

Collins W. 1978. Remote sensing of crop type and maturity. Photogrammetric Engineering and Remote Sensing. 44(1):43-55

Crema A, Boschetti M, Nutini F, Cillis D, Casa R. 2020. Influence of soil properties on maize and wheat nitrogen status assessment from Sentinel-2 data. Remote Sensing. 12(14). doi: https://doi.org/10.3390/rs12142175.

Criddle N. 1922. The western-stem sawfly and its control. Dominion of Canada Department of Agriculture.(6):1–8.

Criddle N. 1923. Popular and practical entomology: The life habits of *Cephus cinctus* Norton in Manitoba. The Canadian Entomologist. 55(1):1–4. doi: 10.4039/Ent551-1.

Dahiya S, Sihag S, Chaudhary C. 2018. Lodging: Significance and preventive measures for increasing crop production. International Journal of Chemical Studies. 6:700–705. E-ISSN: 2321-4902

Danner M, Locherer M, Hank T, Richter K. 2015. Spectral sampling with the ASD Fieldspec 4 EnMAP Field Guides Technical Report. doi: 10.2312/enmap.2015.008.

Davis RA. 2013. Mechanisms for reproductive isolation in two congeneric parasitoids of the wheat stem sawfly. Montana State University - Bozeman, College of Agriculture. [MS Thesis]. Bozeman, MT (USA). Montana State University.

Delaney KJ, Weaver DK, Peterson RKD. 2010. Photosynthesis and yield reductions from wheat stem sawfly (Hymenoptera: Cephidae): Interactions with wheat solidness, Water stress, and phosphorus deficiency. Journal of Economic Entomology. 103(2):516–524. doi: 10.1603/EC09229.

Emerson R, Rabinowitch E. 1960. Red drop and role of auxiliary pigments in photosynthesis. Plant Physiol. 35(4):477–485.

Ermatinger LS, Powell SL, Peterson RKD, Weaver DK. 2024. Multitemporal hyperspectral characterization of wheat infested by wheat stem sawfly, *Cephus cinctus* Norton. Remote Sensing. 16(18):3505. doi: 10.3390/rs16183505.

Everaerts J. 2008. The use of unmanned aerial vehicles (UAVs) for remote sensing and mapping. In: The International Archives of the Photogrammetry, Remote Sensing and Spatial Information Sciences. Vol. 37.

Farstad C. 1940. The development of western wheat stem sawfly (*Cephus cinctus* Norton) in various host plants as an index of resistance. Iowa State College Journal of Science.(15):67–69. doi: 10.31274/RTD-180813-14901.

Farstad CW. 1944. Wheat stem sawfly in flax. Scientific Agriculture. 24(8):383–386. doi: 10.4141/sa-1944-0025.

Fernandez-Cornejo J, Nehring RF, Osteen C, Wechsler S, Martin A, Vialou A. 2014. Pesticide use in U.S. agriculture: 21 selected crops, 1960-2008. USDA-ERS Economic Information Bulletin Number 124. doi: 10.2139/ssrn.2502986.

Fieuzal R, Bustillo V, Collado D, Dedieu G. 2020. Combined use of multi-temporal Landsat-8 and Sentinel-2 images for wheat yield estimates at the intra-plot spatial scale. Agronomy. 10(3):327. doi: 10.3390/agronomy10030327.

Fisher DS, Miller CD, Morgan JO, Parker DC. 1963. Remote sensing of environment. Infrared Laboratory, Institute of Science and Technology, University of Michigan Report No.: 4864-6- F.

Fletcher J. 1896. The western wheat stem sawfly (*Cephus pygmaeus* L.). Dominion of Canada, Department of Agriculture, Report of the Dominion Entomologist. 1(1896):147–149.

Fuentes S, Tongson E, Unnithan RR, Gonzalez Viejo C. 2021. Early detection of aphid infestation and insect-plant interaction assessment in wheat using a low-cost electronic nose (E-Nose), near-infrared spectroscopy and machine learning modeling. Sensors. 21(17):5948. doi: 10.3390/s21175948.

Fulbright J, Wanner K, Bekkerman A, Weaver D. 2017. Wheat stem sawfly biology. Montana State University Extension, MontGuide, MT201107AG.

Gao B-C. 1996. NDWI a normalized difference water index for remote sensing of vegetation liquid water from Space. Remote Sensing of Environment. 58:257-266. doi: 10.1016/S0034-4257(96)00067-3

Gates DM, Keegan HJ, Schleter JC, Weidner VR. 1965. Spectral properties of plants. 4(1):11-20. doi: 10.1364/AO.4.000011

Gausman HW. 1985. Plant leaf optical properties in visible and near-infrared light. [PhD thesis]. Lubbock, TX (USA): Texas Technical University.

Georganos S, Grippa T, Vanhuysse S, Lennert M, Shimoni M, Kalogirou S, Wolff E. 2018. Less is more: optimizing classification performance through feature selection in a very-high-resolution remote sensing object-based urban application. GIScience and Remote Sensing. 55(2):221–242. doi: [10.1080/15481603.2017.1408892](10.1080/15481603.2017.1408892).

Gobbo S, Ghiraldini A, Dramis A, Dal Ferro N, Morari F. 2021. Estimation of hail damage using crop models and remote sensing. Remote Sensing. 13(14):2655. doi: [10.3390/rs13142655](10.3390/rs13142655).

Goodarzi M, Freitas MP. 2009. On the use of PLS and N-PLS in MIA-QSAR: Azole antifungals. Chemometrics and Intelligent Laboratory Systems. 96(1):59–62. doi: 10.1016/j.chemolab.2008.11.007.

Goosey HB. 1999. In field distributions of the wheat stem sawfly, (Hymenoptera: Cephidae), and evaluation of selected tactics for an integrated management program. [MS Thesis] Bozeman, MT (USA). Montana State University.

Gorelick N, Hancher M, Dixon M, Ilyushchenko S, Thau D, Moore R. 2017. Google Earth Engine: Planetary-scale geospatial analysis for everyone. Remote Sensing of Environment. 202(1):18–27. doi: [10.1016/j.rse.2017.06.031](10.1016/j.rse.2017.06.031).

Haack BN. 1982. Landsat: A tool for development. World Development. 10(10):899–909. doi: [10.1016/0305-750X(82)90064-X](10.1016/0305-750X(82)90064-X).

Han W, Yang Z, Di L, Mueller R, 2012. CropScape: A Web service based application for exploring and disseminating US conterminous geospatial cropland data products for decision support. Computers and Electronics in Agriculture, 84, 111–123. doi: 10.1016/j.compag.2012.03.005

Hastie T, Tibshirani R, Friedman J, Franklin J. 2009. The Elements of Statistical Learning: Data Mining, Inference, and Prediction. The Mathematical Intelligencer. 27(2): 83-85

Hatchell DC. 1999. ASD technical guide 3rd ed. section 0-1 technical guide. Boulder, CO.: Analytical Spectral Devices.

Hatfield PL, Pinter PJ. 1993. Remote sensing for crop protection. Crop Protection. 12(6):403–413. doi: [10.1016/0261-2194(93)90001-Y](10.1016/0261-2194(93)90001-Y).

Hervas D, sNPLS. 2022. Available online: https://cran.r-project.org/web/packages/sNPLS/index.html.

Hervás D, Prats-Montalbán JM, García-Cañaveras JC, Lahoz A, Ferrer A. 2019. Sparse n-way partial least squares by l1-penalization. Chemometrics and Intelligent Laboratory Systems. 185:85–91. doi: 10.1016/j.chemolab.2019.01.004.

Hervás D, Prats-Montalbán JM, Lahoz A, Ferrer A. Sparse N-way partial least squares with R package sNPLS. Chemometrics and Intelligent Laboratory Systems. 2018, 179, 54–63.

Holmes ND. 1954. Food relations of the wheat stem Sawfly. The Canadian Entomologist. 86(4):159–167. doi: 10.4039/Ent86159-4.

Holmes ND. 1975. Effects of moisture, gravity, and light on the behavior of larvae of the wheat stem sawfly, *Cephus cinctus* (Hymenoptera: Cephidae). The Canadian Entomologist. 107(4):391–401. doi: 10.4039/ent107391-4.

Holmes ND. 1982. Population dynamics of the wheat stem sawfly, *Cephus cinctus* (Hymenoptera: Cephidae), in wheat. The Canadian Entomologist. 114(9):775–788. doi: 10.4039/Ent114775-9.

Holmes ND, Nelson WA, Peterson LK, Farstad CW. 1963. Causes of variations in effectiveness of *Bracon cephi* (Gahan) (Hymenoptera: Braconidae) as a parasite of the wheat stem sawfly. The Canadian Entomologist. 95(2):133–126. doi: 10.4039/Ent95113-2.

Holmes ND, Peterson LK. 1960. The influence of the host on oviposition by the wheat stem sawfly, *Cephus cinctus* Norton. (Hymenoptera: Cephidae). Can J Plant Sci. 40(1):29–46. doi: 10.4141/cjps60-004.

Holmes RA, MacDonald RB. 1969. The physical basis of system design for remote sensing in agriculture. Proceedings of the IEEE. 57(4):629–639. doi: 10.1109/PROC.1969.7018.

Hu X, Sun L, Gu X, Sun Q, Wei Z, Pan Y, Chen L. 2021. Assessing the self-recovery ability of maize after lodging using UAV-LiDAR data. Remote Sensing. 13(12):2270. doi: 10.3390/rs13122270.

Hughes FG. 1986. On the mean accuracy of statistical pattern recognizers. IEEE. IT-14(1):55–63. doi: 10.1109/TIT.1968.1054102

Hunt ER, Rock BN. 1989. Detection of changes in leaf water content using near- and middle-Infrared reflectances. Remote Sensing of Environment. 30(1):43–54. doi: 10.1016/0034-4257(89)90046-1.

Jensen JR. 1983. Biophysical remote sensing. Annals of the Association of American Geographers. 73(1):111–132. doi: 10.1111/j.1467-8306.1983.tb01399.x.

Jones BH, Blake NK, Heo H-Y, Martin JM, Torrion JA, Talbert LE. 2021. Allelic response of yield component traits to resource availability in spring wheat. Theoretical Applied Genetics. 134(2):603–620. doi: 10.1007/s00122-020-03717-7.

Knipling EB. 1970. Physical and physiological basis for the reflectance of visible and near-infrared radiation from vegetation. Remote sensing of environment. doi:10.1016/S0034-4257(70)80021-9.

Knodel J, Shanower T, Beauzay P. 2016. Distribution and history. Fargo, ND.: North Dakota State University, Extension Service.

Knodel J, Shanower T, Beauzay PB. 2010. Integrated pest management of wheat stem sawfly in North Dakota. North Dakota State University Cooperative Extension Bulletin. E-1479.

Lanning SP, Fox P, Elser J, Martin JM, Blake NK, Talbert LE. 2006. Microsatellite markers associated with a secondary stem solidness locus in wheat. Crop Science. 46(4):1701–1703. doi: 10.2135/cropsci2005.10-0379.

Lee H, Cho S, Lim J, Lee A, Kim G, Song D-J, Chun S-W, Kim M-J, Mo C. 2023. Performance comparison of tungsten-halogen light and phosphor-converted NIR led in soluble solid content estimation of apple. Sensors. 23(4):1961. doi: 10.3390/s23041961.

Lenth RV, Banfai B, Bolker B, Buerkner P, Giné-Vázquez I, Herve M, Jung M, Love J, Miguez F, Piaskowski J, et al. 2024. Emmeans: estimated marginal means, aka least-squares means. doi: 10.32614/CRAN.package.emmeans

Lesieur V, Martin J-F, Weaver DK, Hoelmer KA, Smith DR, Morrill WL, Kadiri N, Peairs FB, Cockrell DM, Randolph TL, et al. 2016. Phylogeography of the wheat stem sawfly, *Cephus cinctus* Norton (Hymenoptera: Cephidae): implications for pest management. PLOS ONE. 11(12):e0168370. doi: 10.1371/journal.pone.0168370.

Lestina J, Cook M, Kumar S, Morisette J, Ode PJ, Peairs F. 2016. MODIS imagery improves pest risk assessment: A case study of wheat stem sawfly (*Cephus cinctus*, Hymenoptera: Cephidae) in Colorado, USA. Environmental Entomology. 45(6):1343–1351. doi: 10.1093/ee/nvw095.

Liu J, van Iersel MW. 2021. Photosynthetic physiology of blue, green, and red light: light intensity effects and underlying mechanisms. Frontiers in Plant Science. 12. doi: 10.3389/fpls.2021.619987.

Lopez-Fornieles E, Brunel G, Rancon F, Gaci B, Metz M, Devaux N, Taylor J, Tisseyre B, Roger JM. 2022. Potential of multiway pls (N-PLS) regression method to analyze time-series of multispectral images: a case study in agriculture. Remote Sensing. 14(1). doi: 10.3390/rs14010216.

Ma H, Huang W, Dong Y, Liu L, Guo A. 2021. Using UAV-based hyperspectral imagery to detect winter wheat *Fusarium* head blight. Remote Sensing. 13(15). doi: 10.3390/rs13153024.

Ma H, Jing Y, Huang W, Shi Y, Dong Y, Zhang J, Liu L. 2018. Integrating early growth information to monitor winter wheat powdery mildew using multi-temporal landsat-8 imagery. Sensors. 18(10) 3290. doi: 10.3390/s18103290.

Macdonald RB, Hall FG, Erb RB. 1975. The use of LANDSAT data in a large area crop inventory experiment (LACIE). In *LARS Symposia*, p. 46. 1975.

Macedo TB, Peterson RKD, Weaver DK, Morrill WL. 2005. Wheat stem sawfly, *Cephus cinctus* Norton, impact on wheat primary metabolism: An ecophysiological approach. Environmental Entomology. 34(3): 719-726. doi: 10.1603/0046-225X-34.3.719

Macedo TB, Weaver DK, Peterson RKD. 2006. Characterization of the impact of wheat stem sawfly, *Cephus cinctus* Norton, on pigment composition and photosystem II photochemistry of wheat heads. Environmental Entomology. 35(4): 1115-1120. doi: 10.1603/0046-225X-35.4.1115

Macedo TB, Weaver DK, Peterson RKD. 2007. Photosynthesis in wheat at the grain filling stage is altered by larval wheat stem sawfly (Hymenoptera: Cephidae) injury and reduced water availability Journal of Entomological Science. 42(2): 228 – 238. doi: 10.18474/0749-8004-42.2.228

Mackay MR. 1955. Cytology and parthenogenesis of the wheat stem sawfly, *Cephus cinctus* Norton. (Hymenoptera: Cephidae). Canadian Journal of Zoology. 33(3):161–174. doi: 10.1139/z55-011.

Main-Knorn M, Pflug B, Louis J, Debaecker V, Müller-Wilm U, Gascon F. 2017. Sen2Cor for Sentinel-2. In: Image and signal processing for remote sensing XXIII. Vol. 10427. SPIE. p. 37–48. doi: 10.1117/12.2278218

McCullough CT, Hein GL, Bradshaw JD. 2020. Phenology and dispersal of the wheat stem sawfly (Hymenoptera: Cephidae) into winter wheat fields in Nebraska. Journal of Economic Entomology. 113(4):1831–1838. doi: 10.1093/jee/toaa093.

Miller P, Lanier W, Brandt S. 2001. Using growing degree days to predict plant stages. Montana State University Extension. MontGuide, MT200103 AG.

Mirik M, Jones DC, Price JA, Workneh F, Ansley RJ, Rush CM. 2011. Satellite remote sensing of wheat infected by wheat streak mosaic virus. Plant Disease. 95(1):4–12. doi: 10.1094/PDIS-04-10-0256.

Montana Department of Agriculture (MDA). (2015). Thimet® 20-G. EPA SLN No.MT-150001.

Moore RK, Simonett DS. 1967. Radar remote sensing in biology. BioScience. 17(6):384–390. doi: 10.2307/1293798.

Morales G, Sheppard JW, Logan RD, Shaw JA. 2021. Hyperspectral dimensionality reduction based on inter-band redundancy analysis and greedy spectral selection. Remote Sensing. 13(18). doi: 10.3390/rs13183649.

Morrill WL, Gabor JW, Kushnak GD. 1992. Wheat stem sawfly (Hymenoptera: Cephidae): Damage and detection. Journal of Economic Entomology. 85(6): 2413-2417. doi: 10.1093/jee/85.6.2413

Morrill WL, Gabor JW, Weaver DK, Kushnak GD, Irish NJ. 2000. Effect of host plant quality on the sex ratio and fitness of female wheat stem sawflies (Hymenoptera: Cephidae). Environmental Entomology. 29(2):195–199. doi: 10.1093/ee/29.2.195.

Morrill WL, Gabor JW, Wichman D. 1993. Mortality of the wheat stem sawfly (Hymenoptera: Cephidae) at low temperatures. Environmental Entomology. 22(6):1358–1361. doi: 10.1093/ee/22.6.1358.

Morrill WL, Kushnak GD. 1999. Planting date influence on the wheat stem sawfly (Hymenoptera: Cephidae) in spring wheat. Journal of Agricultural and Urban Entomology. 16(2): 123-128.

Morrill WL, Kushnak GD, Bruckner PL, Gabor JW. 1994. Wheat stem sawfly (Hymenoptera: Cephidae) damage, rates of parasitism, and overwinter survival in resistant wheat lines. Journal of Economic Entomology. 87(5):1373–1376. doi: 10.1093/jee/87.5.1373.

Morrill WL, Weaver DK, Johnson GD. 2001. Trap strip and field border modification for management of the wheat stem sawfly (Hymenoptera: Cephidae). Journal of Entomological Science. 36(1):34–45. doi: 10.18474/0749-8004-36.1.34.

Munro JA. 1945. Wheat stem sawfly and harvest loss. North Dakota Agricultural Experimental Station Bimonthly Bulletin. 7(4): 12-16.

Myers VI, Allen WA. 1968. Electrooptical remote sensing methods as nondestructive testing and measuring techniques in agriculture. Applied Optics. 7(9):1819–1838. doi: 10.1364/AO.7.001819.

Nansen C, Elliott N. 2016. Remote sensing and reflectance profiling in entomology. Annual Review of Entomoly. 61(1):139–158. doi: 10.1146/annurev-ento-010715-023834.

Nansen C, Macedo T, Swanson R, Weaver DK. 2009. Use of spatial structure analysis of hyperspectral data cubes for detection of insect-induced stress in wheat plants. International Journal of Remote Sensing. 30(10):2447–2464. doi: 10.1080/01431160802552710.

Nansen C, Macedo TB, Weaver DK, Peterson RKD. 2005. Spatiotemporal distributions of wheat stem sawfly eggs and larvae in dryland wheat fields. Canadian Entomologist. 137(4):428–440. doi: 10.4039/n04-094.

Nansen C, Weaver DK, Sing SE, Runyon JB, Morrill WL, Grieshop MJ, Shannon CL, Johnson ML. 2005. Within-field spatial distribution of Cephus cinctus (Hymenoptera: Cephidae) larvae in Montana wheat fields. Canadian Entomologist. 137: 202 – 214.

National Agricultural Statistics Service, Mountain Regional Field Office. 2023. Montana 2023 wheat varieties. United States Department of Agriculture. Available at: https://www.nass.usda.gov/Statistics_by_State/Montana/Publications/Special_Interest_Reports/MT-Wheat-Varieties-2023.pdf.

Neuwirthová E, Lhotáková Z, Albrechtová J. 2017. The effect of leaf stacking on leaf reflectance and vegetation indices measured by contact probe during the season. Sensors. 17(6):1202. doi: 10.3390/s17061202.

Neves AD, Oliveira RF, Parra JRP. 2006. A new concept for insect damage evaluation based on plant physiological variables. An Acad Bras Ciênc. 78:821–835. doi: 10.1590/S0001-37652006000400015.

Nino P, D'Urso G, Vanino S, Di Bene C, Farina R, Falanga Bolognesi S, De Michele C, Napoli R. 2024. Nitrogen status of durum wheat derived from Sentinel-2 satellite data in central Italy. Remote Sensing Applications: Society and Environment. 36:101323. doi: 10.1016/j.rsase.2024.101323.

Norton E. 1872. Notes on North American Tenthredinidae, with descriptions of new species. Transactions of the American Entomological Society (1867-1877). 4:77–86. doi: 10.2307/25076265.

Olfert O, Weiss RM, Catton H, Cárcamo H, Meers S. 2019. Bioclimatic assessment of abiotic factors affecting relative abundance and distribution of wheat stem sawfly (Hymenoptera: Cephidae) in western Canada. The Canadian Entomologist. 151(1):16–33. doi: 10.4039/tce.2018.46.

Payne EH, Hardin JW, Egede LE, Ramakrishnan V, Selassie A, Gebregziabher M. 2017. Approaches for dealing with various sources of overdispersion in modeling count data: Scale adjustment versus modeling. Statistical Methods in Medical Research. 26(4):1802–1823. doi: 10.1177/0962280215588569.

Peirce E, Cockrell D, Mason RE, Haley S, Peairs F, Nachappa P. 2022. Solid stems and beyond: challenges and future directions of resistance to wheat stem sawfly (Hymenoptera: Cephidae). Journal of Integrated Pest Management. 13(1): 29. doi: 10.1093/jipm/pmac023.

Peirce ES, Rand TA, Cockrell DM, Ode PJ, Peairs FB. 2021. Effects of landscape composition on wheat stem sawfly (Hymenoptera: Cephidae) and its associated braconid parasitoids. Journal of Economic Entomology. 114(1):72–81. doi: 10.1093/jee/toaa287.

Perez-Mendoza J, Weaver DK. 2006. Temperature and relative humidity effects on postdiapause larval development and adult emergence in three populations of wheat stem sawfly (Hymenoptera: Cephidae). Environmental Entomology. 35(5):1222–1231. doi: 10.1093/ee/35.5.1222.

Perez-Mendoza J, Weaver DK, Morrill WL. 2006. Infestation of wheat and downy brome grass by wheat stem sawfly and subsequent larval performance. Environmental Entomology. 35(5):1279–1285. doi: 10.1093/ee/35.5.1279.

Peterson RKD, Higley LG. 1993. Arthropod injury and plant gas exchange: current understandings and approaches for synthesis. Trends in Agricultural Science. 1:93–100.

Phillips RE, Thomas GW, Blevins RL, Frye WW, Phillips SH. 1980. No-Tillage agriculture. Science. 208(4448): 1108-1113. doi: 10.1126/science.208.4448.1108.

Piesik D, Weaver DK, Runyon JB, Buteler M, Peck GE, Morrill WL. 2008. Behavioural responses of wheat stem sawflies to wheat volatiles. Agricultural and Forest Entomology. 10(3):245–253. doi: 10.1111/j.1461-9563.2008.00380.x.

Platt AW. 1941. The influence of some environmental factors on the expression of the solid stem character in certain wheat varieties. Scientific Agriculture. 22(3): 139-151.

Platt AW, Farstad CW, Callenbach JA. 1948. The reaction of Rescue wheat to sawfly damage. Scientific Agriculture. 28(4):154–161. doi: 10.4141/sa-1948-0026.

Portman S, Jaronski S, Weaver D, Reddy G. 2018. Advancing biological control of the wheat stem sawfly: new strategies in a 100-yr struggle to manage a costly pest in the Northern Great Plains. Annals of the Entomological Society of America. 111:85–91. doi: 10.1093/aesa/say002.

PRISM Climate Group. 2014. Oregon State University. Available at: https://prism.oregonstate.edu

Qiao M, He X, Cheng X, Li P, Luo H, Zhang L, Tian Z. 2021. Crop yield prediction from multi-spectral, multi-temporal remotely sensed imagery using recurrent 3D convolutional neural networks. International Journal of Applied Earth Observation and Geoinformation. 102:102436. doi: 10.1016/j.jag.2021.102436.

Rabieyan E, Darvishzadeh R, Alipour H. 2023. Identification and estimation of lodging in bread wheat genotypes using machine learning predictive algorithms. Plant Methods. 19(1):109. doi:10.1186/s13007-023-01088-w.

Rand TA, Kula RR, Gaskin JF. 2024. Evaluating the use of common grasses by the wheat stem sawfly (Hymenoptera: Cephidae) and its native parasitoids in rangeland and Conservation Reserve Program grasslands. Journal of Economic Entomology. 117(3):858–864. doi: 10.1093/jee/toae046.

Rand TA, Titus EF, Waters DK. 2019. Do floral resources benefit the herbivorous sawfly, *Cephus cinctus* (Hymenoptera: Cephidae), a major pest of wheat in North America? Journal of Economic Entomology. 112(2):565–570. doi: 10.1093/jee/toy408.

R Core Team. R Language Definition; R Foundation for Statistical Computing: Vienna, Austria, 2023

Reis DA, Hofland ML, Peterson RKD, Weaver DK. 2019. Effects of sucrose supplementation and generation on life-history traits of *Bracon cephi* and *Bracon lissogaster*, parasitoids of the wheat stem sawfly. Physiological Entomology. 44(3–4):266–274. doi: 10.1111/phen.12303.

Roberts DR, Bahn V, Ciuti S, Boyce MS, Elith J, Guillera-Arroita G, Hauenstein S, Lahoz-Monfort JJ, Schröder B, Thuiller W, et al. 2017. Cross-validation strategies for data with temporal, spatial, hierarchical, or phylogenetic structure. Ecography. 40(8):913–929. doi: 10.1111/ecog.02881.

Rodriguez D, Fitzgerald G, Belford R, Christensen L. 2006. Detection of nitrogen deficiency in wheat from spectral reflectance indices and basic crop eco-physiological concepts. Australian Journal of Agricultural Research. 57:781–789. doi: 10.1071/AR05361.

Roemhild GR. 1954. Morphological resistance of some of the Gramineae to the wheat stem sawfly (*Cephus cinctus* Norton) [PhD thesis]. Bozeman, MT (USA): Montana State University.

Romero A, Gatta C, Camps-Valls G. 2016. Unsupervised deep feature extraction for remote sensing image classification. IEEE Transactions on Geoscience and Remote Sensing. 54(3):1349–1362. doi: 10.1109/TGRS.2015.2478379.

Roudier P, Lalibert' E, Asdreader. 2017. Available online: https://cran.r-project.org/web/packages/asdreader/index.html

Runyon JB. 2001. Wheat stem sawfly parasitism in varying field sizes and tillage systems in dryland wheat in Montana. [Master's thesis]. Bozeman, MT (USA): Montana State University.

Runyon JB, Morrill WL, Weaver DK, Miller PR. 2002. Parasitism of the wheat stem sawfly (Hymenoptera: Cephidae) by *Bracon cephi* and *B. lissogaster* (Hymenoptera: Braconidae) in wheat fields bordering tilled and untilled fallow in Montana. Journal of Economic Entomology. 95(6):1130–1134. doi: 10.1603/0022-0493-95.6.1130.

Salt RW. 1947. Some effects of temperature on the production and elimination of diapause in the wheat stem sawfly, *Cephus cinctus* Norton. Canadian Journal of Research. 25d(2): 66–86. doi: 10.1139/cjr47d-004.

Schweiger AK, Cavender-Bares J, Townsend PA, Hobbie SE, Madritch MD, Wang R, Tilman D, Gamon JA. 2018. Plant spectral diversity integrates functional and phylogenetic components of biodiversity and predicts ecosystem function. Nature Ecology and Evolution. 2(6):976–982. doi: 10.1038/s41559-018-0551-1.

Seamans HL. 1928. The value of trap crops in the control of the wheat stem sawfly in Alberta. Annual Report of the Entomological Society of Ontario 59: 59–64.

Seamans HL. 1945. A preliminary report on the climatology of the wheat stem sawfly (*Cephus cinctus* Norton) on the Canadian Prairies. Scientific Agriculture. 25(7):432–457. doi: 10.4141/sa-1945-0012.

Seamans HL, Manson GF, Farstad CW. 1944. The effect of wheat stem sawfly (*Cephus cinctus*) on the heads and grain of infested stems. Annual Report of the Entomological Society of Ontario 75: 10–15.

Seelig HD, Hoehn A, Stodieck LS, Klaus DM, Adams WW, Emery WJ. 2008. The assessment of leaf water content using leaf reflectance ratios in the visible, near-, and short-wave-infrared. International Journal of Remote Sensing. 29(13):3701–3713. doi: 10.1080/01431160701772500.

Segarra J, Buchaillot ML, Araus JL, Kefauver SC. 2020. Remote sensing for precision agriculture: Sentinel-2 improved features and applications. Agronomy. 10(5):641. doi: 10.3390/agronomy10050641.

Serrano L, Peñuelas J, Ustin SL. 2001. Remote sensing of nitrogen and lignin in Mediterranean vegetation from AVIRIS data: Decomposing biochemical from structural signals. Remote Sensing of Environment. 81(2-3): 355-364. 10.1016/S0034-4257(02)00011-1

Shanower T, Waters D. 2006. A survey of five stem-feeding insect pests of wheat in the Northern Great Plains. Journal of Entomological Science. 41. doi: 10.18474/0749-8004-41.1.40.

Sing SE. 2002. Spatial and biotic interactions of the wheat stem sawfly with wild oat and Montana dryland spring wheat. [PhD Thesis]. Bozeman, MT (USA): Montana State University.

Sjolie DM, Willenborg CJ, Vankosky MA. 2024. The causes of wheat stem sawfly (Hymenoptera: Cephidae) larval mortality in the Canadian prairies. The Canadian Entomologist. 156(e3): 1-15. doi: 10.4039/tce.2023.29.

Slaton MR, Raymond Hunt Jr. E, Smith WK. 2001. Estimating near-infrared leaf reflectance from leaf structural characteristics. American Journal of Botany. 88(2):278–284. doi: 10.2307/2657019.

Solgi S, Ahmadi SH, Seidel SJ. 2023. Remote sensing of canopy water status of the irrigated winter wheat fields and the paired anomaly analyses on the spectral vegetation indices and grain yields. Agricultural Water Management. 280:108226. doi: 10.1016/j.agwat.2023.108226.

Song X-P, Huang W, Hansen MC, Potapov P. 2021. An evaluation of Landsat, Sentinel-2, Sentinel-1 and MODIS data for crop type mapping. Science of Remote Sensing. 3:100018. doi: 10.1016/j.srs.2021.100018.

Stein A, Bastiaanssen ,W. G. M., De Bruin, S., Cracknell, A. P., Curran, P. J., Fabbri, A. G., Gorte, B. G. H., Van Groenigen, J. W., Van Der Meer, F. D., and Saldana A. 1998. Integrating spatial statistics and remote sensing. International Journal of Remote Sensing. 19(9):1793–1814. doi: 10.1080/014311698215252.

Stevens A, Ramirez-Lopez L, Prospectr. 2024. Available online: https://cran.r-project.org/web/packages/prospectr/index.html

Strand J, Moya O, Peterson R, Sterling T, Weaver D. 2025. Sensory and behavioral responses of braconid parasitoids to changes in volatile emissions induced by wheat stem sawfly (Hymenoptera: Cephidae) larval feeding in winter wheat and smooth brome. Journal of Insect Science. 25. doi: 10.1093/jisesa/ieaf016.

Strand J, Peterson R, Sterling T, Weaver D. 2024 Oct 28. Agroecological importance of smooth brome in managing wheat stem sawfly (Hymenoptera: Cephidae) via associated braconid parasitoids. Journal of Economic Entomology. doi: 10.1093/jee/toae246.

Subedi M, Cárcamo HA, Knodel JJ, Weaver DK, Cuthbert RD, Pozniak CJ, Nilsen KT, Beres BL. 2021. Stability analysis of stem solidness, grain yield, and grain protein concentration in spring wheat. Canadian Journal of Plant Science. 101(4):456–475. doi: 10.1139/cjps-2020-0089.

Thomas S, Kuska MT, Bohnenkamp D, Brugger A, Alisaac E, Wahabzada M, Behmann J, Mahlein AK. 2018. Benefits of hyperspectral imaging for plant disease detection and plant protection: a technical perspective. Journal of Plant Diseases and Protection. 125(1):5–20. doi: 10.1007/s41348-017-0124-6.

Thoms L-J, Girwidz R. 2015. Training and assessment of experimental competencies from a distance: Optical spectrometry via the Internet. Il Nuovo Cimento C. 38:113. doi: 10.1393/ncc/i2015-15113-3.

Tibshirani R. 1996. Regression shrinkage and selection via the lasso. Journal of the Royal Statistical Society: Series B (Methodological). 58(1): 267-288. doi: 10.1111/j.2517-6161.1996.tb02080.x

Tilling AK, O'Leary GJ, Ferwerda JG, Jones SD, Fitzgerald GJ, Rodriguez D, Belford R. 2007. Remote sensing of nitrogen and water stress in wheat. Field Crops Research. 104(1–3):77–85. doi: 10.1016/j.fcr.2007.03.023.

Tucker CJ. 1979. Red and photographic infrared linear combinations for monitoring vegetation. Remote Sensing of Environment. 8(2): 127-150. doi.org/10.1016/0034-4257(79)90013-0

Tucker CJ. 1980. Remote sensing of leaf water content in the near infrared. Remote Sensing of Environment. 10(1): 23-32. 10.1016/0034-4257(80)90096-6

Tucker CJ, Elgin JH, McMurtrey JE. 1980. Relationship of crop radiance to alfalfa agronomic values. International Journal of Remote Sensing. 1(1). doi: 10.1080/01431168008948211.

Varella AC, Talbert LE, Achhami BB, Blake NK, Hofland ML, Sherman JD, Lamb PF, Reddy GVP, Weaver DK. 2018. Characterization of resistance to *Cephus cinctus* (Hymenoptera: Cephidae) in barley germplasm. Journal of Economic Entomology. 111(2):923–930. doi: 10.1093/jee/toy025.

Varella AC, Weaver DK, Blake NK, Hofland ML, Heo H-Y, Cook JP, Lamb PF, Jordan KW, Akhunov E, Chao S, et al. 2019. Analysis of recombinant inbred line populations derived from wheat landraces to identify new genes for wheat stem sawfly resistance. Theoretical Applied Genetics. 132(8):2195–2207. doi: 10.1007/s00122-019-03347-8.

Villacorta A, Bell RA, Callenbach JA. 1971. Influence of high temperature and light on postdiapause development of the wheat stem sawfly. Journal of Economic Entomology. 64(3):749–751. doi: 10.1093/jee/64.3.749.

Wallace, L. E. and McNeal, F. H. (1966). Stem sawflies of economic importance in grain crops in the United States. Washington, DC: Agricultural Research Service, United States Department of Agriculture.

Wanner K, Tharp C. 2015. Thimet 20-G® for wheat stem sawfly management. Montana State University, Extension, Pesticide News. Available at: https://pesticides.montana.edu/news/msupestnews/20150506_PN_Thimet.html.

Weaver DK. 2023. Wheat stem sawfly (*Cephus cinctus* Norton). Chapter 5, in Eigenbrode, SD, Rashed A, (eds.) Advances in Understanding Insect Pests Affecting Wheat and Other Cereals, pp. 93–134. doi: 10.19103/as.2022.0114.13.

Weaver DK, Sing S, Runyon J, Morrill W. 2004. Potential impact of cultural practices on wheat stem sawfly (Hymenoptera: Cephidae) and associated parasitoids. Journal of Agricultural and Urban Entomology. 21:271–287.

Weaver DK, Tallman S, Lane T. 2024. Wheat stem sawfly best management practices. Montana State University Extension. MSU Extension Bulletin EB0244; USDA-NRCS Agronomy Technical Note MT-95. doi: 10.13140/RG.2.2.19133.88805

Weaver DK, Buteler M, Hofland ML, Runyon JB, Nansen C, Talbert LE, Lamb P, Carlson GR. 2009. Cultivar preferences of ovipositing wheat stem sawflies as influenced by the amount of volatile attractant. Journal of Economic Entomology. 102(3): 1009-1017. doi:10.1603/029.102.0320.

Weiss MJ, Morrill WL. 1992. Wheat stem sawfly (Hymenoptera: Cephidae) revisited. American Entomologist. 38(4):241–245. doi: 10.1093/ae/38.4.241.

Wen W, Timmermans J, Chen Q, van Bodegom PM. 2023. Evaluating crop-specific responses to salinity and drought stress from remote sensing. International Journal of Applied Earth Observation and Geoinformation. 122:103438. doi: 10.1016/j.jag.2023.103438.

Wiersma DJ, Landgrebe DA. 1980. Analytical design of multispectral sensors. IEEE Transactions on Geoscience and Remote Sensing. GE-18(2):180–189. doi: 10.1109/TGRS.1980.350271.

Wold S, Geladi P, Esbensen K, Ohman J. 1987. Multi-way principal components-and pls-analysis. Journal of Chemometrics. 1(1):41-56. doi: 10.1002/cem.1180010107

Woodcock CE, Strahler AH, Jupp DLB. 1988. The use of variograms in remote sensing: real digital images. Remote Sensing of Environment. 25(3):349–379. doi: 10.1016/0034-4257(88)90109-5.

Woolley JT. 1971. Reflectance and transmittance of light by leaves. Plant Physiology. 47(5):656-662. doi: 10.1104/pp.47.5.656

Xiao G, Zhang X, Niu Q, Li Xingang, Li Xuecao, Zhong L, Huang J. 2024. Winter wheat yield estimation at the field scale using sentinel-2 data and deep learning. Computers and Electronics in Agriculture. 216. doi: 10.1016/j.compag.2023.108555.

Yang Z, Rao MN, Elliott NC, Kindler SD, Popham TW. 2009. Differentiating stress induced by greenbugs and Russian wheat aphids in wheat using remote sensing. Computers and Electronics in Agriculture. 67(1):64–70. doi: 10.1016/j.compag.2009.03.003.

Yates HW. 1970. A general discussion of remote sensing of the atmosphere. Applied Optics, AO. 9(9):1971–1975. doi: 10.1364/AO.9.001971.

Yu H, Guo L, Kharbach M, Han W. 2021. Multi-way analysis coupled with near-infrared spectroscopy in food industry: Models and applications. Foods. 10(4). doi: 10.3390/foods10040802.

Zhang W, Li X, Zhao L. 2019. Discovering the representative subset with low redundancy for hyperspectral feature selection. Remote Sensing. 11(11). doi: 10.3390/rs11111341.